POLITECNICO DI TORINO

Master Thesis in Electrical Engineering

Impedance Models of Grid-Tied Converters

Author: Matteo Pasqualini

Supervisor: Prof. Radu Bojoi

Advisor: Fabio Mandrile

March 2020

Abstract

Due to the continuous growth in the number of grid-tied electronic power converters, it has become important to study how they can be represented from the point of view of the grid itself and the system-level problems that can arise once connected. This thesis uses linear analysis to obtain a mathematical model capable of representing the equivalent impedance of a three-phase Voltage Source Converter (VSC) expressed in a rotating (d,q) frame. For this reason, the Small-Signal model of the converter under analysis will be considered to analyze its behavior when it works as a generator (e.g. sun power generation) or when it it works as an active rectifier (e.g. battery charger). From the Small-Signal model, with the chosen mathematical approach, a model is thus obtained which can be used for the analytical calculation of the impedance of the converter. The impedance obtained can either be used as a benchmark to evaluate the accuracy of other methods for measuring the equivalent impedance or can be used for stability analysis using the Nyquist criterion.

Contents

List of Tables

List of Figures

Chapter 1

Introduction

Power electronics, which relies on high efficiency and fast-switching power semiconductor devices, has nowadays been established as a major discipline within electrical engineering: one of the main fields of application of this discipline is the possibility of connecting renewable energy production plants to the power grid. These plants require continuous regulation of the electrical quantities due to several causes, such as the nature of the energy source, climatic conditions etc. Not only that, power converters are also used to connect storage systems to the grid to absorb energy from it and, when the demand for energy is high, to redistribute it to support the network. Therefore, since such regulation is necessary, the growth in the number of renewable plants and the increase in the number of energy storage systems, to enhance the grid reliability, can only lead to an expansion in the number of electronic power converters that make the energy exchange compatible. For example, in Italy for 5 years the share of consumption satisfied by renewable sources has been higher than the 2020 target: this indicator was defined by the directive 2009/28/EC within Europe 2020, a ten year strategy proposed by the European commission in 2010 and based on a vision of smart, sustainable and inclusive growth. In 2018 our country has reached 18.1 % of energy demand supplied by renewable sources, thus exceeding the target, set at 17 % , by the European plan.

In addition to the greater presence of renewable energy sources, the evolution of the power grid itself and its future aspects must also be taken into consideration: the transition from centralized generation to distributed generation, the birth of

microgrids, the interface with the medium voltage distribution network and the future smart grid concept combined with the electrification of transportation all require an increase in the number of front-end AC/DC converters.
The presence of converters connected to the network, in particular Voltage-Source Converters (VSC), is therefore currently increasing and, although these converters are designed to perform a certain function, once connected to the network, the system could weaken to the point of becoming unstable. The problem is determined by the overall system behavior of the VSC and grid: for example, as described in the article *Out of Control Because of Harmonics* [2], during the April of 1995 in Zurich, the interaction through the network of new VSCs mounted on locomotives, that operated with high switching frequency converters, caused the intervention of the protections, thus causing the system shutdown. Through linear analysis it is in fact possible to observe how, for a certain range of frequencies, some elements of the system can influence the equivalent impedance of the converter which begins to have a real part with negative behavior facilitating the amplification of harmonics and making the system unstable. The problem in the presented case was not having foreseen how the power grid would have seen all those converters: to cope with this problem, mathematical models and experimental simulations were used to precisely obtain a model to described the converters in a simple way and with characteristics that could be used in a system study.
The objective of this thesis is to analyze a Active Front End (AFE) for the connection with the three-phase grid of systems that produce or redistributes energy and building an equivalent model, through linear analysis, that expresses the Small-Signal impedances of this converter in a rotating (d,q) frame evaluating its stability once connected to the power grid. Once the converter impedance model has been obtained, it can be used either as a benchmark for experimental results, obtained using other approaches, or to represent a multitude of converters of that type connected to the grid, Fig. 4.1.

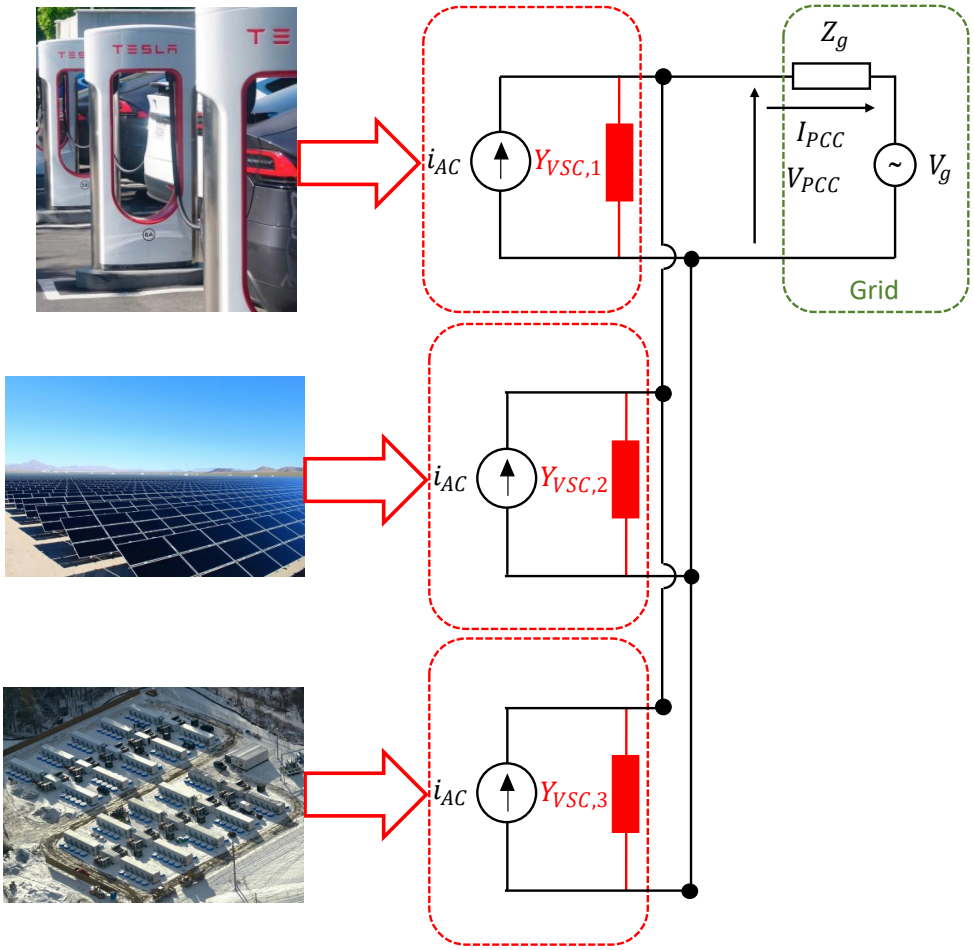

Figure 1.1: Representation via the equivalent Norton circuit of several converters connected to the grid represented by their equivalent admittance.

This type of representation can be used to carry out an analysis of stability, using the Nyquist criterion: in fact, the system in figure Fig. 4.1 can be described as (1.1) using Millman's theorem at the Point of Common Coupling (PCC).

$$I_{PCC} = \frac{V_{PCC} - V_g}{Z_g} = \frac{Z_g \cdot i_{AC} + V_g}{1 + Z_g \cdot (Y_{VSC,1} + Y_{VSC,2} + Y_{VSC,3})} \cdot Z_g^{-1} - V_g \cdot Z_g^{-1}$$

$$I_{PCC} = [i_{AC} - (Y_{VSC,1} + Y_{VSC,2} + Y_{VSC,3}) \cdot V_g] \cdot \frac{1}{1 + Z_g \cdot (Y_{VSC,1} + Y_{VSC,2} + Y_{VSC,3})} \tag{1.1}$$

The stability of a system described in this way can be studied by conderating

the grid voltage as ideal and with a stable i_{AC} current, going to describe a system with negative feedback described in figure Fig. 1.2.

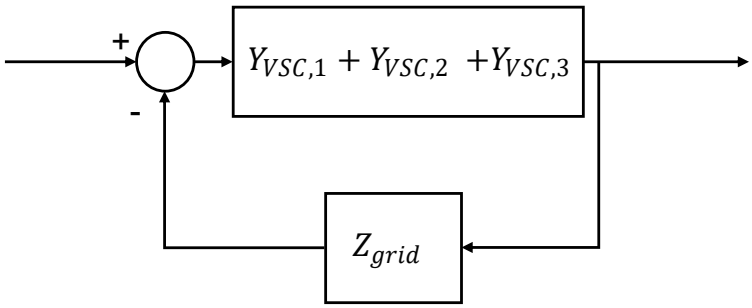

Figure 1.2: Block diagram to study the stability of the system through the Nyquist criterion.

This closed-loop system can be studied by applying the Nyquist stability considering many converters that operate connected in parallel with the grid.
The personal contributions made within the realization of this thesis have been: a bibliographic research concerning the impedance models of converters obtained by linearization, a detailed explanation of the selected approach and obtaining a script capable of calculating, given in input the converter parameters, the equivalent impedance for Small-Signal perturbations. Thanks to this script it has been possible to observe how the equivalent impedance of the converter for Small-Signal disturbances changes when it is used as an active rectifier or when it is used as a generator. The script was also useful for assessing what impact the different converter parameters has, how the currents, in module and sign, influence the results and what influence the PLL has within the control scheme.

1.1 Description of the Examined System

The system under consideration, whose single phase diagram is shown in Fig. 1.3, consists of a DC source connected to a three-phase inverter which has the task of converting electrical energy from DC into AC in order to transfer active power to the grid.

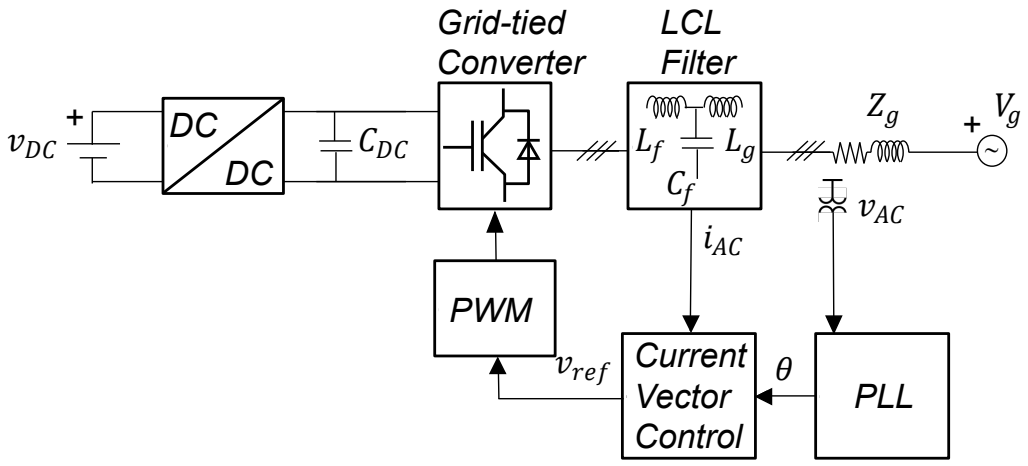

Figure 1.3: Single phase diagram of the analyzed system.

1.1.1 Description of the Blocks that compose the System

The individual parts that make up the system, and their functions, are presented as follows:

Grid Tied Converter

It is the component that converts the voltage from DC to AC or vice versa using controlled switches. In this specific case, a high switching frequency converter will be analyzed to connect a local DC generator to the power grid. The two methods of operation of this converter will be to inject power into the electric grid or to absorb energy from it.

LCL Filter

Linear filters LCL, increasingly used for example in photovoltaic applications for the connection between the inverter and the grid, provide better attenuation of the switching harmonics of the Pulse Width Modulation (PWM) output to the converter compared to a conventional system based on the presence of the inductive element only, also reducing the overall size and weight. It consists of two inductors, one on the network side and one on the inverter side, and a bank of capacitors connected in star connection between the two.

PLL

In order to feed currents and voltages that are in phase with with the grid voltage, a Phase-Locked Loop (PLL) is used. This PLL is able to reconstruct the angle of the grid voltage vector measured across the filter capacitors C_f. The block diagram of the PLL used within the control system is shown in Fig. 1.4.

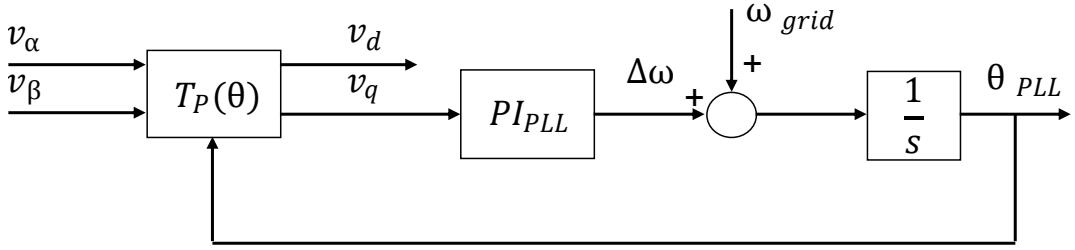

Figure 1.4: PLL block diagram.

The PLL observes the grid angle θ_{PLL}, having as input the measured voltages v_{C_f}. First of all the voltages v_{C_f} are transformed from reference system (123) to the stationary reference system (α, β): the Clarke's transformation T_C matrix is used, which preserves the modules of the electrical quantities of interest by calculating the electrical power differently.

$$T_C = \frac{2}{3} \cdot \begin{bmatrix} 1 & -\frac{1}{2} & -\frac{1}{2} \\ 0 & \frac{\sqrt{3}}{2} & -\frac{\sqrt{3}}{2} \end{bmatrix} \tag{1.2}$$

Multiplying this matrix by the vector of the voltages in the three-phase reference system switches to a two-phase reference system in a stationary reference frame. Through the rotation transform T_P matrix, the measured quantities are then transformed into a rotating frame (d,q). This transform also requires a reference angle to know the position of the rotating reference frame, as shown below.

$$T_P = \begin{bmatrix} cos(\theta) & sen(\theta) \\ -sen(\theta) & cos(\theta) \end{bmatrix} \tag{1.3}$$

So in order to obtain the voltages in the (d,q) reference frame, the operation to be done is as follows:

$$\begin{bmatrix} v_d \\ v_q \end{bmatrix} = \begin{bmatrix} cos(\theta_{PLL}) & sen(\theta_{PLL}) \\ -sen(\theta_{PLL}) & cos(\theta_{PLL}) \end{bmatrix} \cdot \begin{bmatrix} v_\alpha \\ v_\beta \end{bmatrix} \tag{1.4}$$

Since the voltages in (α, β) can be written as functions of the amplitude V and of the grid angle θ_{PCC}, the relationship between voltages in (d,q) frame and voltages in (α, β) frame can be rewritten as:

$$\begin{bmatrix} v_d \\ v_q \end{bmatrix} = \begin{bmatrix} cos(\theta_{PLL}) & sen(\theta_{PLL}) \\ -sen(\theta_{PLL}) & cos(\theta_{PLL}) \end{bmatrix} \cdot \begin{bmatrix} V \cdot cos(\theta_{PCC}) \\ V \cdot sen(\theta_{PCC}) \end{bmatrix} \tag{1.5}$$

By rearranging the sine and cosine functions, a single vector can be obtained to the right of the equal which depends on the difference between the effective network angle and the network angle reconstructed by means of the PLL.

$$\begin{bmatrix} v_d \\ v_q \end{bmatrix} = V \cdot \begin{bmatrix} cos(\theta_{PLL} - \theta_{PCC}) \\ sen(\theta_{PLL} - \theta_{PCC}) \end{bmatrix} \tag{1.6}$$

Since the error between the actual and the measured angle tends to be small, $sen(\theta_{PLL} - \theta_{PCC})$ can be approximated with $\theta_{PLL} - \theta_{PCC}$ and therefore the voltage v_q is used to calculate the measured angle.

$$\Delta\theta = (\theta_{PLL} - \theta_{PCC}) \simeq 0 \tag{1.7}$$

$$\begin{bmatrix} v_d \\ v_q \end{bmatrix} \simeq V \cdot \begin{bmatrix} 1 \\ (\theta_{PLL} - \theta_{PCC}) \end{bmatrix} V \cdot = \begin{bmatrix} 1 \\ (\Delta\theta) \end{bmatrix} \tag{1.8}$$

Using this approximation, the voltage v_q is used as an input in a Proportional Integral (PI) regulator, which returns the difference in rotation speed between the actual mains voltage and the control reference system. Adding then this term to

the rotation speed of the power grid the speed of the reconstructed reference frame (d,q) is obtained: from there, an integrator block is used to obtain the angle to be used in order to perform Park transforms within the control scheme.

Current Vector Control

The current loop in the (d,q) reference frame uses the information deriving from the PLL in order to rotate the measured current and understand what reference voltage to give in the output. The diagram of the current loop used within this elaborate is shown in Fig. 1.5.

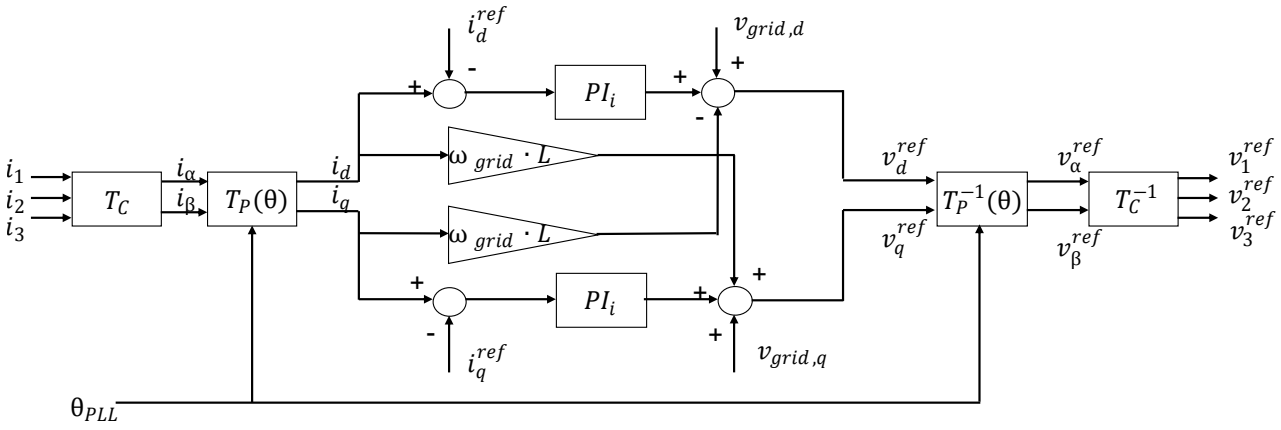

Figure 1.5: Current Vector Control block diagram.

To improve dynamic performance, at the output of the current PI the PCC voltages are given in feedforeward in (d,q) axes and a decoupling is also used to generate the reference voltages in (d,q) axes. The reference voltages are then divided by the DC voltage to obtain the three reference duty cycles comprising between zero and one.

PWM

The Pulse-Width Modulation (PWM) modulator it is the block which, by receiving the reference duty cycles calculated by Current Vector Control as input, generates the signals to be given to the inverter's controllable switches to generate the desired waveforms. The duty cycles are compared with a triangular carrier (so called

because it carries the switching frequency information) and binary signals are obtained at the output.

Voltage Control

Since these systems could receive energy from renewable sources for which the obtainable power levels are directly proportional to the temporary presence or absence of the energy source (wind, or sun for example), it is also necessary to provide a voltage loop in the control, external to the current one and with a lower bandwidth, with its own PI regulator, which manages the voltage levels on the DC-link capacitor to keep the latter constant.

1.1.2 d-q Reference Frame Model

In this section an average model of the system will be obtained in the defined rotating (d,q) frame. What will be considered within this model will be the DC side, modeled as a load resistor, and its capacitors bank in parallel, the inverter and the output $(R - L)$ impedance, not taking into account the filter capacities and the impedance Z_{gf}, on the grid side, such as the grid impedance and the grid itself. If the controllable switches, for this study, are considered on the basis of their function as ideal single-pole double-throw switches, it is possible to write simple relationships that link the instantaneous quantities in input from the DC side to those output from the inverter, AC side.

$$\begin{aligned} \overline{v}_1 &= \overline{d}_1 \cdot \overline{v}_{DC} \\ \overline{v}_2 &= \overline{d}_2 \cdot \overline{v}_{DC} \\ \overline{v}_3 &= \overline{d}_3 \cdot \overline{v}_{DC} \end{aligned} \tag{1.9}$$

$$\begin{aligned} \overline{i}_{DC} &= \overline{d}_1 \cdot \overline{i}_1 \\ \overline{i}_{DC} &= \overline{d}_2 \cdot \overline{i}_2 \\ \overline{i}_{DC} &= \overline{d}_3 \cdot \overline{i}_3 \end{aligned} \tag{1.10}$$

The symbol $-$ above the instantaneous quantities represented in the circuit only indicates that we are in this case in steady state, therefore without the presence of

disturbances absorbed by the gird.

This way, using the load convention for the output impedances, the system taken into account can be represented by three circuits for the three output phases and a single circuit for the DC input, as shown in Fig. 1.6.

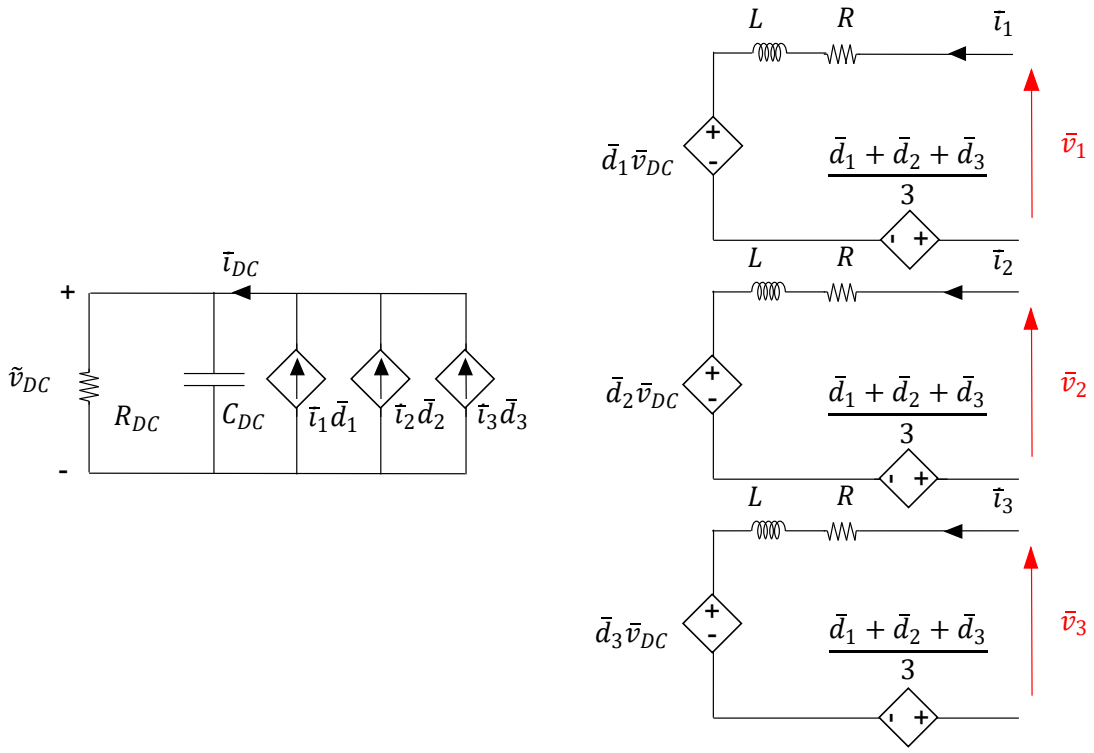

Figure 1.6: Average Model of the three-phase system.

The term $\left(\frac{\bar{d}_1+\bar{d}_2+\bar{d}_3}{3}\right)$ represents the absence of fourth the wire in the inverter, which works as a rejection of the common mode. Using the T_C transform we move into another stationary reference frame, but with one less phase: in this case the homopolar contributions are not considered, therefor removing the controlled generators $\left(\frac{\bar{d}_1+\bar{d}_2+\bar{d}_3}{3}\right)$ from the circuit. The number of controlled generators on the DC side drops to two as well as the number of circuits representing the output phases, Fig. 1.7.

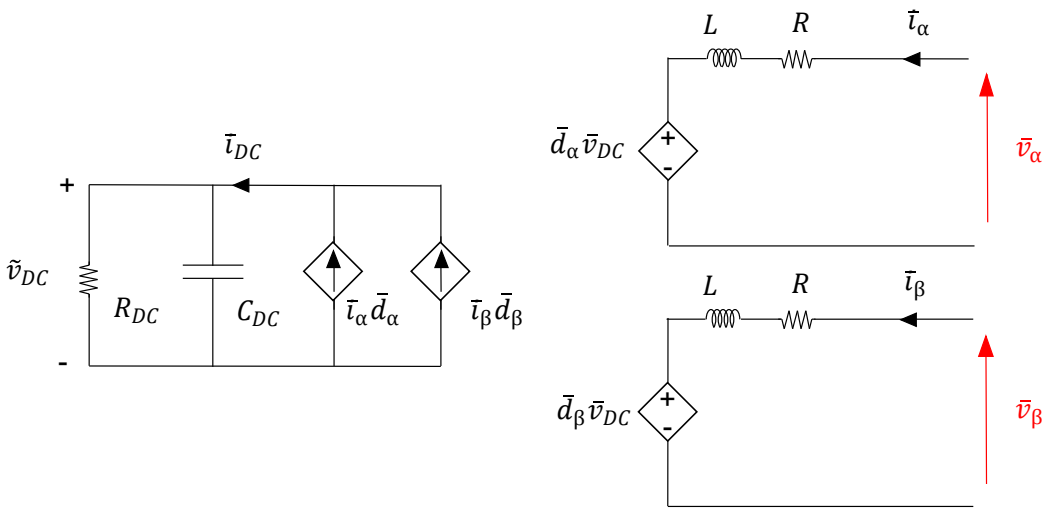

Figure 1.7: Average Model of the system in a stationary (α, β) reference frame.

By subsequently using the transformation T_P the two-phase system begins to rotate following the reference θ_{PLL}, received from the control scheme. Due to this rotation, a coupling term appears in both circuits representative of the output phases: this can be demonstrated by the following equations in vector form with $\mathbf{e}^{-j\theta_{PLL}}$ representing the rotations.

$$\begin{aligned} \mathbf{v}_{\alpha,\beta} &= R \cdot \mathbf{i}_{\alpha,\beta} + L\frac{d(\mathbf{i}_{\alpha,\beta})}{dt} \\ \mathbf{e}^{-j\theta_{PLL}} \cdot \mathbf{v}_{\alpha,\beta} &= R \cdot \mathbf{e}^{-j\theta_{PLL}} \cdot \mathbf{i}_{\alpha,\beta} + L \cdot \mathbf{e}^{-j\theta_{PLL}} \cdot \frac{d}{dt}(\mathbf{i}_{\alpha,\beta}) \\ \mathbf{v}_{d,q} &= R \cdot \mathbf{i}_{d,q} + L \cdot \mathbf{e}^{-j\theta_{PLL}} \cdot \frac{d}{dt}(\mathbf{i}_{\alpha,\beta}) \end{aligned} \tag{1.11}$$

$$\begin{aligned} \frac{d}{dt}(\mathbf{e}^{-j\theta_{PLL}} \cdot \mathbf{i}_{\alpha,\beta}) &= -j\omega_{grid}\mathbf{e}^{-j\theta_{PLL}} \cdot \mathbf{i}_{\alpha,\beta} + \mathbf{e}^{-j\theta_{PLL}} \cdot \frac{d}{dt}(\mathbf{i}_{\alpha,\beta}) \\ \mathbf{e}^{-j\theta_{PLL}} \cdot \frac{d}{dt}(\mathbf{i}_{\alpha,\beta}) &= \frac{d}{dt}(\mathbf{e}^{-j\theta_{PLL}} \cdot \mathbf{i}_{\alpha,\beta}) + j\omega_{grid}\mathbf{e}^{-j\theta_{PLL}} \cdot \mathbf{i}_{\alpha,\beta} \\ \mathbf{e}^{-j\theta_{PLL}} \cdot \frac{d}{dt}(\mathbf{i}_{\alpha,\beta}) &= \frac{d}{dt}(\mathbf{i}_{d,q}) + j\omega_{grid} \cdot \mathbf{i}_{d,q} \end{aligned} \tag{1.12}$$

Substituting (1.12) in (1.11) we obtain the equation which describes how a three-phase impedance is represented in a rotating (d,q) reference frame.

$$\overrightarrow{v}_{d,q} = R \cdot \overrightarrow{i}_{d,q} + L \cdot \frac{d}{dt}(\overrightarrow{i}_{d,q}) + j\omega_{grid} L \cdot \overrightarrow{i}_{d,q} \tag{1.13}$$

Expressing it in matrix form in Laplace domain we obtain:

$$\begin{bmatrix} v_d \\ v_q \end{bmatrix} = \begin{bmatrix} Ls + R & -\omega_{grid} \cdot L \\ \omega_{grid} \cdot L & Ls + R \end{bmatrix} \begin{bmatrix} i_d \\ i_q \end{bmatrix} \tag{1.14}$$

The system's aviation model, without the control scheme, therefore appears in this reference frame as shown in Fig. 1.8.

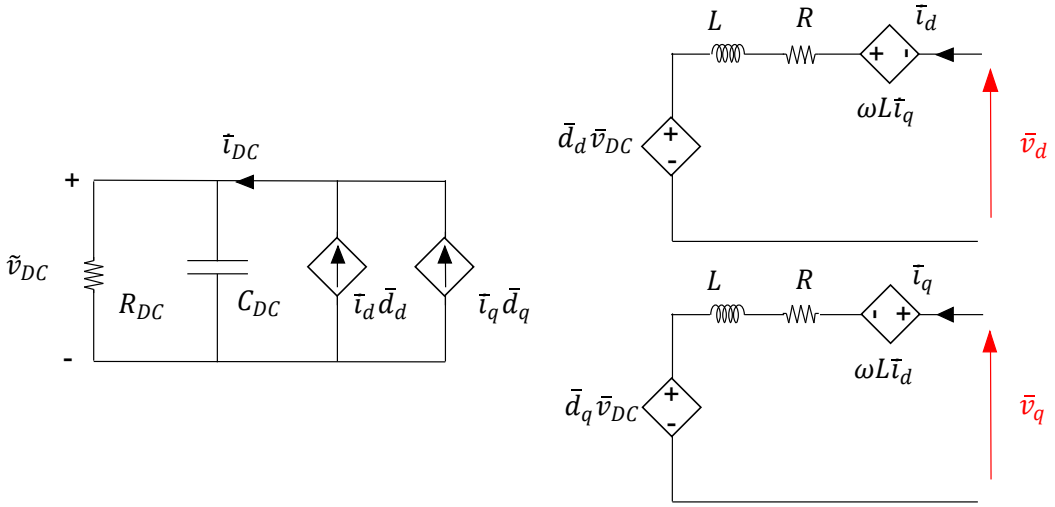

Figure 1.8: Average Model of the system in a rotating (d,q) reference frame.

1.2 Small-Signal Model

The Small-Signal Model is an indispensable tool for studying the behavior of the system under consideration in the presence of harmonics placed on the network: it starts from the Grid-Tied Converter's average model, including PLL and current and voltage control, shown in Fig. 1.9.

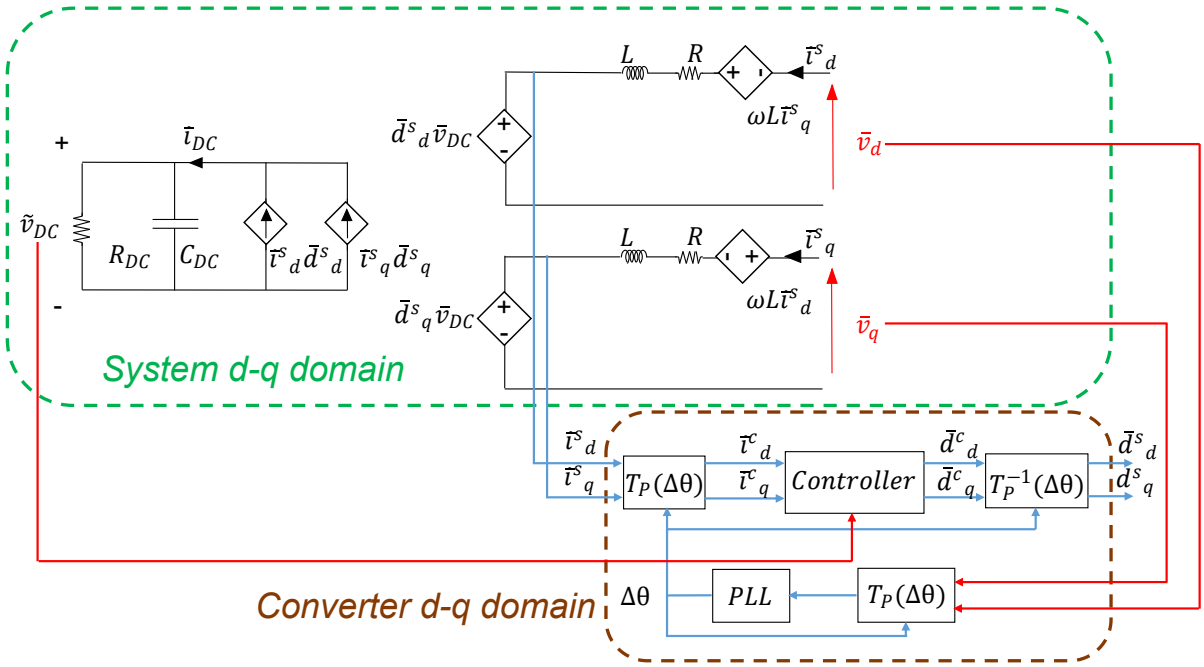

Figure 1.9: Average model of the analyzed system including the control in (d,q) frame.

In this case, the small signal analysis will be carried out in a rotating reference system (d,q) because in a fixed three-phase reference system, such as the actual physical system, there is no stable equilibrium point from which a linearization analysis can start for the study of the response to small signal disturbances: in such a reference system, a balanced three-phase system can be represented as two DC systems coupled together.

The purpose of obtaining a small signal model of a system is precisely to observe how the considered system behaves in the presence of disturbances, at different frequency spectra, of a percentage value with respect to the electrical quantities present in the system. The system, with the insertion of such disturbances, is analyzed around a specific operating point of interest. First of all it can be observed that the inverter system is divided into two domains: the first is the system domain, which is in a reference system (d,q) which is perfectly synchronous with that of the grid; the second is a domain located in a rotating reference system (d,q) defined by the angle calculated by the PLL(Fig 1.10).

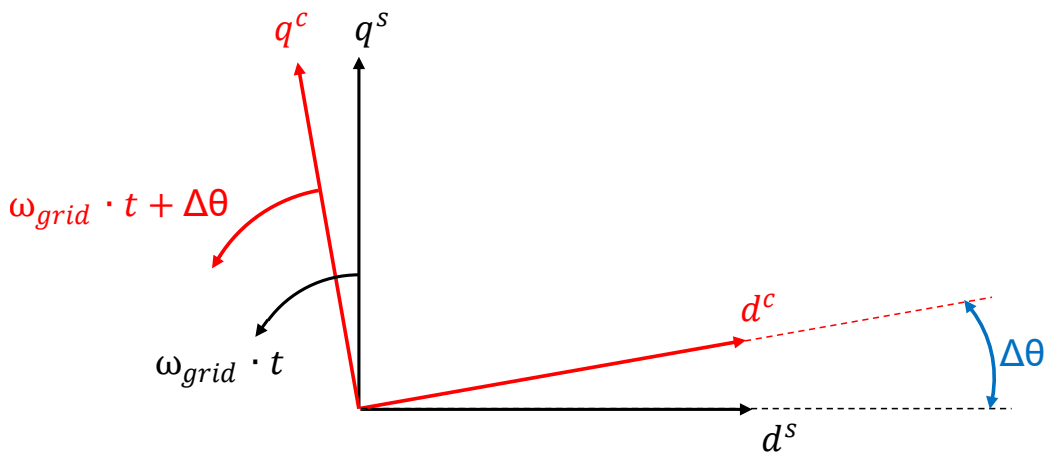

Figure 1.10: difference between the two (d,q) frame domain: the converter reference frame and the system reference frame.

The instantaneous quantities concerning the two systems are identified by the superscript "s" for those referring to the physical system and "c" for those inside the control system. The two systems communicate with each other through the rotation transformation with coefficient $\Delta\theta$, i.e. the difference between the θ reconstructed through the PLL within the control scheme with the actual one of the physical system.
At steady state, the two domains are aligned and there is a single domain, but, due to small signal perturbations coming from the grid, the PLL, which must follow the angle at which the physical system is located, due to its dynamics, will produce a reconstructed angle at the output which will not perfectly coincide with that of the grid and therefore, if we are not in a stable operating state, the angle θ_{PLL} be different from the grid voltage vector angle. Park's transform takes into account this phase difference by passing from one system to another, in the equivalent model, and the $T_P(\Delta\theta)$ matrix that connects the two systems is as follows:

$$T_P(\Delta\theta) = \begin{bmatrix} cos(\theta_{PLL} - \theta_{PCC}) & sen(\theta_{PLL} - \theta_{PCC}) \\ -sen(\theta_{PLL} - \theta_{PCC}) & cos(\theta_{PLL} - \theta_{PCC}) \end{bmatrix} = \begin{bmatrix} cos(\Delta\theta) & sen(\Delta\theta) \\ -sen(\Delta\theta) & cos(\Delta\theta) \end{bmatrix} \tag{1.15}$$

So a small-signal variation of the grid voltage will affect the output of the PLL and, having used the rotation transformation, which needs this angle, to move into a rotating reference system (d,q) for the control, the converter domain will be out of phase with that of the power grid: the error will then spread on the current and, through it, on the duty cycle and on the output voltage of the converter.
In order to study the severity for the system of these voltage disturbances deriving from the network, it is therefore useful, starting from the circuit previously seen, to obtain an equivalent circuit for the study of the propagation of the error, as shown in Fig. 1.11.

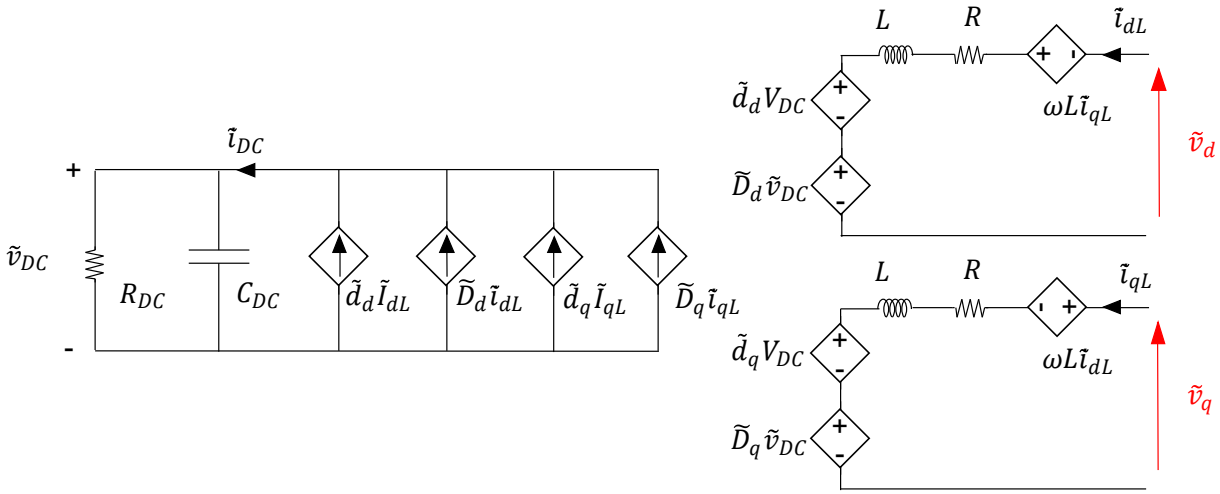

Figure 1.11: Small-Signal Circuit of the Grid-Tied Converter in (d,q) frame [3].

In this case, the symbol $\sim$ above the instantaneous quantities indicates that the propagation of a small-signal signal through the circuit is being analyzed.
This circuit, together with the knowledge of the block diagram of the current loop and the voltage loop, will be used to develop an analytical calculation of the equivalent impedance of the inverter, in (d,q) axes, to be able to determine in which cases the small-signal voltage perturbations present in the network could propagate inside the Grid-Tied Converter causing the intervention of the protections and the consequent system shutdown.

Chapter 2

Analytical Derivation of Equivalent impedance with Only the Current Loop

As previously introduced, linear analysis will be used in this paper to test the behavior of the VSC in the presence of grid perturbations. The approach to the mathematical derivation of the impedance in (d,q) axes will be a modular approach [4]: first the open loop impedances will be calculated and then more and more blocks will be added, increasing the computational complexity, to gradually arrive at a mathematical formulation with a high degree of accuracy. The reference circuit is the one in Fig. 1.11, described in the introduction, through which it will be possible to find the links between the different quantities of interest and then find a relation between small-signal voltage $\tilde{v}_{d,q}$ and small-signal current $\tilde{i}_{d,q}$.

2.1 Analytical Derivation of Blocks

Initially it was considered appropriate to carry out the calculations by not considering the propagation of the disturbance on the voltage loop. In this way, we only have to consider the internal current loop, assuming that the DC voltage does not have overlapping oscillations, also freeing us from the capacitive input dynamics.

In this case the circuit to be considered is the following:

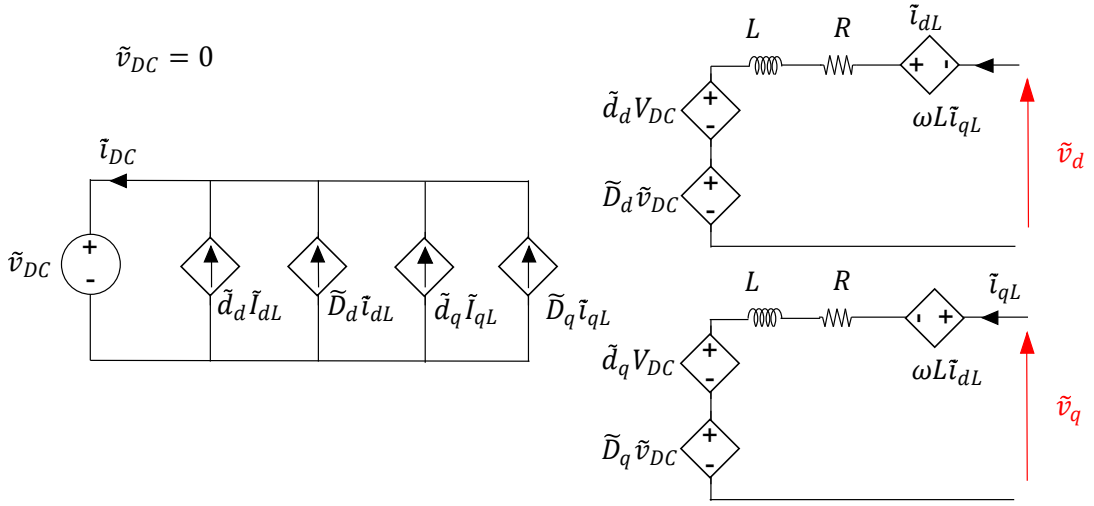

Figure 2.1: Small-Signal Circuit of the Grid-Tied Converter in (d,q) frame with no $\tilde{v}_{DC}$.

2.1.1 Link Between Voltages and Currents

The matrix that relates the voltages on the (d,q) axes to the currents on the (d,q) axis can be found, starting from the circuit in Fig. 2.1, forcing the small-signals of the duty cycles $\tilde{d}_d$ and $\tilde{d}_d$ to zero.
In this case the two equations that can be obtained from the circuit analysis are the following:

$$\tilde{v}_d = L\frac{d(\tilde{i}_d)}{dt} + R\tilde{i}_d - \omega_{grid} L\tilde{i}_q \tag{2.1}$$

$$\tilde{v}_q = L\frac{d(\tilde{i}_q)}{dt} + R\tilde{i}_q + \omega_{grid} L\tilde{i}_d \tag{2.2}$$

In this way it is evident that a matrix relationship can be found, through a 2×2 matrix, between the two terms under analysis (using the load convention). The matrix representation is used in Laplace domain form, for simplicity of expression, obtaining:

$$\begin{bmatrix} \tilde{i}_d \\ \tilde{i}_q \end{bmatrix} = \begin{bmatrix} Ls + R & -\omega_{grid} \cdot L \\ \omega_{grid} \cdot L & Ls + R \end{bmatrix}^{-1} \begin{bmatrix} \tilde{v}_d \\ \tilde{v}_q \end{bmatrix} \tag{2.3}$$

In this case, since this matrix is representative of the inverter's admittance at the output expressed in a rotating (d,q) frame, it will be called $\mathbf{Y}_{RL,dq}$, and its inverse, which has the form of an impedance, will be called $\mathbf{Z}_{RL,dq}$.

$$\mathbf{Y}_{RL,dq} = \frac{1}{(Ls + R)^2 + (\omega_{grid} \cdot L)^2} \begin{bmatrix} Ls + R & +\omega_{grid} \cdot L \\ -\omega_{grid} \cdot L & Ls + R \end{bmatrix} \tag{2.4}$$

$$\mathbf{Z}_{RL,dq} = \begin{bmatrix} Ls + R & -\omega_{grid} \cdot L \\ \omega_{grid} \cdot L & Ls + R \end{bmatrix} \tag{2.5}$$

2.1.2 Link Between Duty Cycles and Currents

To obtain the relationship between the duty cycles $\tilde{d}_{d,q}$ and the system currents $\tilde{i}_{d,q}$ the circuit in Fig. 2.1 is analyzed. In this case, the output voltages $\tilde{v}_d$ and $\tilde{v}_q$ are set to zero instead of the duty cycles $\tilde{d}_{d,q}$.
From the circuit it is possible to obtain that:

$$\tilde{d}_d V_{DC} + L\frac{d(\tilde{i}_d)}{dt} + R\tilde{i}_d - \omega_{grid} L\tilde{i}_q = 0 \tag{2.6}$$

$$\tilde{d}_q V_{DC} + L\frac{d(\tilde{i}_q)}{dt} + R\tilde{i}_q + \omega_{grid} L\tilde{i}_d = 0 \tag{2.7}$$

Rewriting the two relationships in matrix form in the Laplace domain we obtain:

$$\begin{bmatrix} \tilde{i}_d \\ \tilde{i}_q \end{bmatrix} = -V_{DC} \cdot \begin{bmatrix} Ls + R & -\omega_{grid} \cdot L \\ \omega_{grid} \cdot L & Ls + R \end{bmatrix}^{-1} \cdot \begin{bmatrix} \tilde{d}_d \\ \tilde{d}_q \end{bmatrix} \tag{2.8}$$

Then we have obtained the matrix $\mathbf{G}_{d,i}$, defined as:

$$\mathbf{G}_{d,i} = -\frac{V_{DC}}{(Ls+R)^2 + (\omega \cdot L)^2} \begin{bmatrix} Ls+R & +\omega_{grid} \cdot L \\ -\omega_{grid} \cdot L & Ls+R \end{bmatrix}$$
$$\mathbf{G}_{d,i} = -V_{DC} \cdot \mathbf{Y}_{RL,dq} \tag{2.9}$$

2.1.3 Influence of the PLL

We know that, due to its dynamics and disturbances measured from the network, the angle observed by the PLL will not perfectly coincide with the grid reference angle. Taking into account the average model of the system in the (d,q) frame with the two different reference systems (the control reference system and the physical reference system), using the equations (1.7), (1.8) and (1.15) we can define how the PLL affects the impedance of the converter [5].
We know that the DC average value of the currents in (d,q) frame, added to the relative small-signal disturbances, can be brought into the converter reference frame by means of the transform $T_P(\Delta\theta)$ which exploits the difference of phase $\Delta\theta$ between the two systems, therefore:

$$\begin{bmatrix} I_d^c + \tilde{i}_d^c \\ I_q^c + \tilde{i}_q^c \end{bmatrix} = \begin{bmatrix} cos(\Delta\theta) & sen(\Delta\theta) \\ -sen(\Delta\theta) & cos(\Delta\theta) \end{bmatrix} \cdot \begin{bmatrix} I_d^s + \tilde{i}_d^s \\ I_q^s + \tilde{i}_q^s \end{bmatrix} \tag{2.10}$$

This system, taking advantage of the fact that $\Delta\theta$ tends to be almost null since the PLL error tries to cancel itself, can be linearized as follows.

$$\begin{bmatrix} I_d^c + \tilde{i}_d^c \\ I_q^c + \tilde{i}_q^c \end{bmatrix} = \begin{bmatrix} cos(\Delta\theta) & sen(\Delta\theta) \\ -sen(\Delta\theta) & cos(\Delta\theta) \end{bmatrix} \cdot \begin{bmatrix} I_d^s + \tilde{i}_d^s \\ I_q^s + \tilde{i}_q^s \end{bmatrix} \simeq \begin{bmatrix} 1 & \Delta\theta \\ -\Delta\theta & 1 \end{bmatrix} \cdot \begin{bmatrix} I_d^s + \tilde{i}_d^s \\ I_q^s + \tilde{i}_q^s \end{bmatrix} \tag{2.11}$$

The same can be said with duty cuycles, but taking into account that the $T_P(\Delta\theta)$ is there used to transform back the duties from the converter reference system to the physical reference system of the grid.

$$\begin{bmatrix} D_d^s + \tilde{d}_d^s \\ D_q^s + \tilde{d}_q^s \end{bmatrix} = \begin{bmatrix} cos(\Delta\theta) & -sen(\Delta\theta) \\ sen(\Delta\theta) & cos(\Delta\theta) \end{bmatrix} \cdot \begin{bmatrix} D_d^c + \tilde{d}_d^c \\ D_q^c + \tilde{d}_q^c \end{bmatrix} \tag{2.12}$$

$$\begin{bmatrix} D_d^s + \tilde{d}_d^s \\ D_q^s + \tilde{d}_q^s \end{bmatrix} \simeq \begin{bmatrix} 1 & -\Delta\theta \\ \Delta\theta & 1 \end{bmatrix} \cdot \begin{bmatrix} D_d^c + \tilde{d}_d^c \\ D_q^c + \tilde{d}_q^c \end{bmatrix} \tag{2.13}$$

Now we need to be able to express the difference $\Delta\theta$ in order to find the relationship between this error and the operations carried out within the PLL. We know that at the input of the matrix $T_P(\theta)$ at the beginning of the PLL control scheme (Fig. 1.4) there are the voltages in a stationary reference frame (α, β). Starting from (1.7), knowing how fast the grid voltages rotates, we can write that:

$$\Delta\theta = (\theta_{PLL} - \omega_{grid} \cdot t) \tag{2.14}$$

And therefore θ_{PLL} can be expressed as a linear function of the grid angular frequency which multiplies time plus an error.

$$\theta_{PLL} = \Delta\theta + \omega_{grid} \cdot t \tag{2.15}$$

By applying the Park transform with θ_{PLL} the system can be expressed as:

$$\begin{bmatrix} v_d^c \\ v_q^c \end{bmatrix} = T_P(\theta_{PLL}) \cdot \begin{bmatrix} v_\alpha^s \\ v_\beta^s \end{bmatrix} \tag{2.16}$$

Expressing the voltages in (α, β) in the (d,q) reference frame synchronous with the electrical grid and deriving the error on the voltages in (d,q) frame due to external disturbances, it is possible to obtain an expression that depends only on $\Delta\theta$ and that relates the voltages in the two reference systems.

$$\begin{bmatrix} v_d \\ v_q \end{bmatrix} = T_P(\theta_{PLL}) \cdot T_P(\omega_{grid} \cdot t) \cdot \begin{bmatrix} V_d^s + \tilde{v}_d^s \\ \tilde{v}_q^s \end{bmatrix} = T_P(\Delta\theta) \cdot \begin{bmatrix} V_d^s + \tilde{v}_d^s \\ \tilde{v}_q^s \end{bmatrix} \tag{2.17}$$

By linearizing, knowing that there is only v_q at the input of the PLL, an expression of it can be obtained which depends on the error in the q axis of the voltages and on the phase error at the output of the PLL:

$$v_q = cos(\Delta\theta) \cdot (\tilde{v}_q^s) + sen(\Delta\theta) \cdot (V_d^s + \tilde{v}_d^s) \simeq \tilde{v}_q^s + \Delta\theta \cdot (V_d^s + \tilde{v}_d^s) \tag{2.18}$$

Simplifying we obtain:

$$v_q \simeq \tilde{v}_q^s + \Delta\theta \cdot V_d^s \tag{2.19}$$

Observing then the PLL control scheme (Fig. 1.4), removing the feed-forward term ω_{grid}, we see that the voltage v_q passes through the PI of the PLL and through an integrator to generate the output phase with the error and then another formula that take into account how the PLL was structured can be written.

$$\Delta\theta = v_q \cdot \frac{kp_{PLL} + \dfrac{ki_{PLL}}{s}}{s} \tag{2.20}$$

Substituting (2.19) in (2.20) we find a transfer function in the Laplace domain of $\Delta\theta$ that depends exclusively on terms inside the PLL control scheme.

$$\Delta\theta = (\tilde{v}_q^s + \Delta\theta \cdot V_d^s) \cdot \frac{kp_{PLL} + \dfrac{ki_{PLL}}{s}}{s} \tag{2.21}$$

Rearranging the equation it is possible to conclude that:

$$\Delta\theta = \frac{\left(kp_{PLL} + \dfrac{ki_{PLL}}{s}\right)}{s + \left(kp_{PLL} + \dfrac{ki_{PLL}}{s}\right) \cdot V_d} \Delta\tilde{v}_q^s \tag{2.22}$$

Rewriting for convenience the PI transfer function of the PLL as H_{PLL} the transfer

function of the PLL for a small-signal input can be expressed as follows and its transfer function seen as a block diagram appears as in Fig. 2.2.

$$T_{PLL} = \frac{\Delta\theta}{\tilde{v}_q^s} = \frac{H_{PLL}}{s + H_{PLL} \cdot V_d} \tag{2.23}$$

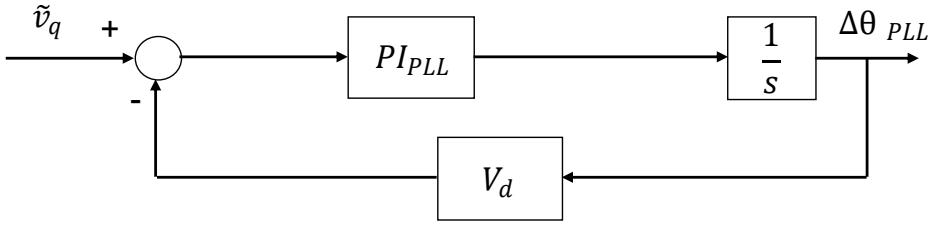

Figure 2.2: Small-Signal Circuit of the PLL.

Having now obtained an expression of $\Delta\theta$ we can replace this relationship in (2.11) and (2.13) to obtain the influence of the PLL on duty cycles and currents.

$$\begin{bmatrix} I_d^c + \tilde{i}_d^c \\ I_q^c + \tilde{i}_q^c \end{bmatrix} \simeq \begin{bmatrix} 1 & T_{PLL} \cdot \tilde{v}_q^s \\ -T_{PLL} \cdot \tilde{v}_q^s & 1 \end{bmatrix} \cdot \begin{bmatrix} I_d^s + \tilde{i}_d^s \\ I_q^s + \tilde{i}_q^s \end{bmatrix}$$

$$\begin{bmatrix} I_d^c + \tilde{i}_d^c \\ I_q^c + \tilde{i}_q^c \end{bmatrix} \simeq \begin{bmatrix} (I_d^s + \tilde{i}_d^s) + T_{PLL} \cdot \tilde{v}_q^s \cdot (I_q^s + \tilde{i}_q^s) \\ -T_{PLL} \cdot \tilde{v}_q^s \cdot (I_d^s + \tilde{i}_d^s) + (I_q^s + \tilde{i}_q^s) \end{bmatrix} \tag{2.24}$$

$$\begin{bmatrix} \tilde{i}_d^c \\ \tilde{i}_q^c \end{bmatrix} \simeq \begin{bmatrix} \tilde{i}_d^s \\ \tilde{i}_q^s \end{bmatrix} + \begin{bmatrix} 0 & T_{PLL} \cdot I_q^s \\ 0 & -T_{PLL} \cdot I_d^s \end{bmatrix} \begin{bmatrix} \tilde{v}_d^s \\ \tilde{v}_q^s \end{bmatrix}$$

$$\begin{bmatrix} D_d^s + \tilde{d}_d^s \\ D_q^s + \tilde{d}_q^s \end{bmatrix} \simeq \begin{bmatrix} 1 & -T_{PLL} \cdot \tilde{v}_q^s \\ T_{PLL} \cdot \tilde{v}_q^s & 1 \end{bmatrix} \cdot \begin{bmatrix} D_d^c + \tilde{d}_d^c \\ D_q^c + \tilde{d}_q^c \end{bmatrix}$$

$$\begin{bmatrix} D_d^s + \tilde{d}_d^s \\ D_q^s + \tilde{d}_q^s \end{bmatrix} \simeq \begin{bmatrix} (D_d^c + \tilde{d}_d^c) - T_{PLL} \cdot \tilde{v}_q^s \cdot (D_q^c + \tilde{d}_q^c) \\ T_{PLL} \cdot \tilde{v}_q^s \cdot (D_d^c + \tilde{d}_d^c) + (D_q^c + \tilde{d}_q^c) \end{bmatrix} \tag{2.25}$$

$$\begin{bmatrix} \tilde{d}_d^s \\ \tilde{d}_q^s \end{bmatrix} \simeq \begin{bmatrix} \tilde{d}_d^c \\ \tilde{d}_q^c \end{bmatrix} + \begin{bmatrix} 0 & -T_{PLL} \cdot D_q^c \\ 0 & T_{PLL} \cdot D_d^c \end{bmatrix} \begin{bmatrix} \tilde{v}_d^s \\ \tilde{v}_q^s \end{bmatrix}$$

So the two matrices useful for identifying the dependence on the PLL are $\mathbf{G}_{PLL,i}$ and $\mathbf{G}_{PLL,d}$, shown below.

$$\mathbf{G}_{PLL}^{i} = \begin{bmatrix} 0 & T_{PLL} \cdot I_q^c \\ 0 & -T_{PLL} \cdot I_d^c \end{bmatrix} \tag{2.26}$$

$$\mathbf{G}_{PLL}^{d} = \begin{bmatrix} 0 & -T_{PLL} \cdot D_q^c \\ 0 & T_{PLL} \cdot D_d^c \end{bmatrix} \tag{2.27}$$

2.1.4 Current PIs and Decoupling Terms

In this case, two current PI's were used for the two axes in the converter reference system. In this case the matrices are easily obtained by observing how the current control has been structured (Fig. 1.5). However, it is important to say that the values of the current PI and the decoupling terms have been set here to obtain the duty cycle at the output.

$$\begin{bmatrix} \tilde{d}_d^c \\ \tilde{d}_q^c \end{bmatrix} = \frac{1}{V_{DC}} \begin{bmatrix} kp_i + \dfrac{ki_i}{s} & 0 \\ 0 & kp_i + \dfrac{ki_i}{s} \end{bmatrix} \begin{bmatrix} \tilde{i}_d^c \\ \tilde{i}_q^c \end{bmatrix} + \begin{bmatrix} 0 & -\dfrac{\omega_{grid} \cdot L}{V_{DC}} \\ \dfrac{\omega_{grid} \cdot L}{V_{DC}} & 0 \end{bmatrix} \begin{bmatrix} \tilde{i}_d^c \\ \tilde{i}_q^c \end{bmatrix} \tag{2.28}$$

The two matrices that will be used are therefore $\mathbf{G}_{PI}$ and $\mathbf{G}_{dec}$, shown below.

$$\mathbf{G}_{PI} = \frac{1}{V_{DC}} \begin{bmatrix} kp_i + \dfrac{ki_i}{s} & 0 \\ 0 & kp_i + \dfrac{ki_i}{s} \end{bmatrix} \tag{2.29}$$

$$\mathbf{G}_{dec} = \begin{bmatrix} 0 & -\dfrac{\omega_{grid} \cdot L}{V_{DC}} \\ \dfrac{\omega_{grid} \cdot L}{V_{DC}} & 0 \end{bmatrix} \tag{2.30}$$

2.1.5 Delay due to PWM and Digital Control and Filters

The time it takes for the digital control to update the values of the reference duty cycles must be taken into account. At each interrupt cycle the control must

sample the analog variables, carry out the control calculations and update the reference value at the output. The average delay considered here is 1.5 of switching period, which is reported as a delay in (d,q) frame by means of a third-order Padè approximation [1].

$$Delay(s) = \frac{120 + 60 \cdot T_{delay} \cdot s + 12 \cdot T_{delay}^2 \cdot s^2 + T_{delay}^3 \cdot s^3}{120 - 60 \cdot T_{delay} \cdot s + 12 \cdot T_{delay}^2 \cdot s^2 - T_{delay}^3 \cdot s^3} \tag{2.31}$$

$$\mathbf{G}_{delay} = \begin{bmatrix} Delay(s) & 0 \\ 0 & Delay(s) \end{bmatrix} \tag{2.32}$$

It should also be considered that the variables under control, before being sampled, are conditioned by an analog circuit, that can be modeled by a transfer function. To ensure that the sampled values that will pass within the control scheme are the instantaneous average values of the quantities under analysis, a second order low pass filter is often inserted in input to model the signal conditioning. In the (d,q) reference frame those filters have only diagonal terms, such as the delay matrix, and can be expressed as:

$$\mathbf{G}_{filter} = \begin{bmatrix} \dfrac{\omega_n^2}{s^2 + 2\zeta\omega_n s + \omega_n^2} & 0 \\ 0 & \dfrac{\omega_n^2}{s^2 + 2\zeta\omega_n s + \omega_n^2} \end{bmatrix} \tag{2.33}$$

In the previous matrix ω_n is the natural frequency of the signal conditioning filter and ζ is the damping factor of the signal conditioning filter.

2.2 Calculated Impedances with only the Current Loop

Having obtained all the matrices useful for describing the impedance model in the (d,q) reference frame in this section, a way of composing these matrices together

will be proposed. We start by considering the internal current loop dividing the two reference systems, Fig. 2.3.

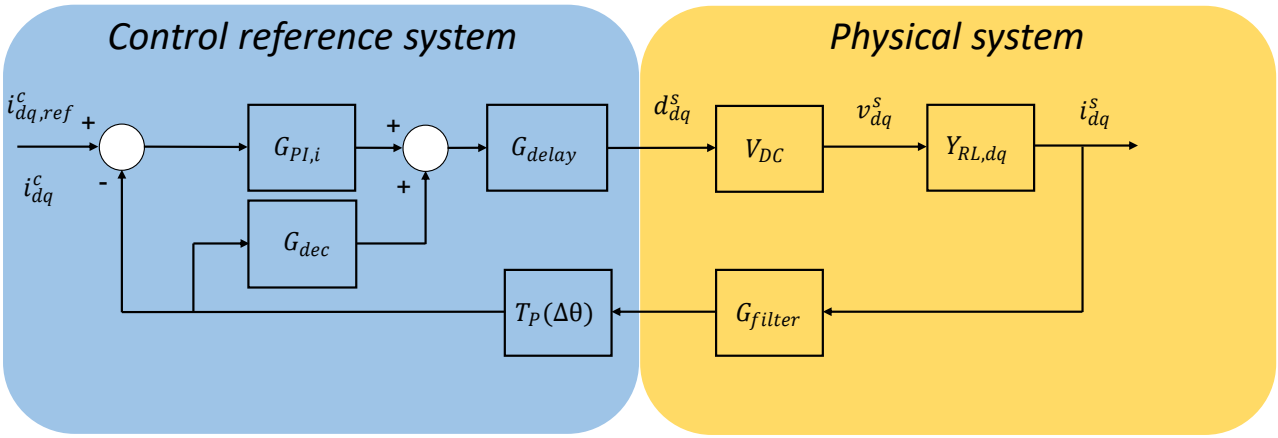

Figure 2.3: Current Loop of the Active Front End Converter.

As can be seen, the output of $\mathbf{G}_{PI}$ and $\mathbf{G}_{dec}$ have been defined to get the duty cycles to be applied on the d axis and the q axis which, through the $\mathbf{G}_{delay}$ matrix, are reported in the reference system of the power grid.
Considering the sampled voltage, and the analog filtering, the matrices inherent to the PLL can be added: through the $\mathbf{G}^d_{PLL}$, a contribution will be added to the duty cycle before it is transformed in the physical reference system and, through the $\mathbf{G}^i_{PLL}$, the feedback currents will be modified. At the output, through the $\mathbf{Y}_{RL}$, the small-signal variations of voltage will influence the feedback current. The system thus described can therefore be represented by a block diagram Fig. 2.4.

As can be seen in this system, designed to study the propagation of small-signals, the reference, imposed constant and equal to zero, is not considered. In addition, $\tilde{i}^s_{d,q}$ and $\tilde{v}^s_{d,q}$ were highlighted, i.e. the voltages and currents small-signals: considering $\tilde{v}^s_{d,q}$ as the input and $\tilde{i}^s_{d,q}$ as the output, the link that binds them expresses the system's impedance (or admittance) for small-signal disturbances in the (d,q) reference frame.
By rearranging the scheme presented in Fig. 2.4, it can be better observed that what connects the two signals must necessarily be expressed in $[\Omega]$ or in $\left[\frac{1}{\Omega}\right]$ and has the form of a 2×2 matrix, Fig. 2.5.

Having said that, to reduce any errors, we start to define what is the impedance

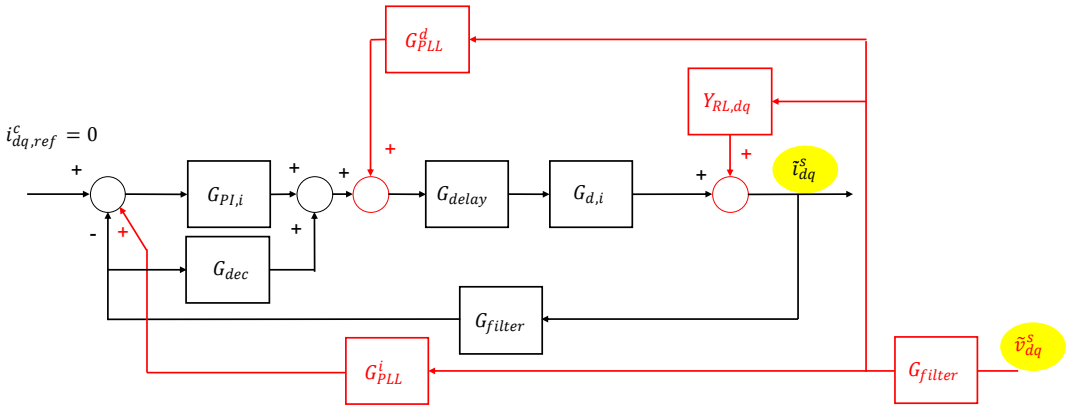

Figure 2.4: Small-Signal analysis of the Current Loop considering the PLL influences.

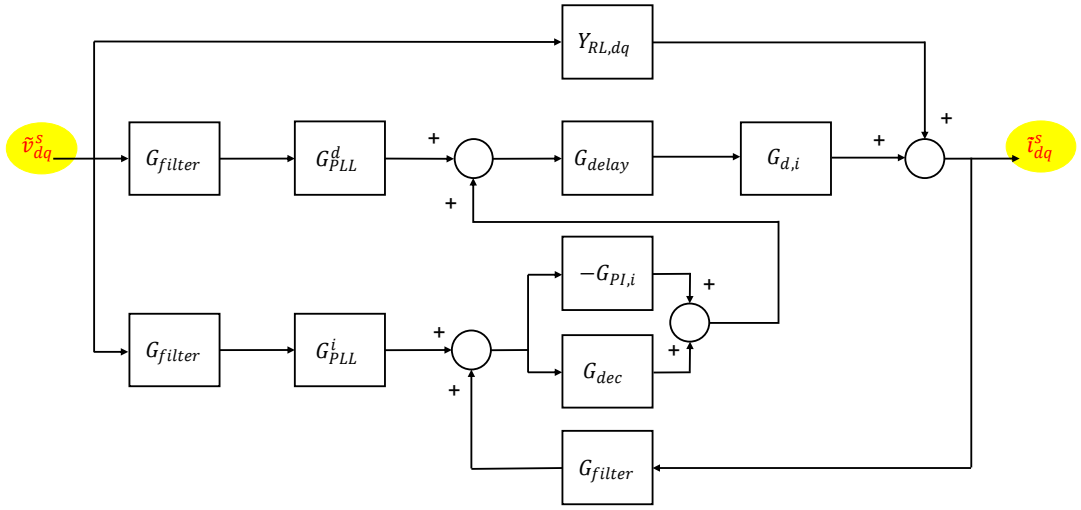

Figure 2.5: Matrix composition of the impedance in (d,q) reference frame.

of the system analyzed starting from a simple case and updating the results one step at a time: for this reason the impedance of the open-loop system will first be calculated without considering the dynamics of the PLL making the system more complex gradually, to arrive to a final sulution understanding the steps to take.
The data relating to the inverter system, the DC source, the LCL filter and the power grid are shown in the Table 2.1.

Table 2.1: Converter Parameters

Parameter	**Value**	**Unit of Measure**
f_{sw}	10000	Hz
V_{DC}	370	V
f_g	50	Hz
C_{DC}	1.8	mF
L_f	545	µH
R_f	15	mΩ
C_f	18	µF
L_g	170	µH
Z_g	$0.01 + 0.0471i$	Ω at 50 Hz
V_g	120	V_{rms}

As for the PIs used within this system, the bandwidths values are shown in the table 2.2:

Table 2.2: Control Bandwidths

Parameter	**Value**	**Unit of Measure**
$f_{bandwidth}$ *current loop*	1000	Hz
$f_{bandwidth}$ *voltage loop*	100	Hz
$f_{bandwidth}$ *PLL*	20	Hz

2.2.1 Impedances at Open Current-Loop with no PLL dynamic

Considering the open current loop and not taking into account the dynamics of the PLL and how it affects the results, the block diagram taken into consideration becomes that shown in Fig. 2.6.

In this case, therefore, what connects input and output is simply the matrix $\mathbf{Y}_{RL,dq}$ which expresses the output admittance from the converter.
A Matlab script was used to represent the transfer functions in the Laplace domain and obtain the Bode diagrams that describe the module and phase of the impedances in the (d,q) reference frame. For convenience, the Bode diagrams are shown here on a logarithmic scale both on the frequency axis and on the magnitude

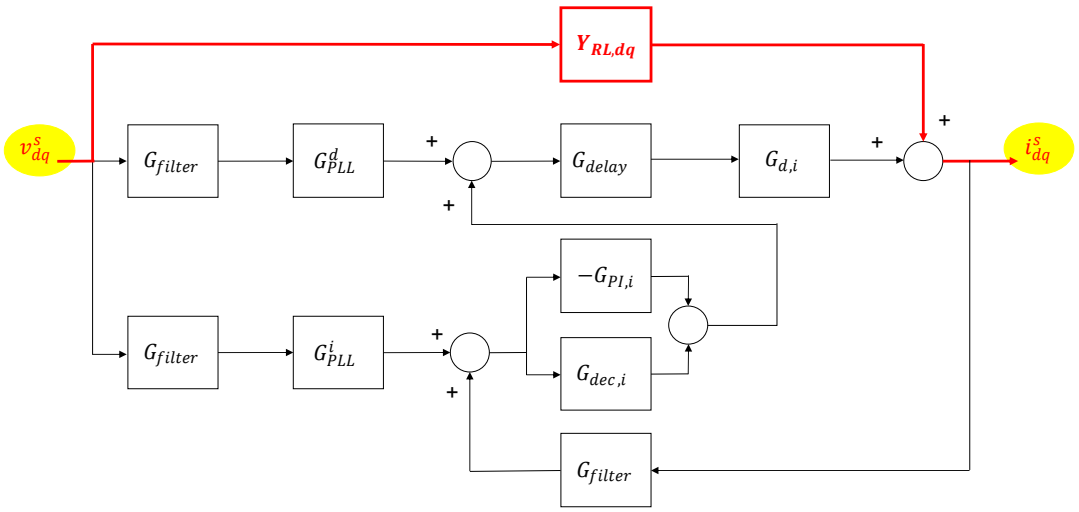

Figure 2.6: Output Impedence without PLL influences and no current feedback.

axis. The module was set in "*abs*" and not "*dB*", so what is represented is actually the impedance module in [Ω]; the phase is expressed in degrees with a phase wrapping between -180° and +180°. The frequency is expressed in Hz. Having set a switching frequency of 10 kHz, the maximum frequency analyzed is half that frequency: starting from 1 Hz, impedances up to 5000 Hz will be analyzed.
In the case initially analyzed, the impedance can be expressed by simply taking into account the upper branch (Fig. 2.6) of the block diagram obtaining:

$$\begin{bmatrix} \tilde{v}^s_d \\ \tilde{v}^s_q \end{bmatrix} = \begin{bmatrix} Ls + R & -\omega_{grid} \cdot L \\ \omega_{grid} \cdot L & Ls + R \end{bmatrix}^{-1} \cdot \begin{bmatrix} \tilde{i}^s_d \\ \tilde{i}^s_q \end{bmatrix} \tag{2.34}$$

$$\tilde{\mathbf{v}}^s = \mathbf{Y}^{-1}_{RL,dq} \cdot \tilde{\mathbf{i}}^s$$

$$\frac{\tilde{\mathbf{v}}^s}{\tilde{\mathbf{i}}^s} = \mathbf{Z}_{O-L} = \mathbf{Y}^{-1}_{RL,dq} \tag{2.35}$$

Starting the Matlab calculation with the parameters in the table and the formula above, the results obtained are those presented in Fig. 2.7.

The results in this case are independent of the direction given to the (d,q) currents imposed and it can be observed that, with increasing frequency, the impedances dd and qq change from a resistive behavior to an inductive behavior by increasing the module and going from phase 0° to phase 90°. The impedances

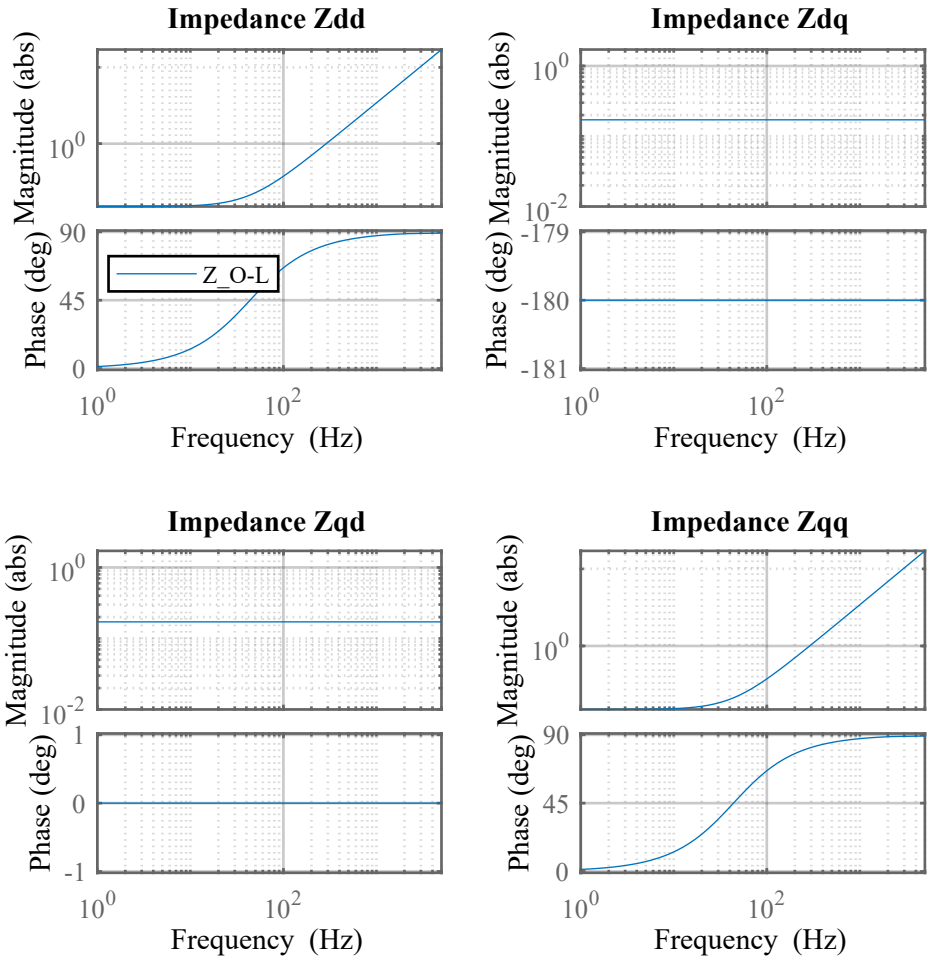

Figure 2.7: Output Impedence without PLL influence and no current feedback.

dq and *qd* are instead constant and proportional to the output inductance and the frequency of the power grid.

2.2.2 Impedances at Open Current-Loop WITH PLL dynamic

If the second branch is also considered (Fig. 2.8), in addition to the output impedance of the converter, the influence of the PLL on the duty cycles of the system is also taken into consideration.

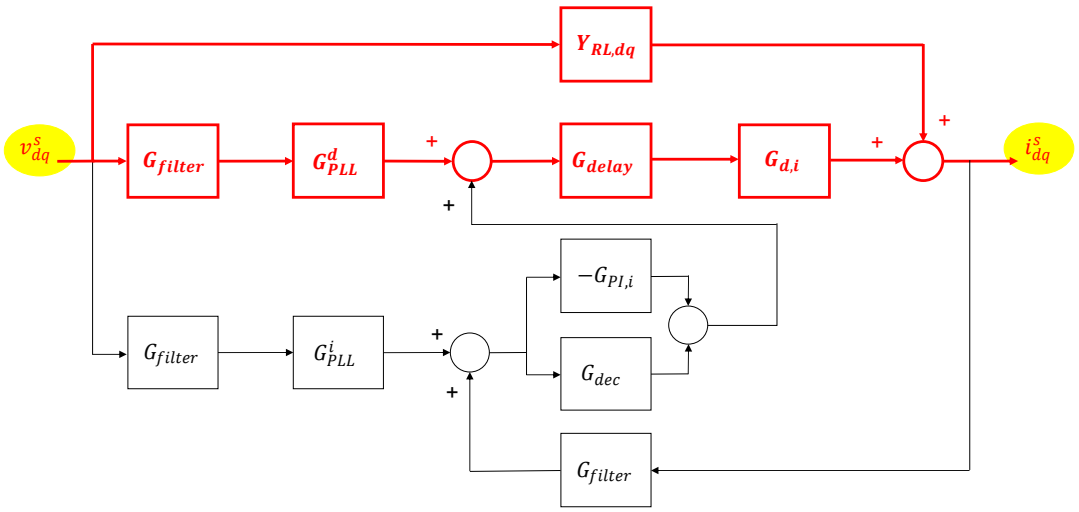

Figure 2.8: Output Impedence with PLL influences and no current feedback.

The matrices $\mathbf{G}_{d,i}$, $\mathbf{G}^d_{PLL}$ and $\mathbf{G}_{delay}$, in addition to the matrix that expresses the conditioning of the analog voltage signals, are considered in the formula, which becomes more complex. Also, having now to consider a system of several matrices that interface the output Small-Signal currents with the input Small-Signal voltages in the block diagram, the order in which the multiplication operations are indicated is important: in this case, for example, the Small-Signal voltages are conditioned by the filter before being multiplied by the $\mathbf{G}^d_{PLL}$ matrix. In this case the expression for the impedance can be written as follows:

$$\begin{aligned} \tilde{\mathbf{i}}^s &= \mathbf{Y}_{RL,dq}\tilde{\mathbf{v}}^s + \left(\mathbf{G}_{d,i}\mathbf{G}_{delay}\mathbf{G}^d_{PLL}\mathbf{G}_{filter}\right)\cdot\tilde{\mathbf{v}}^s \\ \frac{\tilde{\mathbf{v}}^s}{\tilde{\mathbf{i}}^s} &= \mathbf{Z}_{O-L,PLL} = \left(\mathbf{Y}_{RL,dq} + \mathbf{G}_{d,i}\mathbf{G}_{delay}\mathbf{G}^d_{PLL}\mathbf{G}_{filter}\right)^{-1} \end{aligned} \tag{2.36}$$

So in this case the output impedance depends on the values of the average duty cycles $D_{q,d}$, that can be computed as:

$$\begin{aligned} D_d &= V_d + R_f \cdot I_d - \omega_{grid} \cdot L_f \cdot I_q \\ D_q &= V_q + R_f \cdot I_q + \omega_{grid} \cdot L_f \cdot I_d \end{aligned} \tag{2.37}$$

The impedance therefore depends on the sign and the intensity of the current

imposed on the d axis and the q axis as well as on the V_d and V_q values. Table 2.3 shows the values of the variables inside the matrices if the AFE works as a three-phase rectifier, and therefore absorbs power from the electric grid, or if it works as an inverter connected to the grid, and therefore operates as a generator feeding the power grid.

Table 2.3: Rectifier and Generator parameters

Rectifier Parameter	**Value**	**Generator Parameter**	**Value**
V_d	$120\sqrt{2}$ V	V_d	$120\sqrt{2}$ V
V_d	0 V	V_d	0 V
I_d	10 A	I_d	-10 A
I_q	0 A	I_q	0 A
D_d	0.4627	D_d	0.4546
D_q	0.0046	D_q	-0.0046

Once the parameters which define the two different AFE functions are highlighted, the formula 2.36 can be applied to calculate the new impedance, always in an open current loop, in the two cases. The results computed on Matlab are shown in figures 2.9 and 2.10: the new impedances calculated with 2.36 are indicated with $Z_O - L, PLL$ and confronted with $Z_O - L$, previously calculated with (2.35).

As can can be seen, the diagonal impedances dd and qq deviate from the resistive-inductive behavior at low frequencies while they return to coincide with it as the frequency rises. The non-diagonal terms, dq and qd, generally have a very low impedance value deriving from a weak coupling between the d and q axes.

2.2.3 Impedances at Closed Current-Loop WITH PLL Dynamic

Closing the current loop we consider the whole transfer function between $\tilde{\mathbf{i}}^s$ and $\tilde{\mathbf{v}}^s$ (Fig. 2.5). Considering within the formula also the matrices of the current control and the influence of the PLL on the currents themselves will affect the output impedances arriving to a first result.
The analytical transfer function used to calculate the impedance of the converter in the (d,q) reference frame will be calculated below.

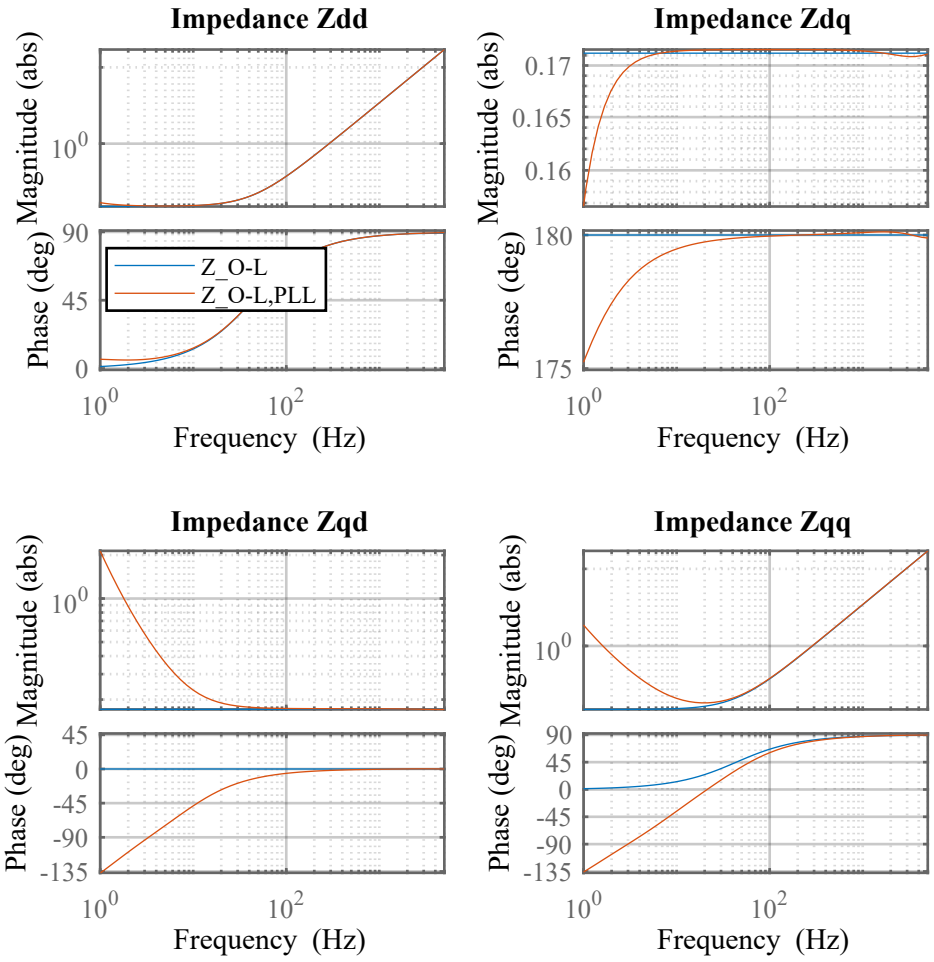

Figure 2.9: Comparison between output Impedence with and without PLL influences and no current feedback when the converter works as a Rectifier.

$$\tilde{\mathbf{i}}^s = \mathbf{Y}_{RL,dq}\tilde{\mathbf{v}}^s + \mathbf{G}_{d,i}\mathbf{G}_{delay}\cdot \left[\mathbf{G}^d_{PLL}\mathbf{G}_{filter}\cdot\tilde{\mathbf{v}}^s + (\mathbf{G}_{dec}-\mathbf{G}_{PI,i})\cdot\left(\mathbf{G}^i_{PLL}\mathbf{G}_{filter}\cdot\tilde{\mathbf{v}}^s + \mathbf{G}_{filter}\cdot\tilde{\mathbf{i}}^s\right)\right]$$

$$\tilde{\mathbf{i}}^s = \mathbf{Y}_{RL,dq}\tilde{\mathbf{v}}^s + \mathbf{G}_{d,i}\mathbf{G}_{delay}\mathbf{G}^d_{PLL}\mathbf{G}_{filter}\cdot\tilde{\mathbf{v}}^s + \mathbf{G}_{d,i}\mathbf{G}_{delay}(\mathbf{G}_{dec}-\mathbf{G}_{PI,i})\cdot \cdot\mathbf{G}^i_{PLL}\mathbf{G}_{filter}\cdot\tilde{\mathbf{v}}^s + \mathbf{G}_{d,i}\mathbf{G}_{delay}(\mathbf{G}_{dec}-\mathbf{G}_{PI,i})\mathbf{G}_{filter}\cdot\tilde{\mathbf{i}}^s$$

$$\frac{\tilde{\mathbf{v}}^s}{\tilde{\mathbf{i}}^s} = \mathbf{Z}_{Closed-Loop} = \frac{\mathbf{1}-\mathbf{G}_{d,i}\mathbf{G}_{delay}(\mathbf{G}_{dec}-\mathbf{G}_{PI,i})\mathbf{G}_{filter}}{\mathbf{Y}_{RL,dq}+\mathbf{G}_{d,i}\mathbf{G}_{delay}\left(\mathbf{G}^d_{PLL}+(\mathbf{G}_{dec}-\mathbf{G}_{PI,i})\mathbf{G}^i_{PLL}\right)\mathbf{G}_{filter}} \quad (2.38)$$

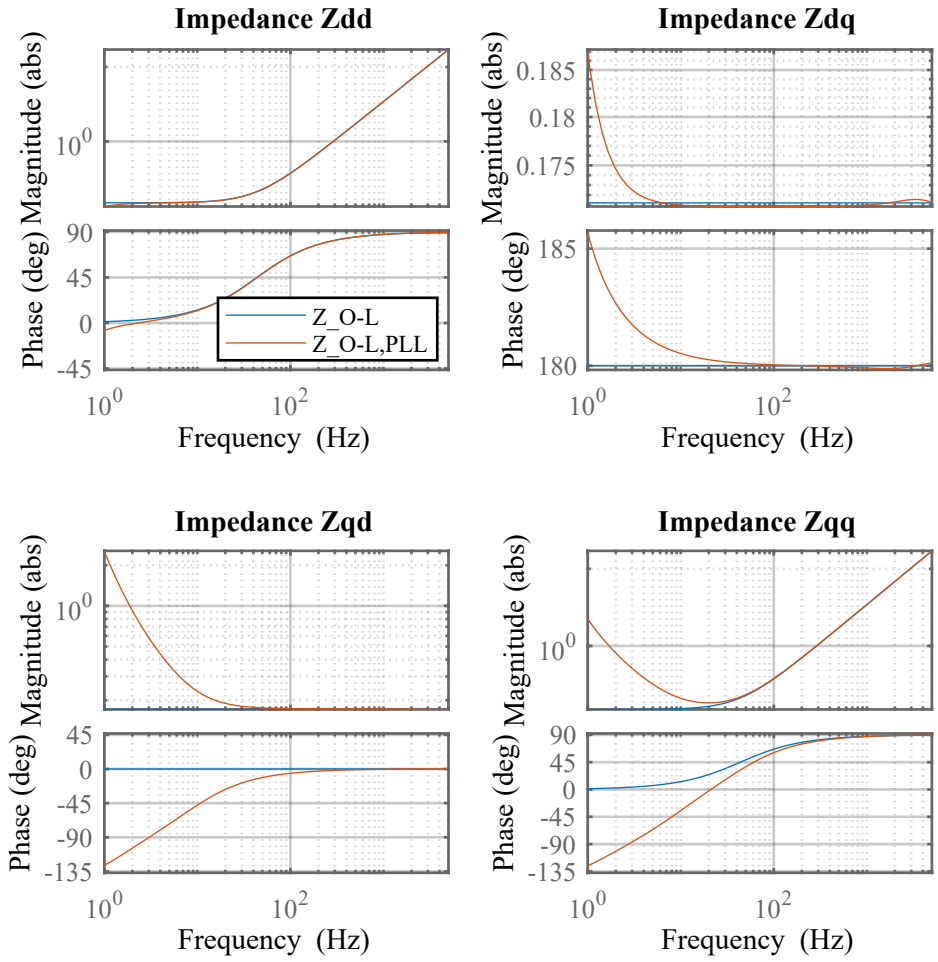

Figure 2.10: Comparison between output Impedence with and without PLL influences and no current feedback when the converter works as a Generator.

From this with a Matlab script the impedance is computated and compared with the previous ones to highlight the differences at each step and the evolution of the results, which corresponds to a heavier computational burden.

As can be seen from Fig. 2.11 and 2.12, the non-diagonal impedances have a module that remains very small compared to the impedances *dd* and *qq* which, even at low frequencies, received an increment in both cases. Z_{dq} and Z_{qd} are small in the frequency range analyzed as a unit power factor is being used for these tests.

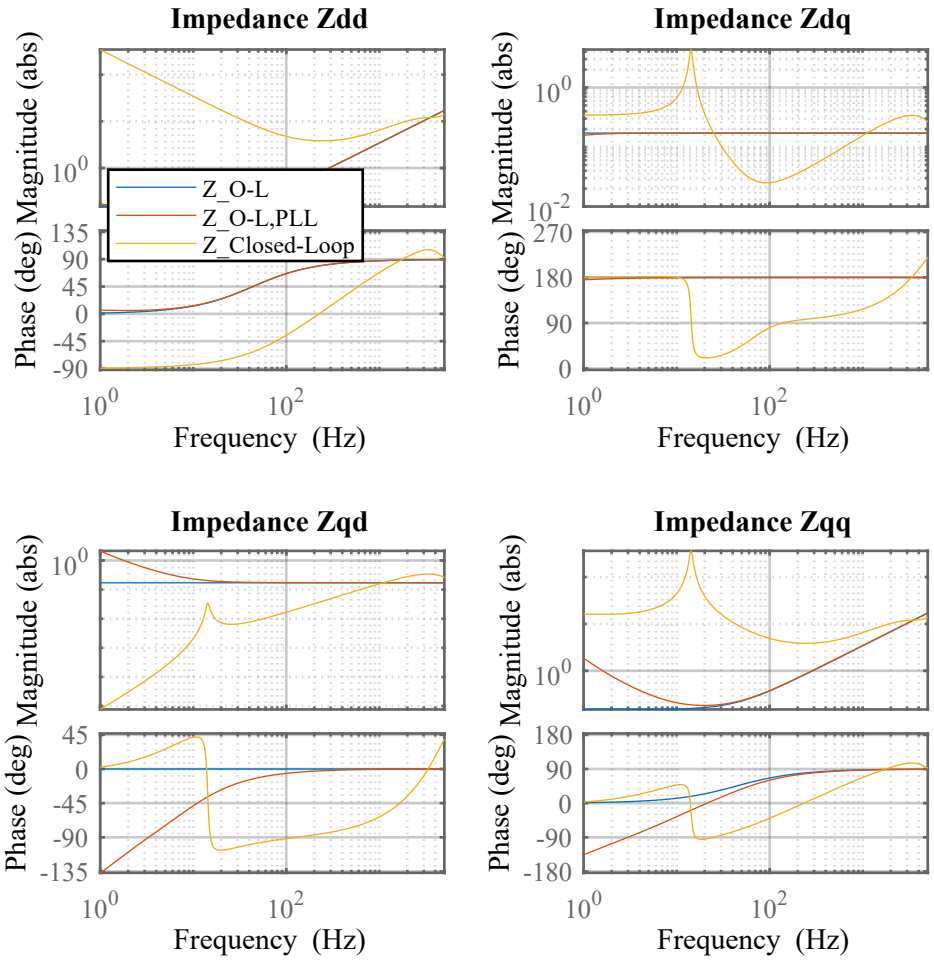

Figure 2.11: Comparison between output Impedence with and without PLL influences and Open Current-Loop/Closed Current-Loop when the converter works as a Rectifier.

They are also further decreased by the presence of decoupling in the current control, which has in fact the objective of reducing the coupling between the two axes. Z_{dd} shows the behavior of the current source: at low frequencies it is greatly influenced by the integrative part of the PI controller and has therefore a delayed phase of 90°, while at high frequencies it has an inductive type behavior due to the output impedance of the converter. The important thing to notice is that, while

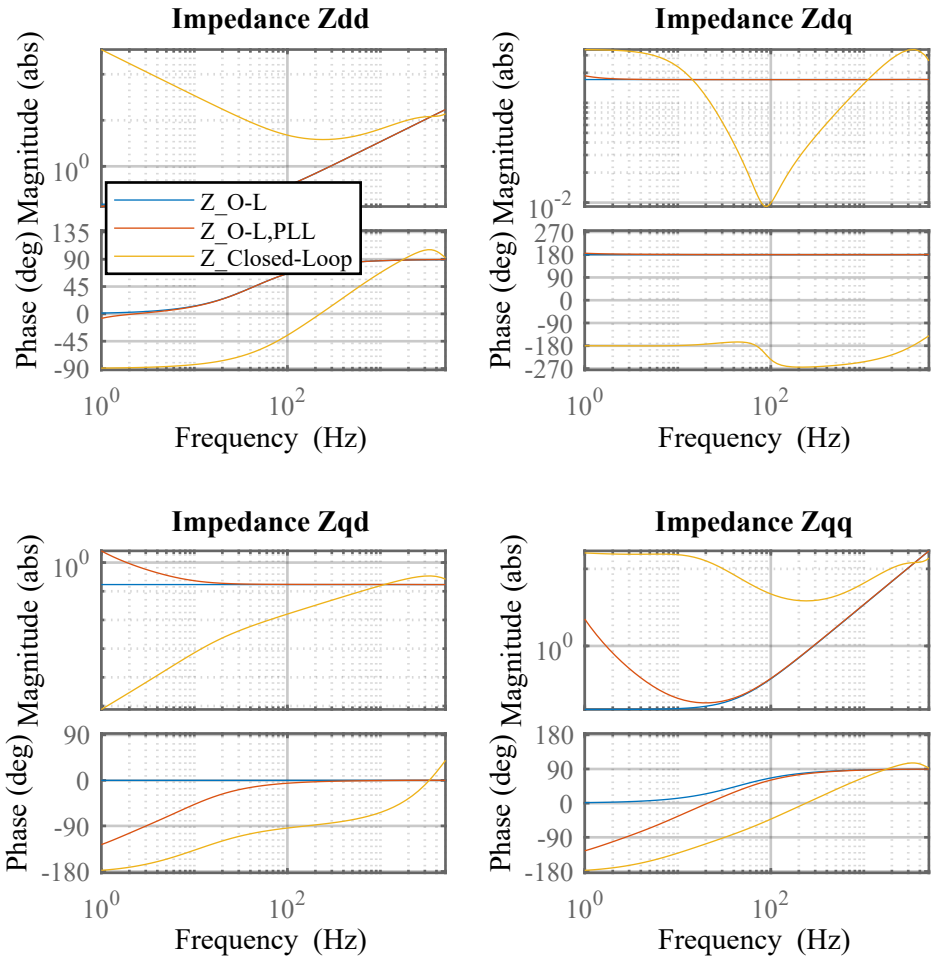

Figure 2.12: Comparison between output Impedence with and without PLL influences and Open Current-Loop/Closed Current-Loop when the converter works as a Generator.

the impedance Z_{dd} both in generator mode and in rectifier mode, has a initial capacitive behavior and then comes to have inductive behavior for high frequencies, the impedance Z_{qq} has two very different behaviors if the converter is absorbing current or if it is injecting current into the grid. While in rectifier mode the phase of Z_{qq} is always between -90° and +90°, making it comparable with something related to the physical system. If the converter is used to inject power into the grid the impedance Z_{qq} has an incremental negative resistive behaviour, which is something

that does not exists as a physical electrical object. This type of behaviour could lead to system instability: the negative resistance behaviour, together with a weak grid, can lead to a negative resistance oscillator so that, for a voltage small-signal, entering the converter at the PCC, the oscillation amplitude and energy grow exponentially with time forcing the control current loop to open at some point, as it exited the range of controllability, causing a system shoutdown.
The converter can also perform the function of supporting the grid when it requires to absorb or to dispose of reactive power. During these requests, the converter must produce a non-null I_q current with a sign that depends on the application. The impedances computed in the two converter functioning cases are shown below, Fig. 2.13 and Fig. 2.14, differentiating according to the value and sign of the current required on the q axis. The blu line shows the behaviour of the system when I_q is set to zero, the red line shows the case in which the converter absorbs reactive power into the grid and lastly the yellow line shows the impedances when the converter injects reactive power.

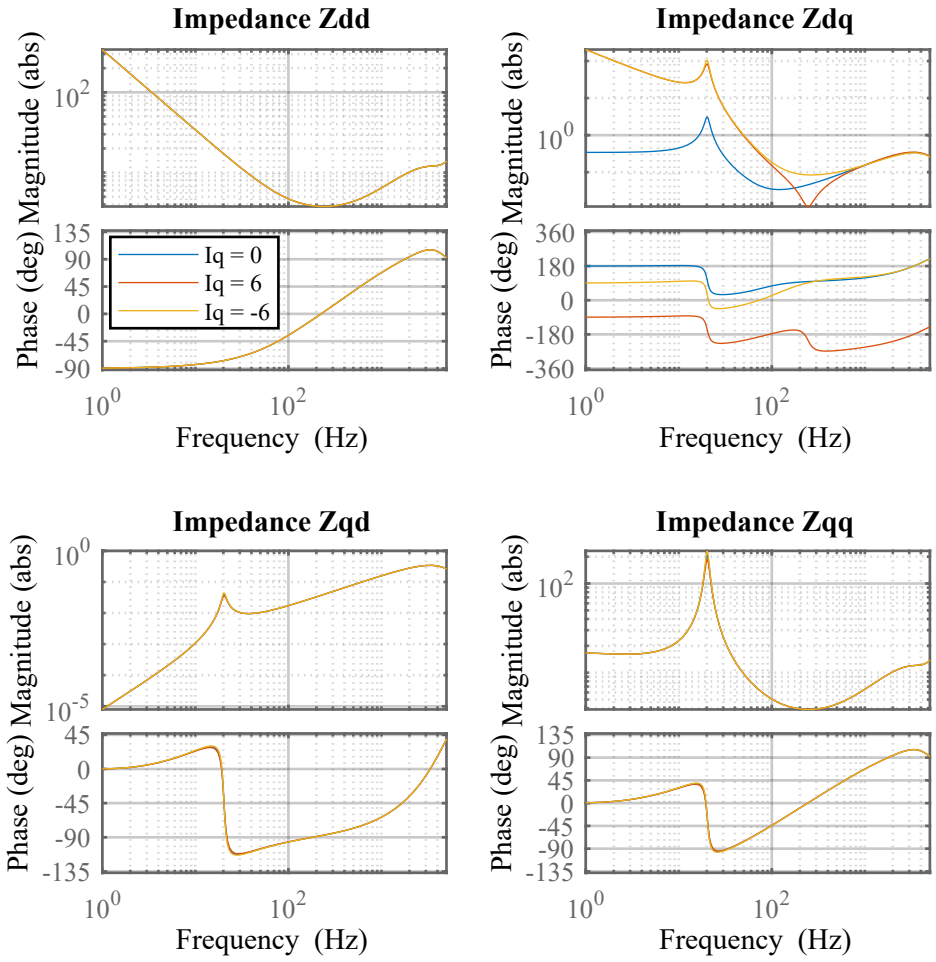

Figure 2.13: Comparison between output Impedence with Closed Current-Loop with different I_q when the converter works as a Rectifier.

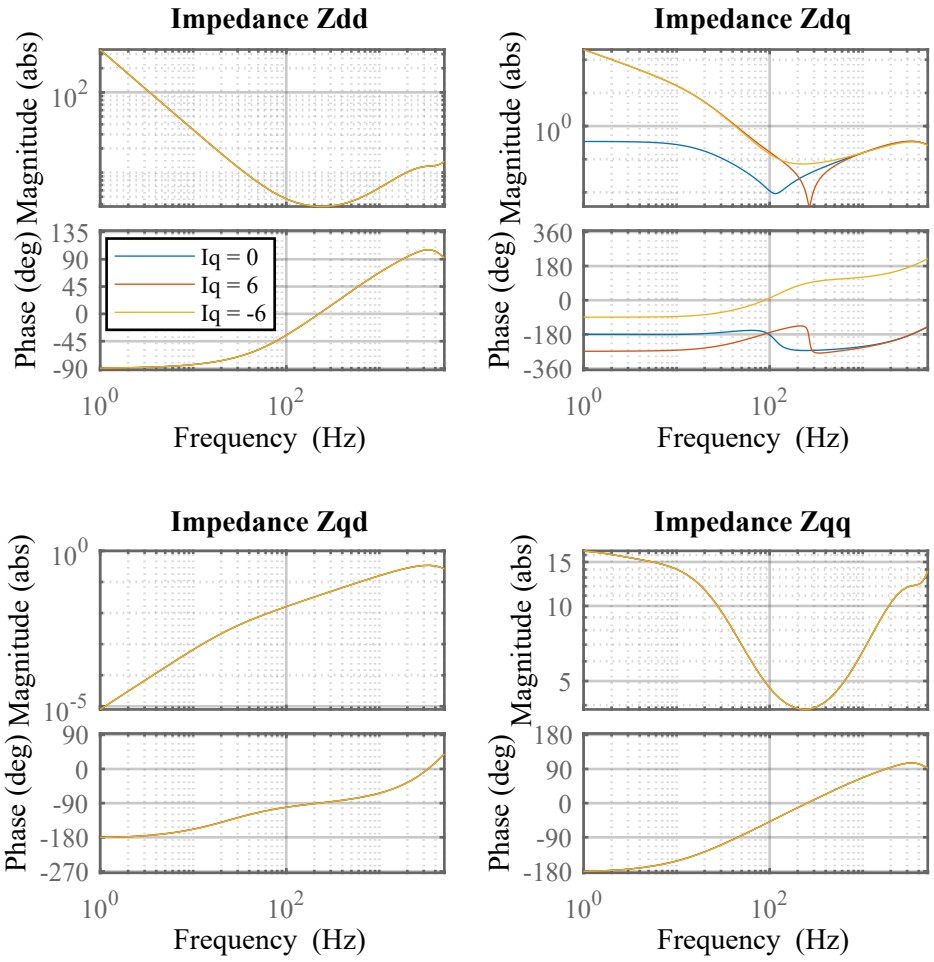

Figure 2.14: Comparison between output Impedence with Closed Current-Loop with different I_q when the converter works as a Generator.

It is possible to note that, as previously mentioned, in the both cases with unit power factor, the impedances Z_{dq} and Z_{qd} are both very small in module with respect to the other two. When I_q module rises the Z_{dq} impedance tends to be higher a low frequencies: while the rest of the impedances are unaffected by this effect, the cross coupling term Z_{dq} increases becoming of the same magnitude order as Z_{dd} and Z_{qq}.

2.2.4 Influence of the PLL Bandwidth on the Output Impedance

In this section we want to see how the PLL affects the different impedances of the converter in (d,q) reference frame. For this reason, several bandwidths have been used to obtain the PI values within the PLL and the results are shown below (Fig. 2.15 and Fig. 2.16).

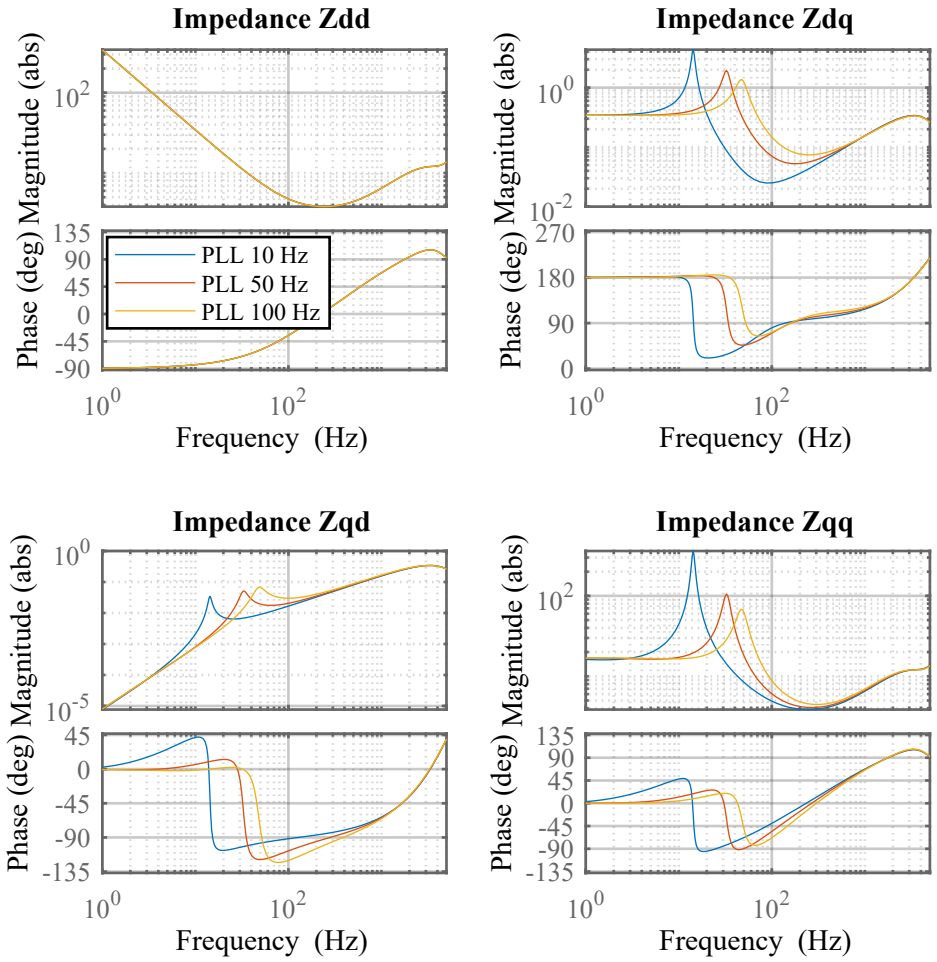

Figure 2.15: Comparison between output Impedence with Closed Current-Loop with different PLL bandwidths when the converter works as a Rectifier.

It is possible to notice that the PLLs with higher bandwidths, although they are faster and therefore, intuitively, the best for following the voltage vector on the

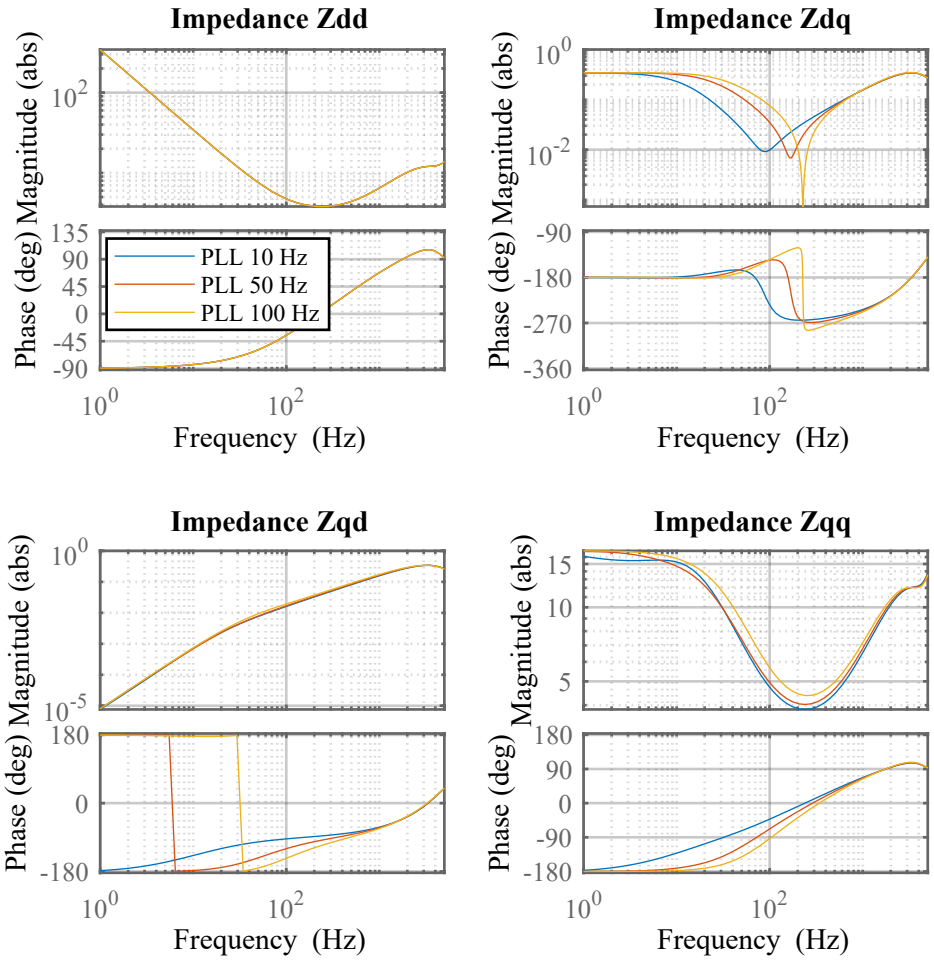

Figure 2.16: Comparison between output Impedence with Closed Current-Loop with different PLL bandwidths when the converter works as a Generator.

PCC, have a negative influence on the behavior of the converter regarding Small-Signal disturbances. In fact, the higher the PLL band, the more the impedance Z_{qq} will have a wider region in which it will act as a negative incremental resistance, when the AFE is asked to inject power into the grid.

As for the other impedances, the impedance Z_{dd} is not altered, while the two coupling impedances Z_{dq} and Z_{qd} do not change their shape much depending on the PLL: they remain of negligible magnitude compared to the others, when unit power factor is required, and their phase undergoes a shift to the right similar to

that of the Z_{qq}.

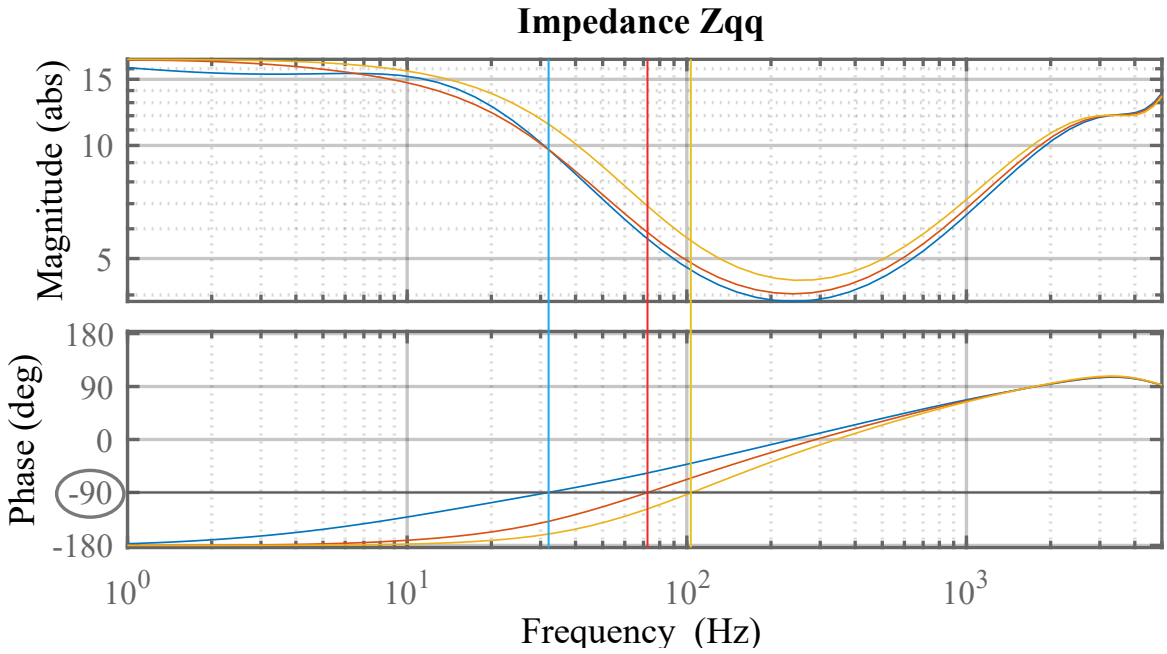

Figure 2.17: Impedance Z_{qq} with different PLL bandwidths when the converter works as a Generator.

As can be seen in Fig. 2.17, while the magnitude of the impedance depends mostly on the power rating of the AFE, when the PLL bandwidth is set to 10 Hz it is possible to observe how the point where the phase reaches -90° is around 30 Hz, moreover, the behavior from almost pure negative incremental resistance remains for a very reduced frequency spectrum. With a bandwidth of 100 Hz, the point where the impedance of the converter returns to having a real part greater than or equal to zero is located at about 100 Hz.

Chapter 3

Analytical Derivation of Equivalent impedance considering also the DC-Link Voltage Loop

3.1 Analytical Derivation of Blocks

If, in addition to the current loop, the converter also has a slower external voltage loop, to manage the voltage levels on the DC-Link and keep them constant, some of the matrices identified in the previous chapter will be modified. At the end of the introduction, the average equivalent circuit for the study of the propagation of Small-Signals was introduced, Fig. 1.11: that circuit already included the voltage control and represents what will be taken into account for this analysis. In this case, however, contrary to what is done with the internal current loop only, Fig. 2.1, the $\tilde{v}_{DC}$ will not be forced to zero obtaining a Small-Signal variation on the voltage on the DC-Link: this will introduce the capacitive dynamics inside the system study.

3.1.1 Link Between Voltages and Currents Considering the DC-Link Dynamics

The matrix that relates the voltages on the (d,q) axes to the currents on the (d,q) axis can be found like before: forcing the small-signals of the duty cycles $\tilde{d}_{d,q}$ to zero, only considering the $\tilde{v}_{DC}$ this time. By forcing $\tilde{d}_{d,q}$ to zero we obtain that on the left circuit (Fig. 1.11), among the four controlled generators, only two remain and the equation can be expressed in the Laplace domain as follows:

$$\tilde{v}_{DC} = \frac{R_{DC}}{R_{DC}C_{DC}s + 1}\left(\tilde{i}_d D_d + \tilde{i}_q D_q\right) \tag{3.1}$$

The two equations of the two right circuits are instead expressed as:

$$\tilde{v}_d = \tilde{v}_{DC}D_d + L\tilde{i}_d + R\tilde{i}_d - \omega_{grid}L\tilde{i}_q \tag{3.2}$$

$$\tilde{v}_q = \tilde{v}_{DC}D_q + L\tilde{i}_q + R\tilde{i}_q + \omega_{grid}L\tilde{i}_d \tag{3.3}$$

Substituting (3.1) into (3.2) and (3.3) we obtain a relationship between the voltages and currents in (d,q) reference frame that is independent from the duties $\tilde{d}_{d,q}$ and in which is included the dynamics on the capacitive DC-Link. For simplicity, the expression $\left(\frac{R_{DC}}{R_{DC}C_{DC}s+1}\right)$ has been abbreviated with Z_P.

$$\begin{bmatrix}\tilde{v}_d\\ \tilde{v}_q\end{bmatrix} = \begin{bmatrix}Ls + R + D_d^2 Z_P & D_d D_q Z_P - \omega_{grid}L\\ D_d D_q Z_P + \omega_{grid}L & Ls + R + D_q^2 Z_P\end{bmatrix}\begin{bmatrix}\tilde{i}_d\\ \tilde{i}_q\end{bmatrix} \tag{3.4}$$

Like in the case where $\tilde{v}_{DC}$ was not considered, being what binds voltages and currents in the (d,q) reference frame, this matrix has the form of an impedance (or an admittance).

$$\mathbf{Z}_{dq} = \begin{bmatrix}Ls + R + D_d^2 Z_P & D_d D_q Z_P - \omega_{grid}L\\ D_d D_q Z_P + \omega_{grid}L & Ls + R + D_q^2 Z_P\end{bmatrix} \tag{3.5}$$

$$\mathbf{Y}_{dq} = \begin{bmatrix} Ls + R + D_d^2 Z_P & D_d D_q Z_P - \omega_{grid} L \\ D_d D_q Z_P + \omega_{grid} L & Ls + R + D_q^2 Z_P \end{bmatrix}^{-1} =$$

$$= \frac{1}{det(\mathbf{Z}_{dq})} \begin{bmatrix} Ls + R + D_q^2 Z_P & -\left(D_d D_q Z_P + \omega_{grid} L\right) \\ -\left(D_d D_q Z_P - \omega_{grid} L\right) & Ls + R + D_d^2 Z_P \end{bmatrix} \tag{3.6}$$

with $det(\mathbf{Z}_{dq})$ equal to $(R + Ls + Z_P D_d^2)\left(R + Ls + Z_P D_q^2\right) - \left[\left(Z_P D_d D_q\right)^2 - \left(\omega_{grid} L\right)^2\right]$

3.1.2 Link Between Duty Cycles and Currents Considering the DC-Link Dynamics

To obtain the relationship between the duty cycles $\tilde{d}_{d,q}$ and the system currents $\tilde{i}_{d,q}$ in this case, as said before, $\tilde{v}_{DC}$ is not set to zero. This leads, for both right circuits (Fig. 1.11), to have the controlled generators $D_d \tilde{v}_{DC}$ and $D_q \tilde{v}_{DC}$ to be taken into account for the computations. Is always true however that the output voltages $\tilde{v}_d$ and $\tilde{v}_q$ are set to zero to get $\mathbf{G}_{d,i}$. The equations to be considered in Laplace domain are:

$$\tilde{d}_d V_{DC} + D_d \tilde{v}_{DC} + L\tilde{i}_d s + R\tilde{i}_d - \omega_{grid} L\tilde{i}_q = 0 \tag{3.7}$$

$$\tilde{d}_q V_{DC} + D_q \tilde{v}_{DC} + L\tilde{i}_q s + R\tilde{i}_q + \omega_{grid} L\tilde{i}_d = 0 \tag{3.8}$$

$$\tilde{v}_{DC} = \frac{R_{DC}}{R_{DC} C_{DC} s + 1}\left(\tilde{d}_d I_d + \tilde{d}_q I_q + \tilde{i}_d D_d + \tilde{i}_q D_q\right) \tag{3.9}$$

Substituting the last equation in the first two we obtain the following system:

$$\begin{aligned} &\tilde{d}_d\left(V_{DC} + D_d I_d Z_P\right) + \tilde{d}_q\left(I_q D_d Z_P\right) + \tilde{i}_d\left(Ls + R + D_d^2 Z_P\right) + \tilde{i}_q\left(D_d D_q Z_P - \omega_{grid} L\right) = 0 \\ &\tilde{d}_q\left(V_{DC} + D_q I_q Z_P\right) + \tilde{d}_d\left(I_d D_q Z_P\right) + \tilde{i}_q\left(Ls + R + D_q^2 Z_P\right) + \tilde{i}_d\left(D_d D_q Z_P + \omega_{grid} L\right) = 0 \end{aligned} \tag{3.10}$$

with Z_P being $\left(\frac{R_{DC}}{R_{DC}C_{DC}s+1}\right)$, as before. Thanks to (3.10) the system can be rewritten in matrix form as:

$$\begin{bmatrix} V_{DC}+D_dI_dZ_P & I_qD_dZ_P \\ I_qD_dZ_P & V_{DC}+D_qI_qZ_P \end{bmatrix} \begin{bmatrix} \tilde{d}_d \\ \tilde{d}_q \end{bmatrix} = \\ = -\begin{bmatrix} Ls+R+D_d^2Z_P & D_dD_qZ_P-\omega_{grid}L \\ D_dD_qZ_P+\omega_{grid}L & Ls+R+D_q^2Z_P \end{bmatrix} \begin{bmatrix} \tilde{i}_d \\ \tilde{i}_q \end{bmatrix} \tag{3.11}$$

And therefore the new $\mathbf{G}_{d,i}$, in which the non-ideality of the DC side is taken into account, can be written as:

$$\mathbf{G}_{d,i} = -\begin{bmatrix} Ls+R+D_d^2Z_P & D_dD_qZ_P-\omega_{grid}L \\ D_dD_qZ_P+\omega_{grid}L & Ls+R+D_q^2Z_P \end{bmatrix}^{-1} \cdot \begin{bmatrix} V_{DC}+D_dI_dZ_P & I_qD_dZ_P \\ I_qD_dZ_P & V_{DC}+D_qI_qZ_P \end{bmatrix}$$

$$\mathbf{G}_{d,i} = -\mathbf{Y}_{dq} \cdot \begin{bmatrix} V_{DC}+D_dI_dZ_P & I_qD_dZ_P \\ I_qD_dZ_P & V_{DC}+D_qI_qZ_P \end{bmatrix} \tag{3.12}$$

It is also possible to observe that when the source on the DC-link is ideally replaced with an ideal voltage source, by making the capacitance a $+\infty$, the term Z_P tends to zero and the two $\mathbf{G}_{d,i}$ and $\mathbf{Y}_{RL,dq}$ matrices return to be equal to the previous ones.

$$\mathbf{Z}_{dq} = \begin{bmatrix} Ls+R+D_d^2\cdot 0 & D_dD_q\cdot 0-\omega_{grid}L \\ D_dD_q\cdot 0+\omega_{grid}L & Ls+R+D_q^2\cdot 0 \end{bmatrix} = \begin{bmatrix} Ls+R & -\omega_{grid}L \\ \omega_{grid}L & Ls+R \end{bmatrix} = \mathbf{Z}_{RL,dq} \tag{3.13}$$

$$\mathbf{Y}_{dq} = \begin{bmatrix} Ls + R + D_d^2 \cdot 0 & D_d D_q \cdot 0 - \omega_{grid} L \\ D_d D_q \cdot 0 + \omega_{grid} L & Ls + R + D_q^2 \cdot 0 \end{bmatrix}^{-1} =$$

$$= \begin{bmatrix} Ls + R & -\omega_{grid} L \\ \omega_{grid} L & Ls + R+ \end{bmatrix}^{-1} = \frac{1}{(Ls+R)^2 + (\omega_{grid} L)^2} \begin{bmatrix} Ls + R & +\omega_{grid} L \\ -\omega_{grid} L & Ls + R \end{bmatrix} = \mathbf{Y}_{RL,dq}$$

(3.14)

$$\mathbf{G}_{d,i} = - \begin{bmatrix} Ls + R + D_d^2 \cdot 0 & D_d D_q \cdot 0 - \omega_{grid} L \\ D_d D_q \cdot 0 + \omega_{grid} L & Ls + R + D_q^2 \cdot 0 \end{bmatrix}^{-1} \cdot \begin{bmatrix} V_{DC} + D_d I_d \cdot 0 & I_q D_d \cdot 0 \\ I_q D_d \cdot 0 & V_{DC} + D_q I_q \cdot 0 \end{bmatrix} =$$

$$= - \begin{bmatrix} Ls + R \cdot 0 & -\omega_{grid} L \\ \omega_{grid} L & Ls + R \end{bmatrix}^{-1} \cdot V_{DC} \begin{bmatrix} 1 & 0 \\ 0 & 1 \end{bmatrix} =$$

$$-V_{DC} \begin{bmatrix} Ls + R \cdot 0 & -\omega_{grid} L \\ \omega_{grid} L & Ls + R \end{bmatrix}^{-1} = -\frac{V_{DC}}{(Ls+R)^2 + (\omega \cdot L)^2} \begin{bmatrix} Ls + R & +\omega_{grid} \cdot L \\ -\omega_{grid} \cdot L & Ls + R \end{bmatrix}$$

(3.15)

In this case (3.13) corresponds to (2.5), (3.14) corresponds to (2.4) and (3.15) corresponds to (2.9).

3.1.3 Link Between DC-Link Voltage and the D-Q Voltages

Now we need to find what binds the Small-Signal voltage variations in the (d,q) reference frame and the voltage variation on the DC-Link. Knowing that, to find the two semi-effects of Small-Signal duty cycles and of Small-Signal voltages on Small-Signal currents, the principle of overlapping effects is applied, as regards the effect of the voltages $\tilde{v}_{d,q}$ the Small-Signal variations of duty cycles will be forced to zero. We have a system of three equations as follows:

$$\tilde{v}_d = \tilde{v}_{DC} D_d + L\tilde{i}_d + R\tilde{i}_d - \omega_{grid} L\tilde{i}_q \tag{3.16}$$

$$\tilde{v}_q = \tilde{v}_{DC} D_q + L\tilde{i}_q + R\tilde{i}_q + \omega_{grid} L\tilde{i}_d \tag{3.17}$$

$$\tilde{v}_{DC} = \frac{R_{DC}}{R_{DC} C_{DC} s + 1} \left(\tilde{i}_d D_d + \tilde{i}_q D_q \right) \tag{3.18}$$

Those are the same equations used to find the link between the Small-Signal (d,q) voltages and the Samall-Signal (d,q) currents, but will be rearranged in a different way to find the new link.
In this case (3.18) will be rearranged as:

$$\frac{\tilde{v}_{DC} \cdot (R_{DC} C_{DC} s + 1)}{R_{DC}} = \begin{bmatrix} D_d & D_q \end{bmatrix} \begin{bmatrix} \tilde{i}_d \\ \tilde{i}_q \end{bmatrix} \tag{3.19}$$

The other two equations, instead, are rewritten to see on what the Small-Signals currents depend.

$$\begin{aligned} \tilde{v}_d - \tilde{v}_{DC} D_d &= Ls\tilde{i}_d + R\tilde{i}_d - \omega_{grid} L\tilde{i}_q \\ \tilde{v}_q - \tilde{v}_{DC} D_q &= Ls\tilde{i}_q + R\tilde{i}_q + \omega_{grid} L\tilde{i}_d \end{aligned} \tag{3.20}$$

The two expressions can be written in matrix form and rearranged to obtain an expression of the Small-Signal current vector in the (d,q) reference frame.

$$\begin{aligned} \begin{bmatrix} \tilde{v}_d - \tilde{v}_{DC} D_d \\ \tilde{v}_q - \tilde{v}_{DC} D_q \end{bmatrix} &= \begin{bmatrix} Ls + R & -\omega_{grid} L \\ \omega_{grid} L & Ls + R \end{bmatrix} \begin{bmatrix} \tilde{i}_d \\ \tilde{i}_q \end{bmatrix}; \\ \begin{bmatrix} \tilde{i}_d \\ \tilde{i}_q \end{bmatrix} &= \begin{bmatrix} Ls + R & -\omega_{grid} L \\ \omega_{grid} L & Ls + R \end{bmatrix}^{-1} \begin{bmatrix} \tilde{v}_d - \tilde{v}_{DC} D_d \\ \tilde{v}_q - \tilde{v}_{DC} D_q \end{bmatrix} \end{aligned} \tag{3.21}$$

Replacing the latter equation inside (3.19) gives the following system:

$$\frac{\tilde{v}_{DC}\cdot(R_{DC}C_{DC}s+1)}{R_{DC}}=\begin{bmatrix}D_d & D_q\end{bmatrix}\cdot\begin{bmatrix}Ls+R & -\omega_{grid}L\\ \omega_{grid}L & Ls+R\end{bmatrix}^{-1}\begin{bmatrix}\tilde{v}_d-\tilde{v}_{DC}D_d\\ \tilde{v}_q-\tilde{v}_{DC}D_q\end{bmatrix}=$$

$$\frac{1}{(Ls+R)^2+(\omega_{grid}L)^2}\cdot\begin{bmatrix}D_d\cdot(Ls+R)-D_q\omega_{grid}L & D_q\cdot(Ls+R)+D_d\omega_{grid}L\end{bmatrix}\cdot$$

$$\cdot\begin{bmatrix}\tilde{v}_d-\tilde{v}_{DC}D_d\\ \tilde{v}_q-\tilde{v}_{DC}D_q\end{bmatrix} \tag{3.22}$$

At this point, is easier to re-transform the matrix system into an equation to isolate the $\tilde{v}_{DC}$ and find an expression of it.

$$\tilde{v}_{DC}\cdot\left(C_{DC}s+\frac{1}{R_{DC}}\right)\cdot(Ls+R)^2+(\omega_{grid}L)^2=$$

$$\tilde{v}_{DC}\left[(Ls+R)\cdot\left(-D_d^2-D_q^2\right)\right]+ \tag{3.23}$$

$$+\tilde{v}_d\left[D_d\left(Ls+R\right)-\omega_{grid}LD_q\right]+\tilde{v}_q\left[D_q\left(Ls+R\right)+\omega_{grid}LD_d\right]$$

This equation can be rearranged to express the $\tilde{v}_{DC}$ as a function of the voltage vector in the (d,q) axes, obtaining what links the two variables of the system.

$$\tilde{v}_{DC}=\frac{1}{\left[\left(C_{DC}s+\frac{1}{R_{DC}}\right)\cdot(Ls+R)^2+(\omega_{grid}L)^2\right]+(Ls+R)\cdot\left(D_d^2+D_q^2\right)}$$

$$\begin{bmatrix}D_d\left(Ls+R\right)-\omega_{grid}LD_q & D_q\left(Ls+R\right)+\omega_{grid}LD_d\end{bmatrix}\begin{bmatrix}\tilde{v}_d\\ \tilde{v}_q\end{bmatrix} \tag{3.24}$$

In order to compose the matrices together in the future so that they will all have the same dimensions (2×2), it was decided to treat $\tilde{v}_{DC}$ as a 2×1 vector with the value in the second row equal to zero. In this way it is possible to write a 2×2 matrix that links the two voltages:

$$\mathbf{G}_{v,v} = \frac{1}{\left[\left(C_{DC}s + \frac{1}{R_{DC}}\right) \cdot (Ls+R)^2 + (\omega_{grid}L)^2\right] + (Ls+R) \cdot \left(D_d^2 + D_q^2\right)} \cdot$$

$$\begin{bmatrix} [D_d\,(Ls+R) - \omega_{grid}LD_q] & [D_q\,(Ls+R) + \omega_{grid}LD_d] \\ 0 & 0 \end{bmatrix} \tag{3.25}$$

3.1.4 Link Between Duty Cycles and DC-Link Voltage

The process is very similar to the one previously seen: in this case, to use the superposition of the effects subsequently, the voltage contributions in the (d,q) reference frame are considered null and instead the contribution of the Small-Signal duty cycles is taken into account. We start from the same equations defined for finding the link between Small-Signal duty cycles and Small-Signal currents.

$$\tilde{d}_d V_{DC} + D_d \tilde{v}_{DC} + L\tilde{i}_d s + R\tilde{i}_d - \omega_{grid} L\tilde{i}_q = 0 \tag{3.26}$$

$$\tilde{d}_q V_{DC} + D_q \tilde{v}_{DC} + L\tilde{i}_q s + R\tilde{i}_q + \omega_{grid} L\tilde{i}_d = 0 \tag{3.27}$$

$$\tilde{v}_{DC} = \frac{R_{DC}}{R_{DC}C_{DC}s + 1}\left(\tilde{d}_d I_d + \tilde{d}_q I_q + \tilde{i}_d D_d + \tilde{i}_q D_q\right) \tag{3.28}$$

As previously done, the equation that expresses the different contributions of $\tilde{v}_{DC}$ is rewritten in matrix form:

$$\tilde{v}_{DC} \cdot \left(C_{DC}s + \frac{1}{R_{DC}}\right) = \begin{bmatrix} I_d & I_q \end{bmatrix} \begin{bmatrix} \tilde{d}_d \\ \tilde{d}_q \end{bmatrix} + \begin{bmatrix} D_d & D_q \end{bmatrix} \begin{bmatrix} \tilde{i}_d \\ \tilde{i}_q \end{bmatrix} \tag{3.29}$$

The other two equations, on the other hand, also written in the form of matrices, are shown below and arranged in such a way to make the vector of the Small-Signal currents in the (d,q) reference frame in evidence.

$$\tilde{d}_d V_{DC} + \tilde{v}_{DC} D_d = -Ls\tilde{i}_d - R\tilde{i}_d + \omega_{grid} L\tilde{i}_q$$

$$\tilde{d}_q V_{DC} + \tilde{v}_{DC} D_q = -Ls\tilde{i}_q - R\tilde{i}_q - \omega_{grid} L\tilde{i}_d$$

$$\begin{bmatrix} \tilde{d}_d V_{DC} + \tilde{v}_{DC} D_d \\ \tilde{d}_q V_{DC} + \tilde{v}_{DC} D_q \end{bmatrix} = - \begin{bmatrix} Ls + R & -\omega_{grid} L \\ \omega_{grid} L & Ls + R \end{bmatrix} \begin{bmatrix} \tilde{i}_d \\ \tilde{i}_q \end{bmatrix}; \tag{3.30}$$

$$\begin{bmatrix} \tilde{i}_d \\ \tilde{i}_q \end{bmatrix} = - \begin{bmatrix} Ls + R & -\omega_{grid} L \\ \omega_{grid} L & Ls + R \end{bmatrix}^{-1} \cdot \begin{bmatrix} \tilde{d}_d V_{DC} + \tilde{v}_{DC} D_d \\ \tilde{d}_q V_{DC} + \tilde{v}_{DC} D_q \end{bmatrix}$$

Substituting (3.30) inside (3.29) the expression that describes the contribution of the Small-Signal duty cycle vector inside the $\tilde{v}_{DC}$ is obtained.

$$\tilde{v}_{DC} \cdot \left(C_{DC} s + \frac{1}{R_{DC}} \right) = \begin{bmatrix} I_d & I_q \end{bmatrix} \begin{bmatrix} \tilde{d}_d \\ \tilde{d}_q \end{bmatrix} +$$

$$+ \begin{bmatrix} D_d & D_q \end{bmatrix} \cdot \frac{-1}{(Ls + R)^2 + (\omega_{grid} L)^2} \begin{bmatrix} Ls + R & +\omega_{grid} L \\ -\omega_{grid} L & Ls + R \end{bmatrix} \cdot \begin{bmatrix} \tilde{d}_d V_{DC} + \tilde{v}_{DC} D_d \\ \tilde{d}_q V_{DC} + \tilde{v}_{DC} D_q \end{bmatrix} \tag{3.31}$$

As previously done, it is more convenient at this point to bring the system back into linear form, perform the calculations, simplify where necessary and then eventually bring the system back to a matrix form.

$$\tilde{v}_{DC} \cdot \left(C_{DC}s + \frac{1}{R_{DC}} \right) = \tilde{d}_d I_d + \tilde{d}_q I_q + \left(\frac{-1}{(Ls+R)^2 + (\omega_{grid}L)^2} \right) \cdot$$

$$\cdot \left\{ \tilde{v}_{DC} \left[(Ls+R) \cdot \left(D_d^2 + D_q^2 \right) \right] \right\} + \left(\frac{-1}{(Ls+R)^2 + (\omega_{grid}L)^2} \right) \cdot$$

$$\cdot \left\{ \tilde{d}_d \left[D_d V_{DC} \left(Ls+R \right) - D_q V_{DC} \omega_{grid} L \right] + \tilde{d}_q \left[D_q V_{DC} \left(Ls+R \right) + D_d V_{DC} \omega_{grid} L \right] \right\}$$

(3.32)

$\tilde{v}_{DC}$ can now be obtained by reporting the system in matrix form, expressing it as a multiplicative term and a 1×2 vector that multiplies the duty cycle vector, a 2×1 vector.

$$\tilde{v}_{DC} \cdot \left\{ C_{DC}s + \frac{1}{R_{DC}} - \left[\frac{-\left(Ls+R\right) \cdot \left(D_d^2 + D_q^2 \right)}{(Ls+R)^2 + (\omega_{grid}L)^2} \right] \right\} = \begin{bmatrix} I_d & I_q \end{bmatrix} \begin{bmatrix} \tilde{d}_d \\ \tilde{d}_q \end{bmatrix} +$$

$$- \frac{V_{DC}}{(Ls+R)^2 + (\omega_{grid} \cdot L)^2} \cdot$$

$$\cdot \begin{bmatrix} \left[D_d \left(Ls+R \right) - D_q \omega_{grid} L \right] & \left[D_q \left(Ls+R \right) + D_d \omega_{grid} L \right] \end{bmatrix} \begin{bmatrix} \tilde{d}_d \\ \tilde{d}_q \end{bmatrix};$$

$$\tilde{v}_{DC} = \frac{1}{\left\{ C_{DC}s + \frac{1}{R_{DC}} - \left[\frac{-\left(Ls+R\right) \cdot \left(D_d^2 + D_q^2 \right)}{(Ls+R)^2 + (\omega_{grid}L)^2} \right] \right\}} \cdot$$

$$\begin{bmatrix} I_d - \frac{V_{DC} \left[D_d \left(Ls+R \right) - D_q \omega_{grid} L \right]}{(Ls+R)^2 + (\omega_{grid} \cdot L)^2} & I_q - \frac{V_{DC} \left[D_q \left(Ls+R \right) + D_d \omega_{grid} L \right]}{(Ls+R)^2 + (\omega_{grid} \cdot L)^2} \end{bmatrix} \begin{bmatrix} \tilde{d}_d \\ \tilde{d}_q \end{bmatrix}$$

(3.33)

As previously mentioned, for simplicity, this matrix will however be treated as a 2×2 which produces a vector of DC components (2×1) with the second component equal to zero. So the matrix that expresses the ratio between the Small-Signal DC

voltage and the Small-Signal (d,q) voltages is expressed as follows:

$$\mathbf{G}_{d,v} = \frac{1}{\left\{ C_{DC}s + \frac{1}{R_{DC}} - \left[\frac{-(Ls+R)\cdot\left(D_d^2 + D_q^2\right)}{(Ls+R)^2 + (\omega_{grid}L)^2} \right] \right\}} \cdot$$

$$\begin{bmatrix} I_d - \frac{V_{DC}\left[D_d\left(Ls+R\right) - D_q\omega_{grid}L\right]}{(Ls+R)^2 + (\omega_{grid}\cdot L)^2} & I_q - \frac{V_{DC}\left[D_q\left(Ls+R\right) + D_d\omega_{grid}L\right]}{(Ls+R)^2 + (\omega_{grid}\cdot L)^2} \\ 0 & 0 \end{bmatrix} \tag{3.34}$$

3.1.5 DC-Link Voltage PI

As regards the PI controller of the voltage loop, it works by attempting to generate an output signal which aim is to keep the voltage on the DC-Link constant at the desired rated value. This output signal is the reference current to be forced in the $d-$axis and therefore, in this case, the reference current will also have a Small-Signal perturbation superimposed on it. The values according to which the PI was calibrated have already been introduced in tables 2.2 and 2.1.
Since there is a single controller to manage the voltage level on the DC-Link, the matrix that binds the reference Small-Signal current, output from the PI, and the Small-Signal DC voltage is as follows:

$$\begin{bmatrix} \tilde{i}_d^{ref} \\ \tilde{i}_q^{ref} \end{bmatrix} = \begin{bmatrix} kp_v + \frac{ki_v}{s} & 0 \\ 0 & 0 \end{bmatrix} \begin{bmatrix} \tilde{v}_{DC} \\ 0 \end{bmatrix} \tag{3.35}$$

As can be seen from the formula presented, the current control imposes only the current reference on the $d-$axis, the reference on the $q-$axis is autonomous and independent from this control.

3.2 Calculated Impedances with the Voltage Loop

The matrices concerning the contributions of the PLL, the delay, the sampling filters and the current PIs are unchanged with respect to the previously analyzed system and therefore have not been obtained again in the previous paragraphs.
Once all the contributions considered have been obtained, it is necessary to find a way to combine them together and obtain a formula to calculate the impedance of the system. In this case also, to minimize errors, we will proceed by adding the different contributions one at a time to gradually arrive at a final solution. Starting from the block diagram previously used for the impedance with current control only (Fig. 2.5), the points where are expressed the Small-Signal voltages and the Small-Signal duty cycles are used: they are respectively multiplied by $\mathbf{G}_{v,v}$ and $\mathbf{G}_{d,v}$ and then added together to obtain, by overlapping the semi-effects, the Small-Signal voltage on the DC-Link. This latter is then sampled via an acquisition filter on the DC-Link and enters the voltage PI. Since we are dealing with a Small-Signal circuit, the reference DC voltage $\tilde{v}_{DC}^{ref}$ is null, as $\tilde{i}_{d,q}^{ref}$ was previously null. The output of the voltage PI becomes the reference of the current PI.
All of this can be represented in a block diagram, as shown in Fig. 3.1.

The problem of the block diagram presented is represented by the impossibility, as it appears, to derive a transfer function: in addition to the Small-Signal current feedback there is another ring within the block diagram. The input of $\mathbf{G}_{delay}$ depends on its output through the newly introduced voltage-loop control, which makes it impossible, starting from this scheme, to find an equation that links input and output considering also the red blocks. For this reason, calculations have been carried out on the blocks in order to avoid other closed rings within the system. The Small-Signal DC voltage reference was first eliminated and the minus of the feedback was integrated with the matrix that describes the voltage PI. The matrix of the current PI and the delay were extracted to better highlight the loop due to the insertion of the current control, Fig 3.2.

The block diagram was then rearranged, Fig 3.3, to better highlight the internal ring created by the insertion of the matrices inherent in the voltage control.

Once you get to this block diagram it is possible, observing it, to extract a link between inputs and outputs. To do this, in such a system it is useful to use the

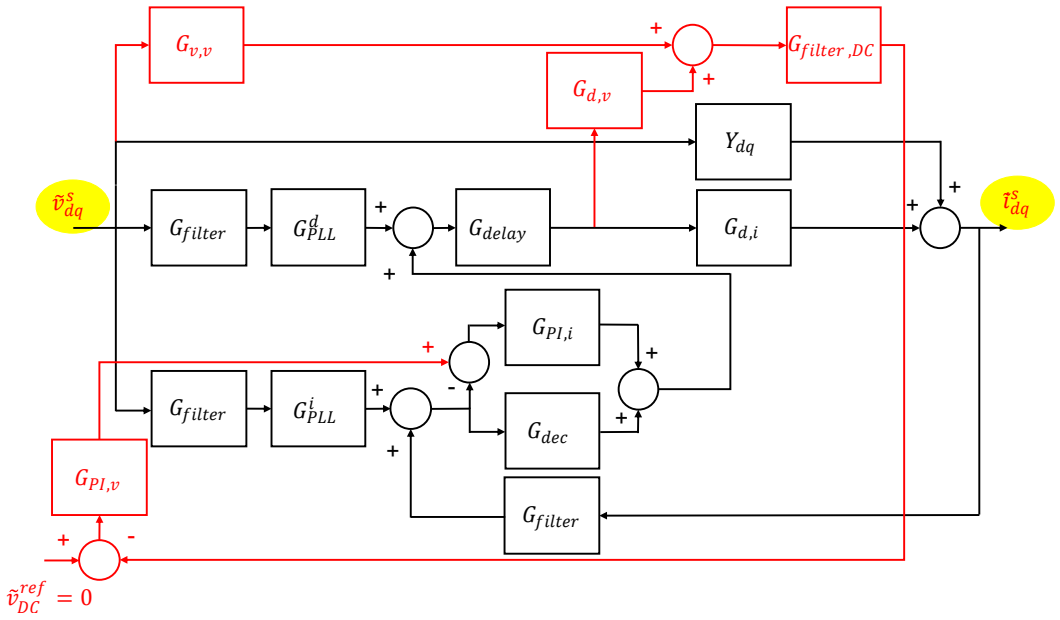

Figure 3.1: Matrix composition of the impedance in (d,q) reference frame considering the voltage-loop contribution (in red).

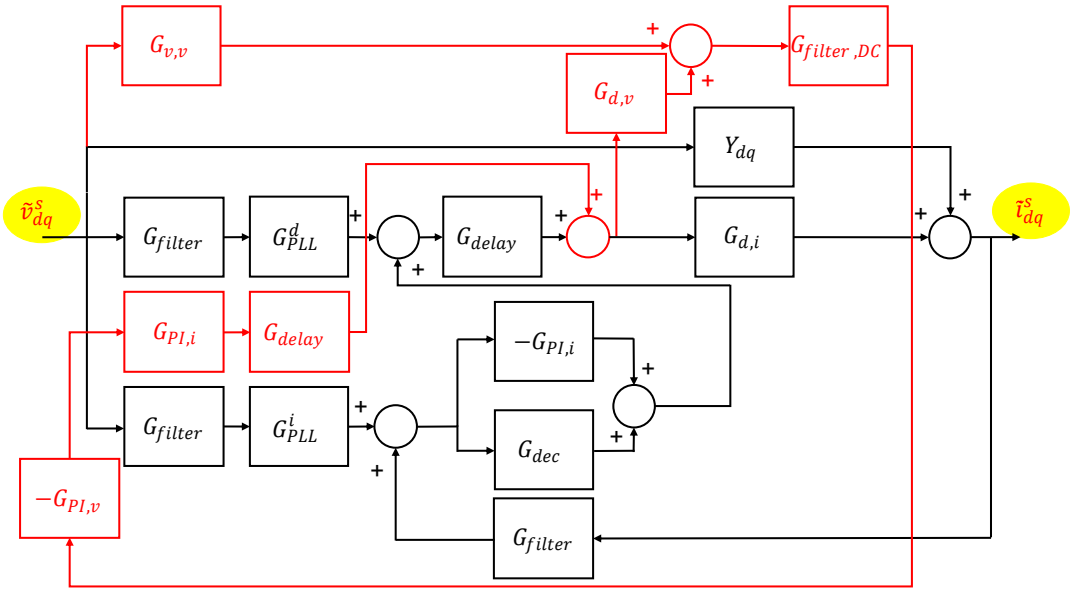

Figure 3.2: Matrix composition of the impedance in (d,q) reference frame considering the voltage-loop contribution (in red).

principle of overlapping effects to obtain the result. In figure Fig. 3.4 a generic block diagram with a single feedback is shown: the transfer function between the

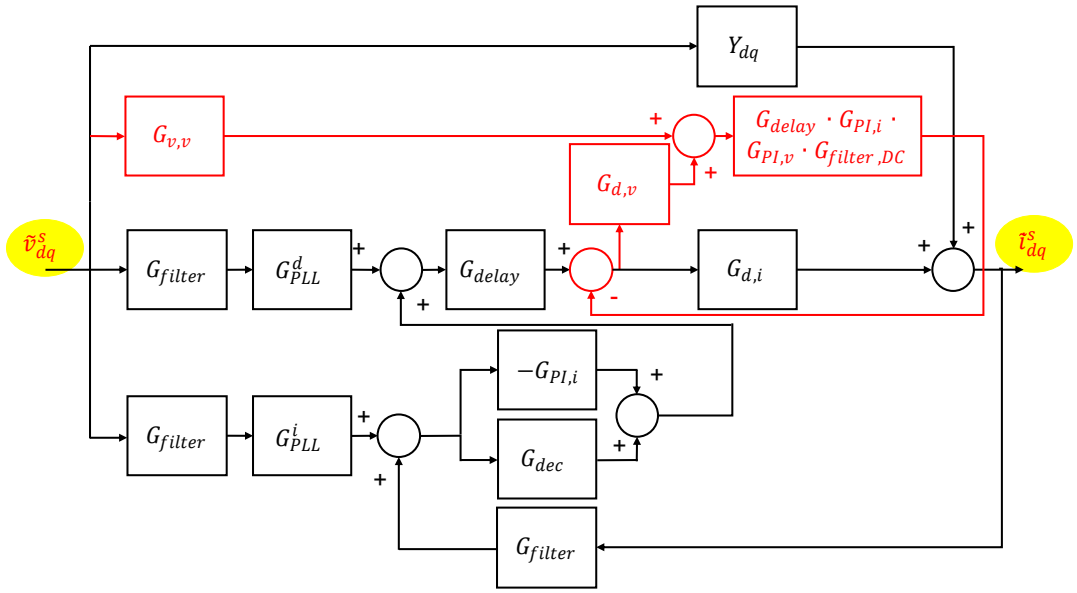

Figure 3.3: Matrix composition of the impedance in (d,q) reference frame considering the voltage-loop contribution (in red).

generic output y and the generic input x in this case is easily calculated and is equal to $\left(\frac{A}{1+A\cdot B}\right)$. To obtain the transfer function, one could proceed by setting the input x to zero first, to see how the output affects itself, and then calculating the transfer function between input and output without feedback. Once the results are obtained in these two conditions they can be put together to obtain the total transfer function of the system.

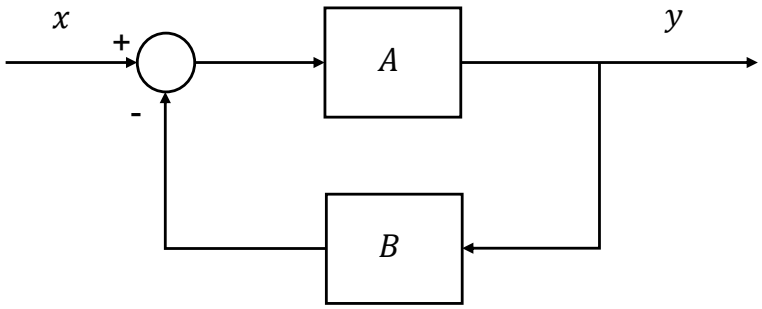

Figure 3.4: Generic transfer function block diagram with feedback.

$$\begin{cases} y &= -y \cdot A \cdot B; \\ y &= x \cdot A; \end{cases} \\ \begin{cases} 0 &= y \cdot (1 + A \cdot B) \\ y &= x \cdot A; \end{cases} \tag{3.36}$$

$$\Rightarrow y \cdot (1 + A \cdot B) = x \cdot A; \\ \frac{y}{x} = \frac{A}{1 + A \cdot B} \tag{3.37}$$

For the system under consideration we can do the same thing: at first we look for the transfer function in case the input is set to zero and the focus is on how the output affects itself.

$$\tilde{\dot{i}}_{d,q} = \left\{ \left[\frac{\mathbf{G}_{d,i}}{\mathbf{1} + \mathbf{G}_{delay}\mathbf{G}_{PI,i} \cdot \mathbf{G}_{PI,v}\mathbf{G}_{filter,DC}\mathbf{G}_{d,v}} \right] \mathbf{G}_{delay} \left(\mathbf{G}_{dec} - \mathbf{G}_{PI,i} \right) \mathbf{G}_{filter} \right\} \tilde{\dot{i}}_{d,q};$$

$$\left\{ \mathbf{1} + \mathbf{G}_{d,i} \left[\mathbf{1} + \mathbf{G}_{delay}\mathbf{G}_{PI,i}\mathbf{G}_{PI,v}\mathbf{G}_{filter,DC}\mathbf{G}_{d,v} \right]^{-1} \cdot \mathbf{G}_{delay} \left(\mathbf{G}_{PI,i} - \mathbf{G}_{dec} \right) \mathbf{G}_{filter} \right\} \cdot \tilde{\dot{i}}_{d,q} = 0;$$

$$\mathbf{A} \cdot \tilde{\dot{i}}_{d,q} = 0 \tag{3.38}$$

To find the transfer function to be used with the one previously found that links the Small-Signal voltage to the output currents, instead, the feedback is not considered.

$$\tilde{\dot{i}}_{d,q} = \mathbf{Y}_{dq} + \mathbf{G}_{d,i} \left[\mathbf{1} + \mathbf{G}_{delay}\mathbf{G}_{PI,i}\mathbf{G}_{PI,v}\mathbf{G}_{filter,DC}\mathbf{G}_{d,v} \right]^{-1} \mathbf{G}_{delay} \cdot$$

$$\cdot \left[\left(\mathbf{G}_{dec} - \mathbf{G}_{PI,i} \right) \mathbf{G}^{i}_{PLL}\mathbf{G}_{filter} - \mathbf{G}_{PI,i}\mathbf{G}_{PI,v}\mathbf{G}_{filter}\mathbf{G}_{v,v} + \mathbf{G}^{d}_{PLL}\mathbf{G}_{filter} \right] \tilde{v}_{d,q};$$

$$\tilde{\dot{i}}_{d,q} = \mathbf{B} \cdot \tilde{v}_{d,q} \tag{3.39}$$

If the two expressions obtained are put together, the total transfer function is obtained for the calculation of the impedances in the (d,q) reference frame with closed voltage and current loop.

$$\begin{aligned} \mathbf{A} \cdot \tilde{\dot{i}}_{d,q} &= \mathbf{B} \cdot \tilde{v}_{d,q}; \\ \frac{\tilde{v}_{d,q}}{\tilde{\dot{i}}_{d,q}} &= \mathbf{Z}_{converter,dq} = \mathbf{A}^{-1} \cdot \mathbf{B} \end{aligned} \tag{3.40}$$

However, this formula will be the final one to calculate the impedance in (d,q) reference frame with the voltage loop: as for the current loop alone, a step-by-step solution for reducing errors is presented here.

3.2.1 Impedances at Open Current-Loop with no PLL dynamic

In this case the impedance, also represented in this case only by the $\mathbf{Y}_{dq}$ (Fig. 2.6), depends on the average duty cycles both as regards diagonal and non-diagonal terms. Since $D_{d,q}$ are high square on the diagonal terms there will not be much difference based on the direction of the current, on which the signs of the two duty cycles depend, while on the non-diagonal terms it will be possible to observe a difference based on the direction of the current. For this reason, two impedances are shown, Fig. 3.5 and Fig. 3.6, Depending on whether the AFE is operating as a generator or as a rectifier. The data used remains that of the tables 2.1, 2.3 and 2.2.

Due to the presence of the capacity in parallel to the R_{DC}, the difference is seen above all at low frequencies for impedances D_{dd}, D_{dq} and D_{qd} while at high frequencies the inductive contribution prevails. As regards the impedance D_{qq}, being the average duty cycle in the q axis very small, the new contribution is greatly reduced and the impedance is almost identical to that calculated with an ideal voltage source for both cases. Furthermore, in both operating cases, the impedance Z_{dd} undergoes a phase lowering and an increase in the module, for low frequencies, due to the presence of R_{DC} and C_{DC}.

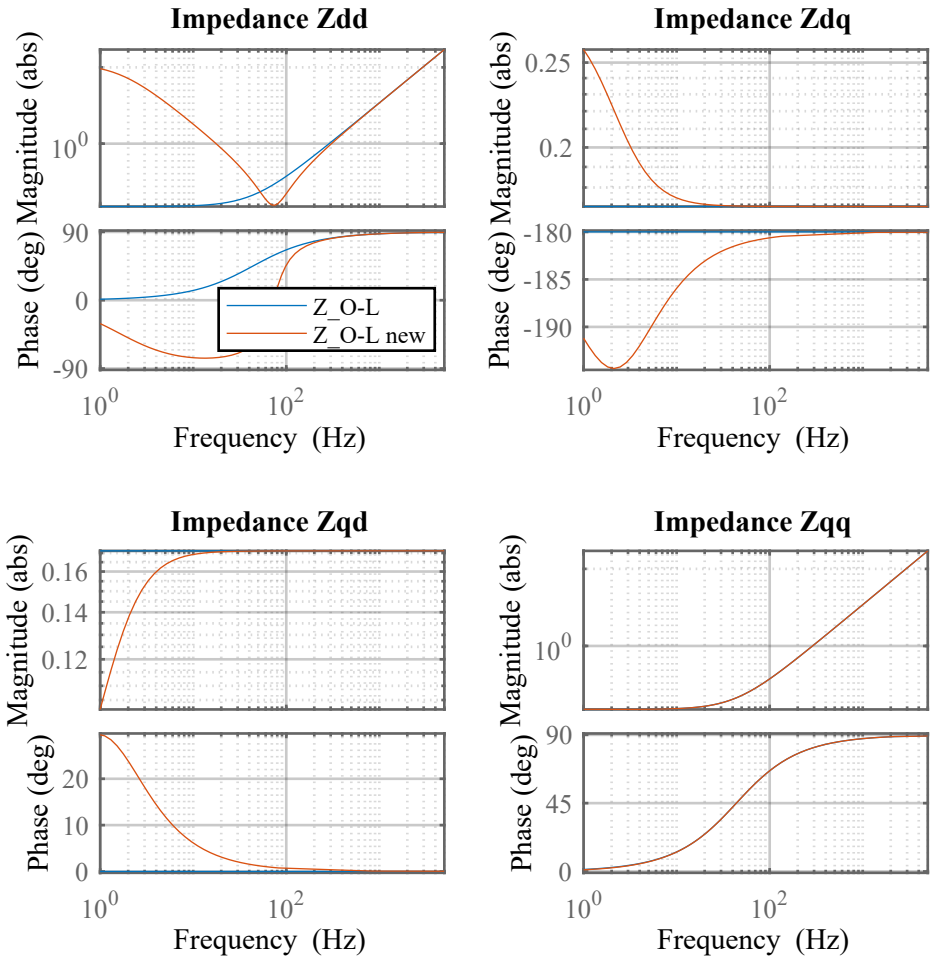

Figure 3.5: Comparison between Z_{dq} and $Z_{RL,dq}$ when the converter works as a Rectifier.

3.2.2 Impedances at Closed Current-Loop WITH PLL Dynamic

By closing the current loop it can be observed how the results in both cases are very similar to those obtained previously considering an ideal voltage generator on the DC side.

Also in this case, whether the converter works by feeding power into the grid or absorbing power from it, there is an increase in the impedance module Z_{dq} and

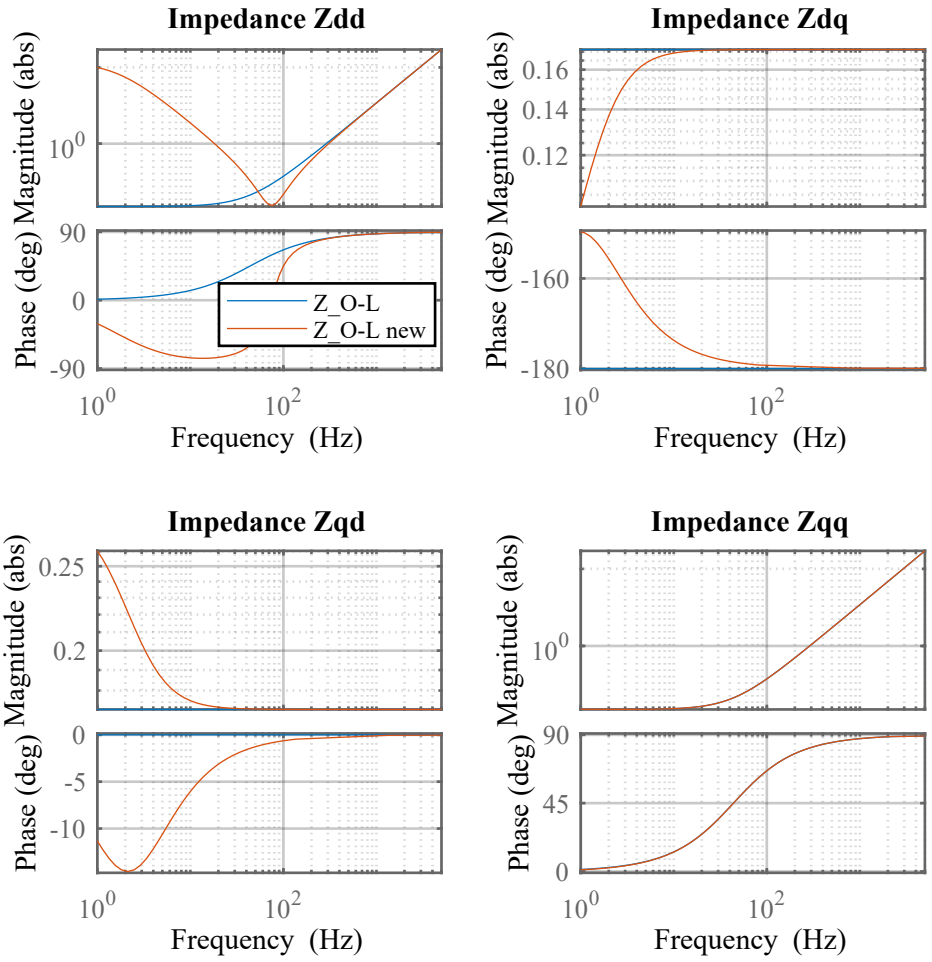

Figure 3.6: Comparison between Z_{dq} and $Z_{RL,dq}$ when the converter works as a Generator.

Z_{qd} at low frequencies. The phases vary for non-diagonal terms depending on the converter function, while, again due to the average duety cycles, the impedance Z_{qq} remains almost identical to that calculated in the previous chapter. By closing the current loop, you can instead start to observe how the impedance Z_{dd}, which shows the behavior of the current source, changes its behavior according to the function of the AFE. The low frequency phase continues to be around -90° due to the integrative part of the current PI, but undergoes a further phase decrease and an increase in modulus if the converter is used as an active rectifier while, in the

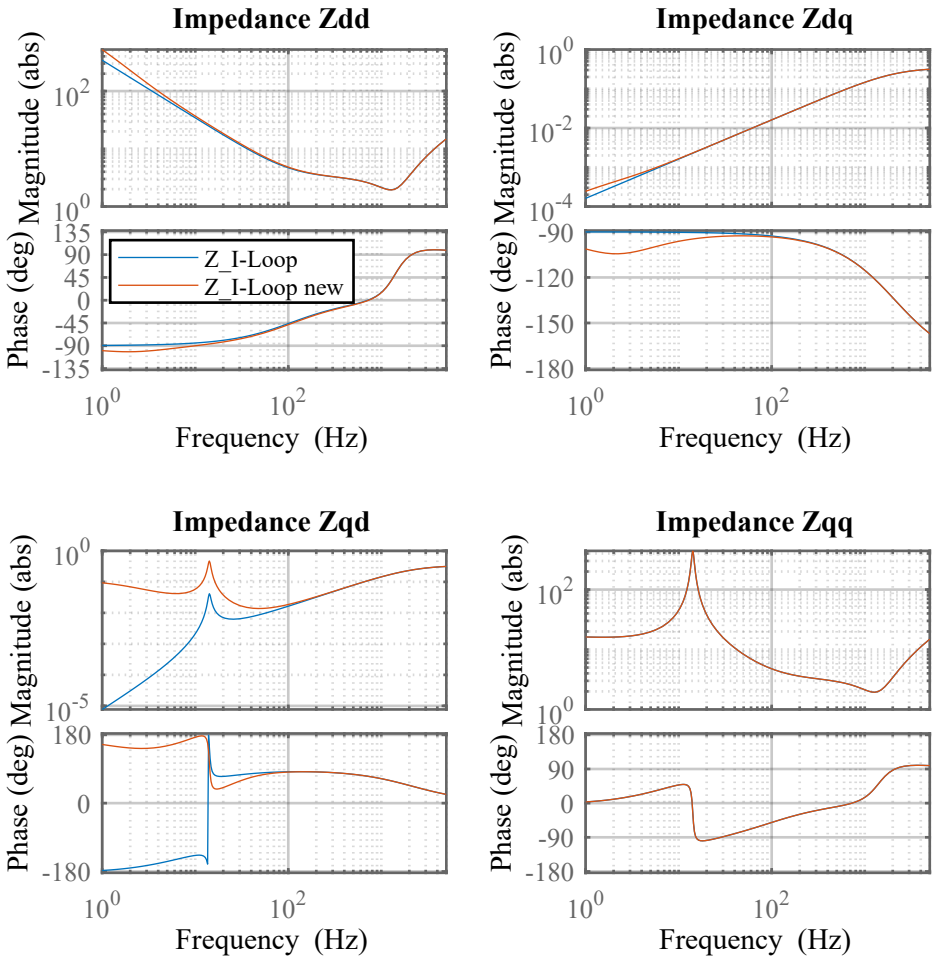

Figure 3.7: Comparison between the impedances with current closed-loop with and without considering an idel voltage source when the converter works as a Rectifier.

case is used to inject power into the grid, undergoes an increase in phase and a decrease in modulus.

3.2.3 Impedances at Closed Voltage-Loop

By closing the voltage loop, using the formula (3.40) for the calculation of the impedance, we obtain the total impedance of an AFE converter with PLL to synchronize to the grid voltage vector that works with current control in (d,q) reference

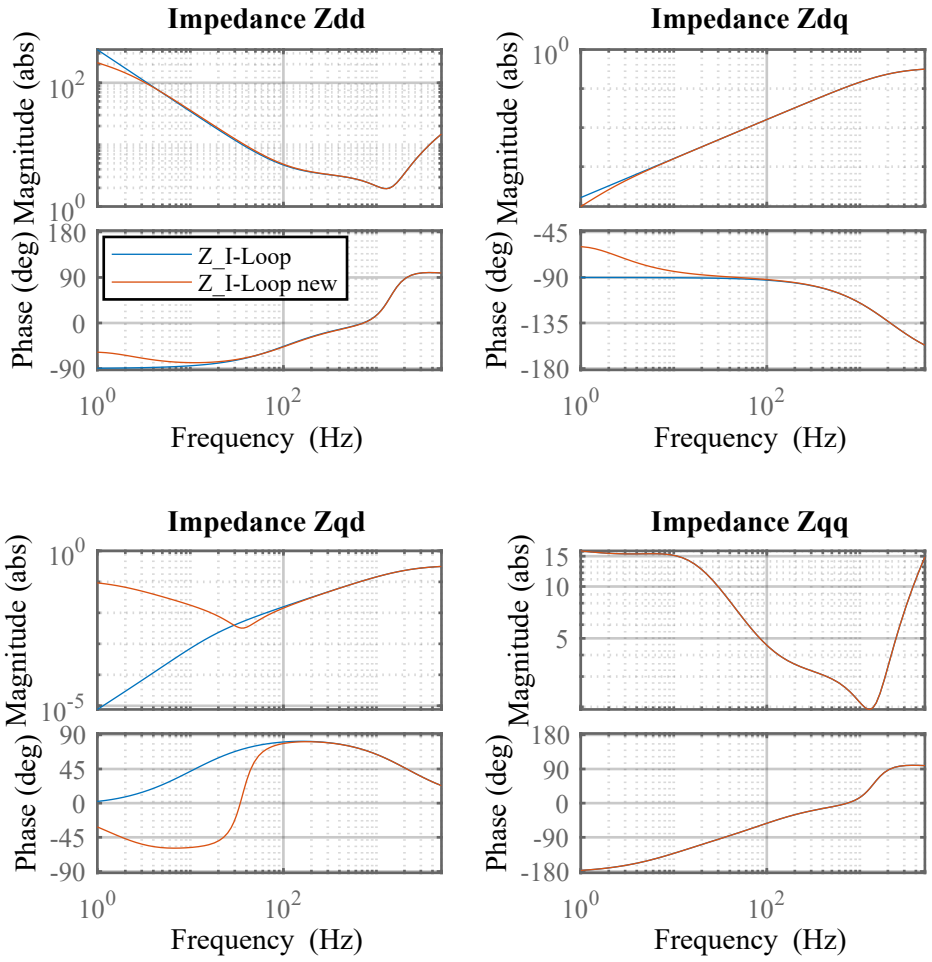

Figure 3.8: Comparison between the impedances with current closed-loop with and without considering an idel voltage source when the converter works as a Generator.

frame and voltage control.

The results obtained are shown below, Fig. 3.9 and 3.10, comparing them to those obtained previously having closed only the current loop.

It can be observed that with the voltage loop closed the impedance Z_{qq} has not changed in either of the two operating modes from the one calculated in the previous chapter. When the converter works as an active rectifier, it does not present problems as it is always included, in this specific case, between approximately -90° and +90°. When it works to withdraw energy from a DC source and transfer it

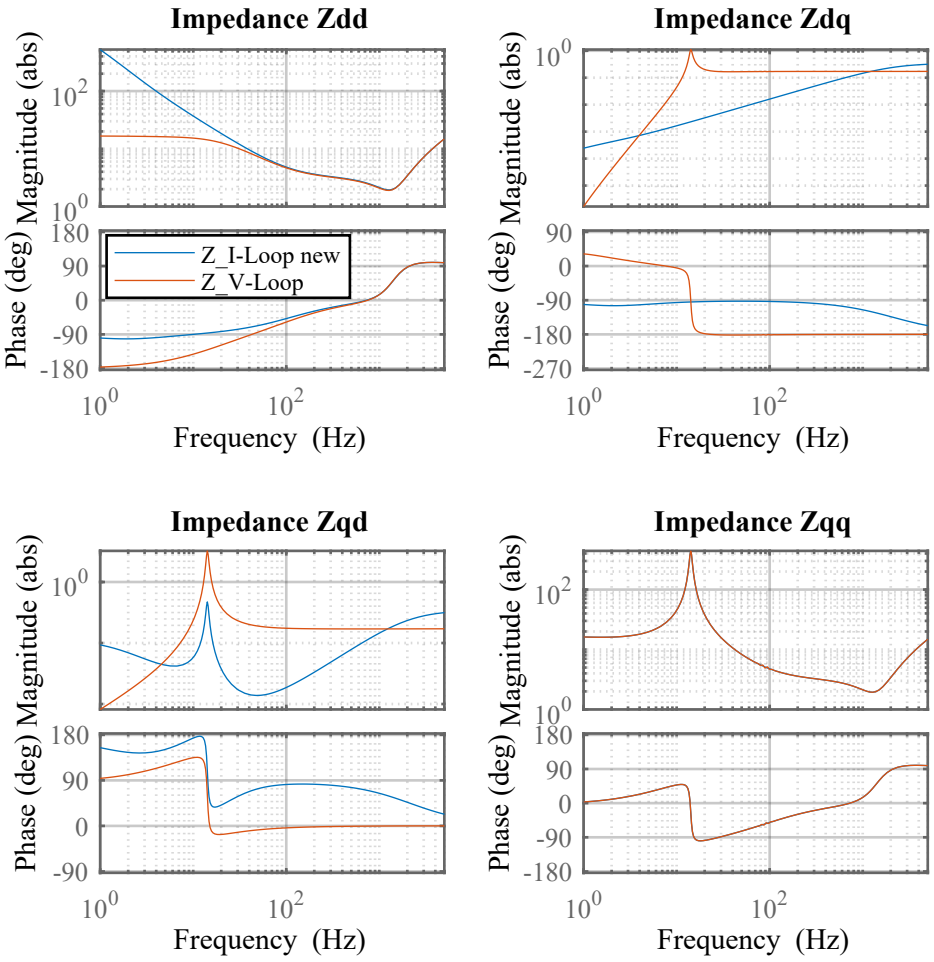

Figure 3.9: Comparison between the new impedances with current closed-loop and with the voltage closed-loope when the converter works as a Rectifier.

to the grid, this impedance behaves as a negative incremental resistance for low frequencies.

The impedances Z_{dq} and Z_{qd} gain modulus with respect to those with only the closed loop of current for a certain spectrum of frequencies and their phase is modified but, since the current in the q axis for these calculations is set to zero and there is the decoupling in the control scheme, their values are always smaller than those of diagonal terms.

Finally, the Z_{dd} impedance is identical to the previous one for high frequencies

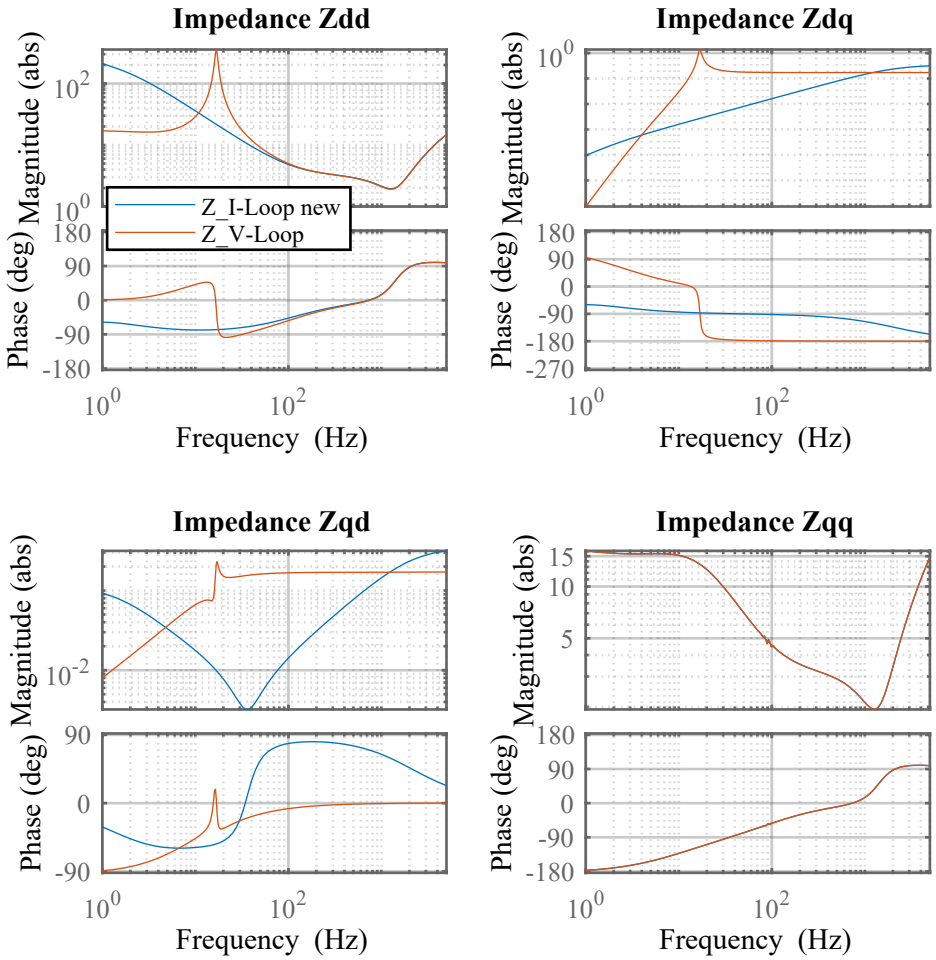

Figure 3.10: Comparison between the new impedances with current closed-loop and with the voltage closed-loope when the converter works as a Generator.

while, due to the voltage control, it gains 90° of phase for the low frequencies if the converter gives power to the power grid and instead loses 90° if it is absorbing power. In the analyzed case of active rectifier, Fig. 3.9, the frequency spectrum for which the phase of impedance Z_{dd} is -180° is almost negligible and depends exclusively on how the converter and its control are sized and not on the PLL, as will be seen in the following paragraph.

As said before, the converter can also perform the function of supporting the grid when it requires to absorb or to dispose of reactive power. During these requests

the converter produces an I_q current that has an impact on the impedance Z_{dq} only, as previously seen.

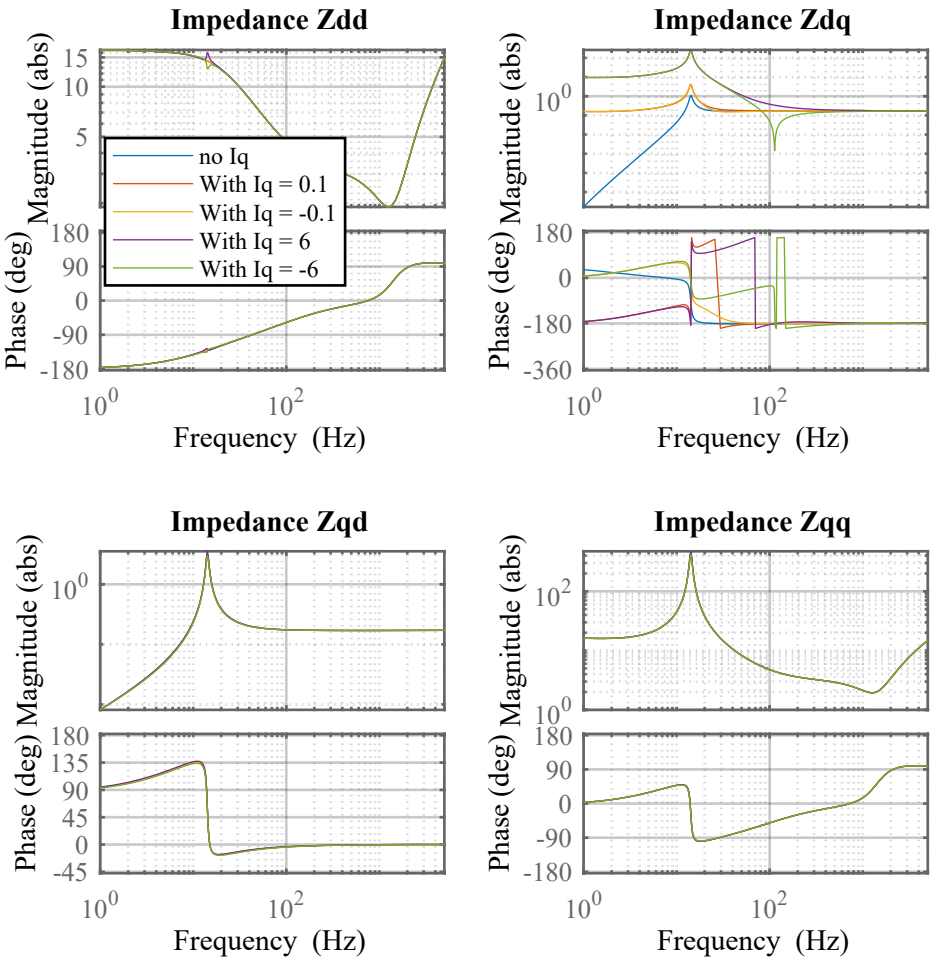

Figure 3.11: Comparison between output Impedence with Closed Voltage-Loop with different I_q when the converter works as a Rectifier.

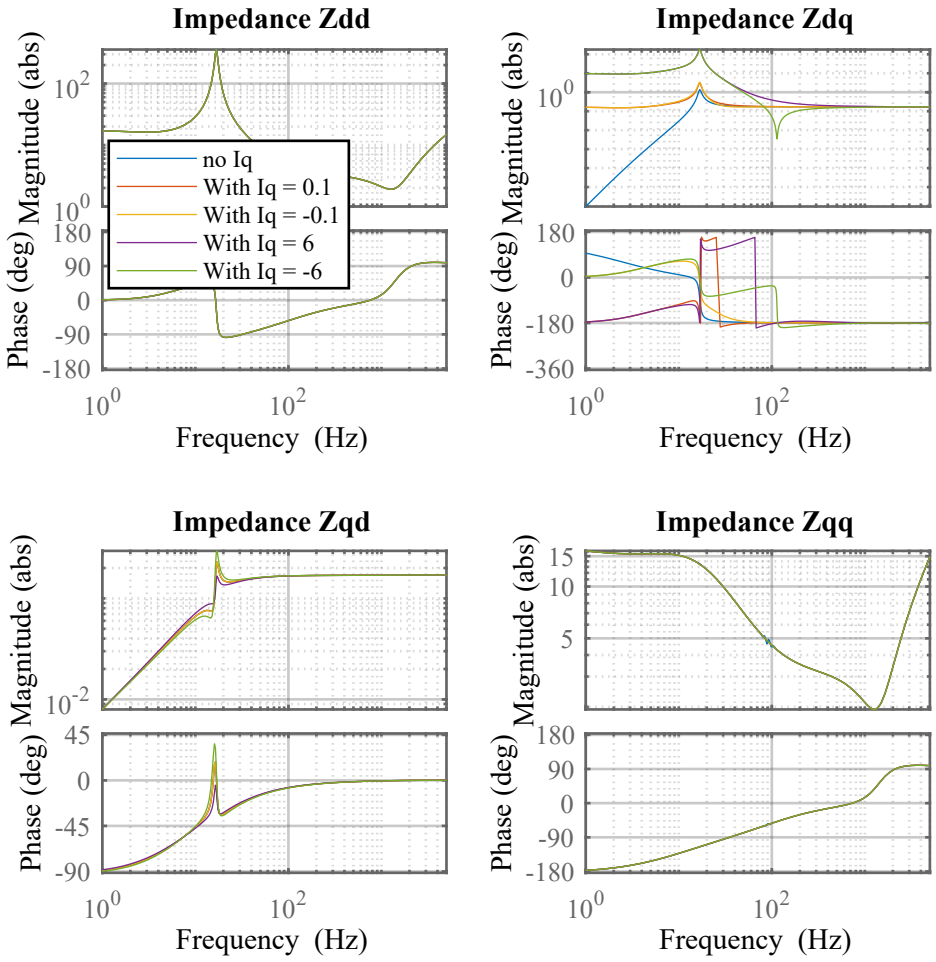

Figure 3.12: Comparison between output Impedence with Closed Voltage-Loop with different I_q when the converter works as a Generator.

Even in this case, the impedance module Z_{dq} increases for the lower frequency disturbances in proportion to the current flowing in the q axis.

3.2.4 Influence of the PLL Bandwidth on the Output Impedance with Voltage-Loop

Since the impedance Z_{qq} is almost unchanged with respect to those calculated previously; Fig. 2.15 and 2.16, the same reasoning already seen previously can

be appied here: a wider PLL bandwidth, which determines the ability to pursue faithfully the reference angle of the grid , determines a greater sensitivity to voltage disturbances that travel within the network. In fact, the aspect that the impedance Z_{qq} assumes in generator mode operation is that of a negative incremental resistance which increases its frequency spectrum depending on the PLL bandwidth. On the other hand, the impedance Z_{dd}, as already anticipated, when the converter operates as an active rectifier, also has a similar behavior which, however, does not depend on how the PLL was sized for this system. This behaviour depends exclusively on the parameters used for the current and voltage control and from the circuit parameters of the converter itself. As can be seen, in fact, as the bandwidth of the PLL changes, the impedance Z_{dd} does not change neither in module nor in phase.

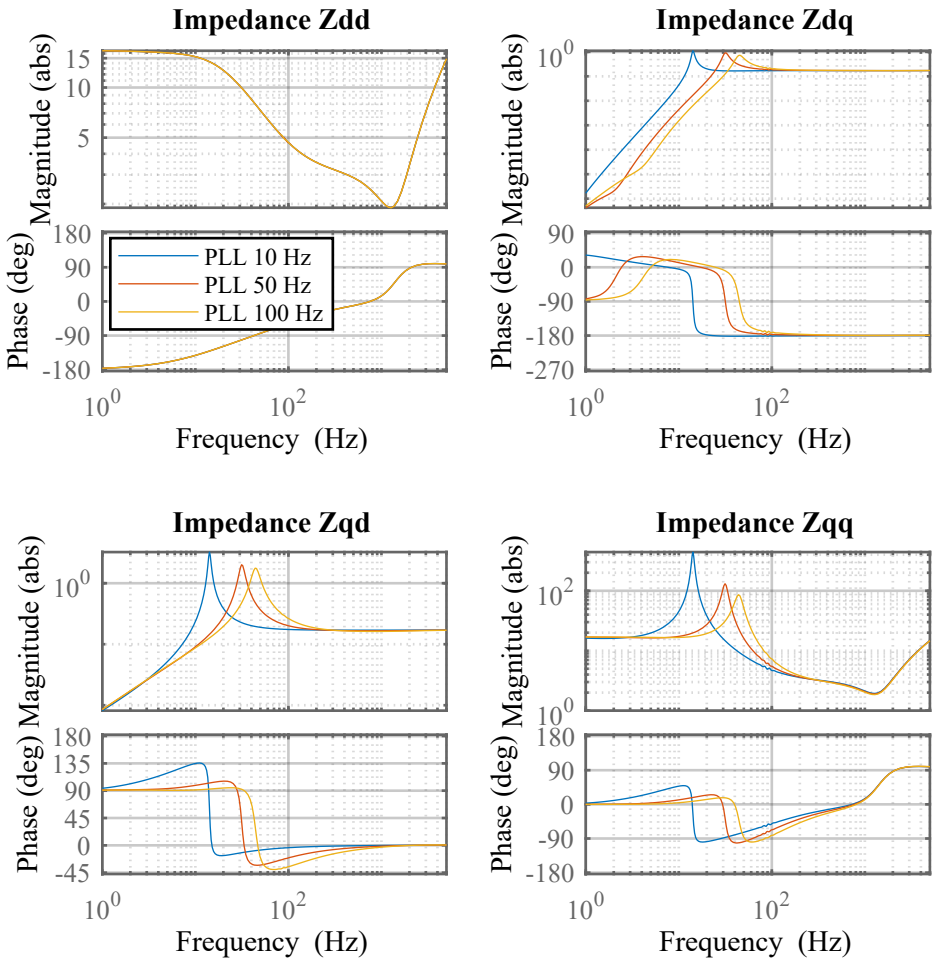

Figure 3.13: Comparison between the new voltage closed-loop impedances with different PLL bandwidths when the converter works as a Rectifier.

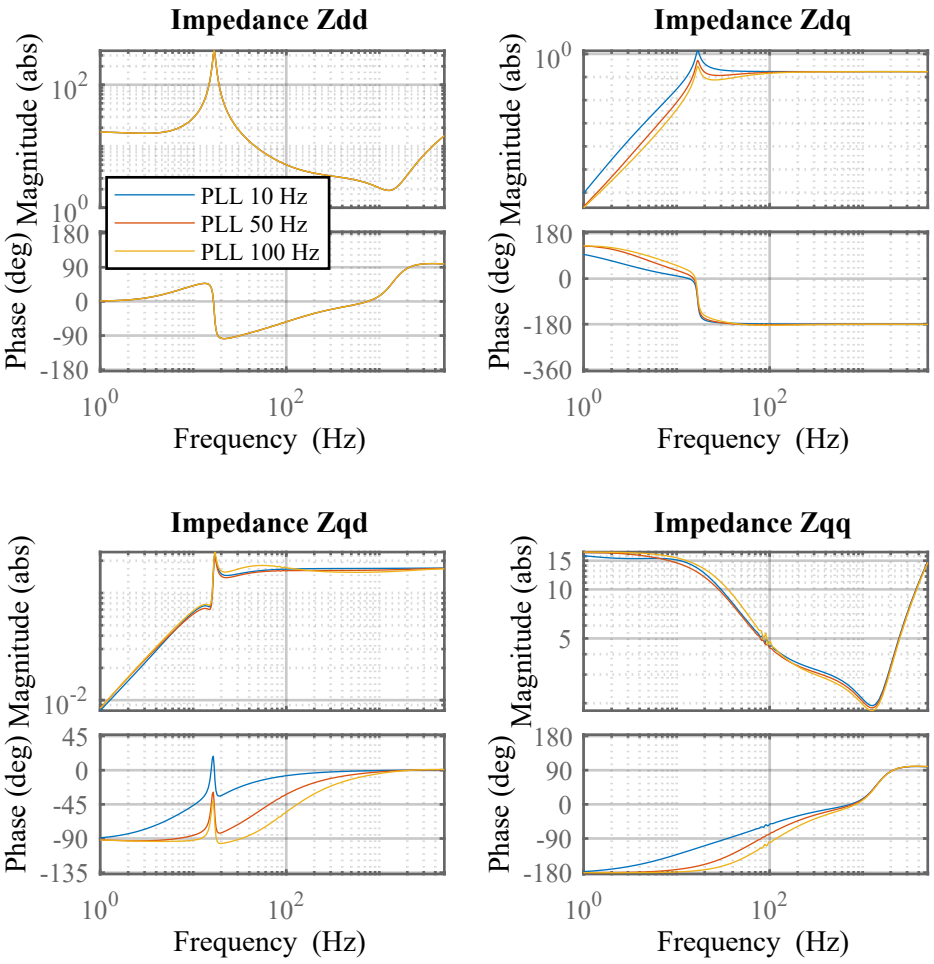

Figure 3.14: Comparison between the new voltage closed-loop impedances with different PLL bandwidths when the converter works as a Generator.

Chapter 4

Conclusions

This thesis focused on a single method to describe, through linear analysis, the behavior of an Voltage Source Converter representing it as a 2×2 impedance in a totating (d,q) reference frame. The result obtained can be put together with the elements previously not considered to represent the whole system: if also the remaining part of the LCL filter and the grid are represented in the reference (d,q) frame system, the equivalent of the system in figure Fig. 1.3 can be represented for the study of the propagation of Small-Signals as in figure Fig. 4.1.

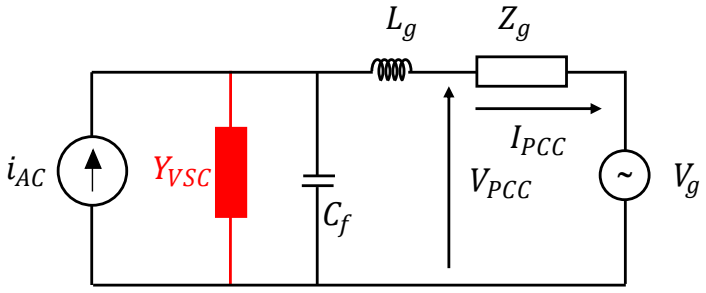

Figure 4.1: Average equivalent model for Small-Signals propagation study.

Once the calculations have been developed, it is possible, by changing the parameters of the simulation, to obtain an impedance model of any converter of this type: it would be simple, in the design phase, to observe what the impact of this converter could be once connected to the power grid, but it is necessary to know the parameters of the components used for the production and the values of the PI

controllers. In the industrial practice, other methods can derive these models by injecting signals into the converter without knowing the internal components.
This method can however be used to test, in the design phase, the validity and accuracy of such experimental caracterization methods. For example, voltage injection methods or system identification techniques [6] can be used.
Here are some examples taken from [6] that show the experimental results compared with the calculations I developed.
It is therefore important to note the versatility of the method developed: it is possible to modify the code elaborated and to insert other circuit parameter values, change them, or even the structure of the current and voltage controllers, add or remove parts if necessary (e.g. Decoupling matrix) adapting the code to the converter under analysis.

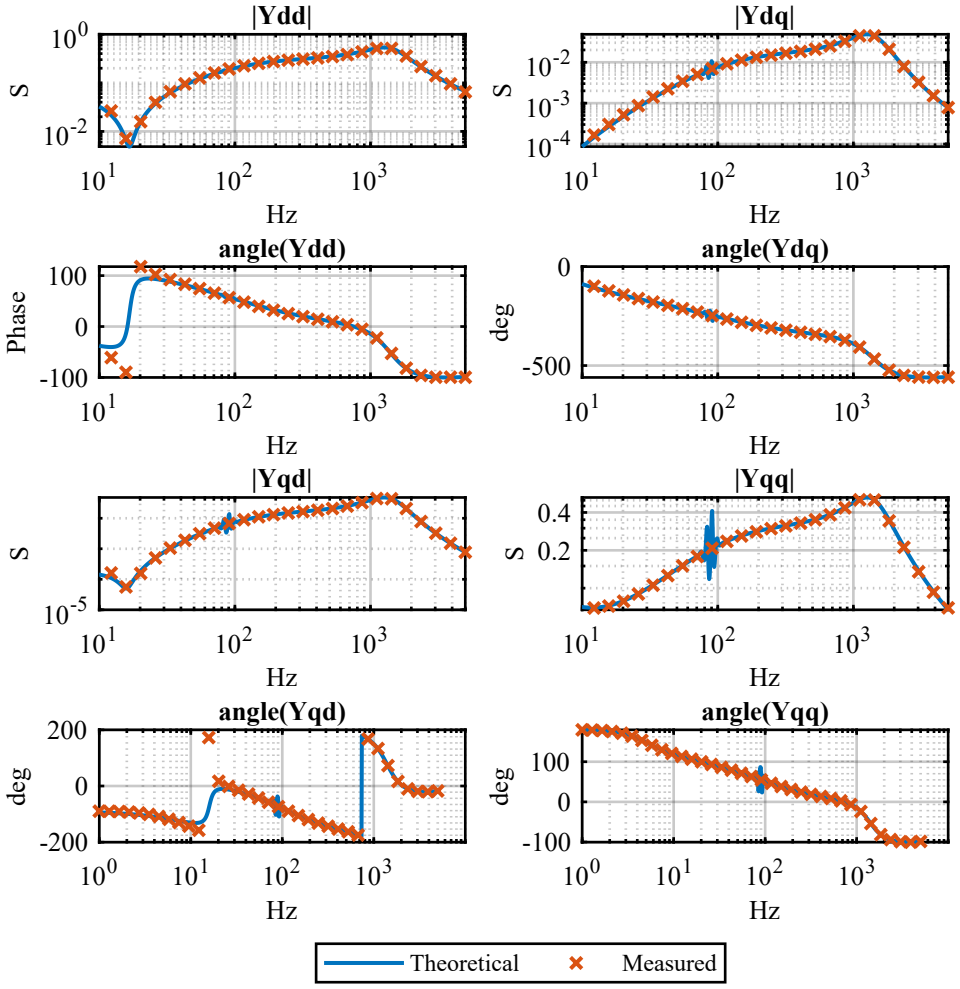

Figure 4.2: Comparison between the results obtained in a PLECS simulation using the Small-Signal voltage injection and the theoretical results calculated for a converter with closed voltage-loop operating in Generator Mode.

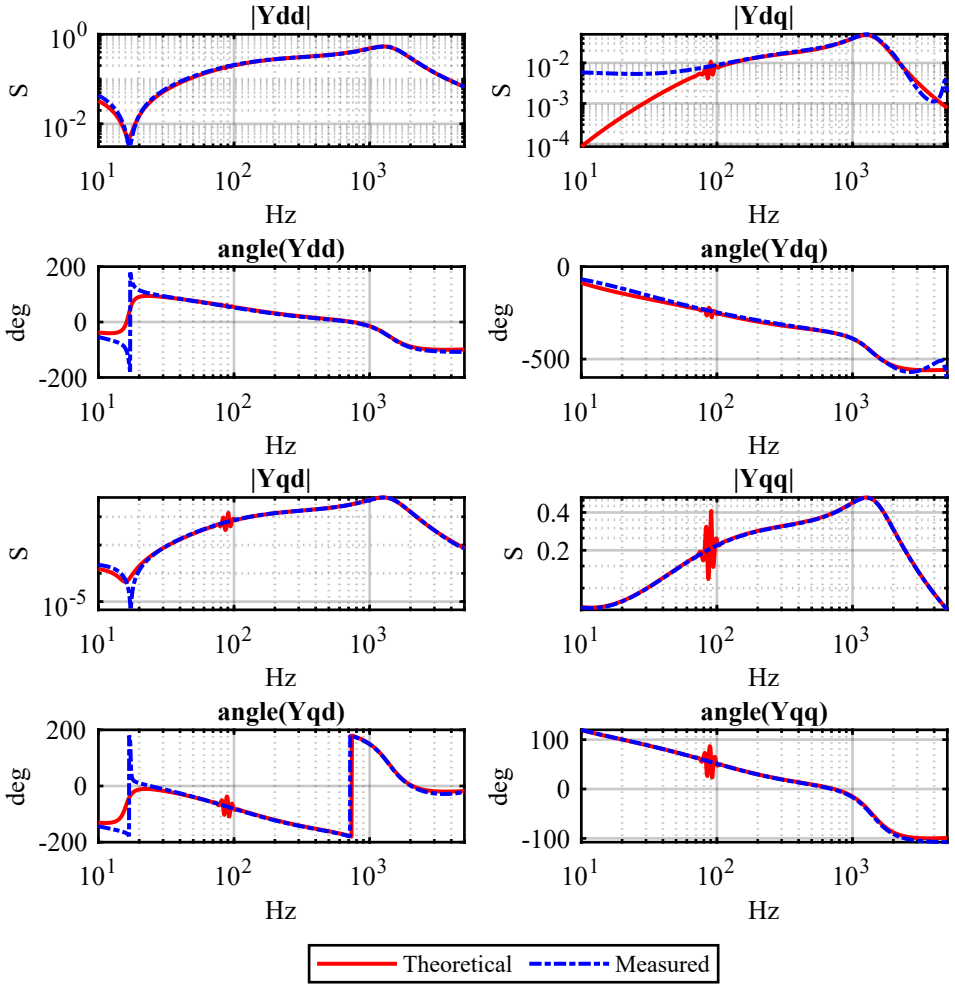

Figure 4.3: Comparison between the results obtained in a PLECS simulation using the Transient Analysis and the theoretical results calculated for a converter with closed voltage-loop operating in Generator Mode.

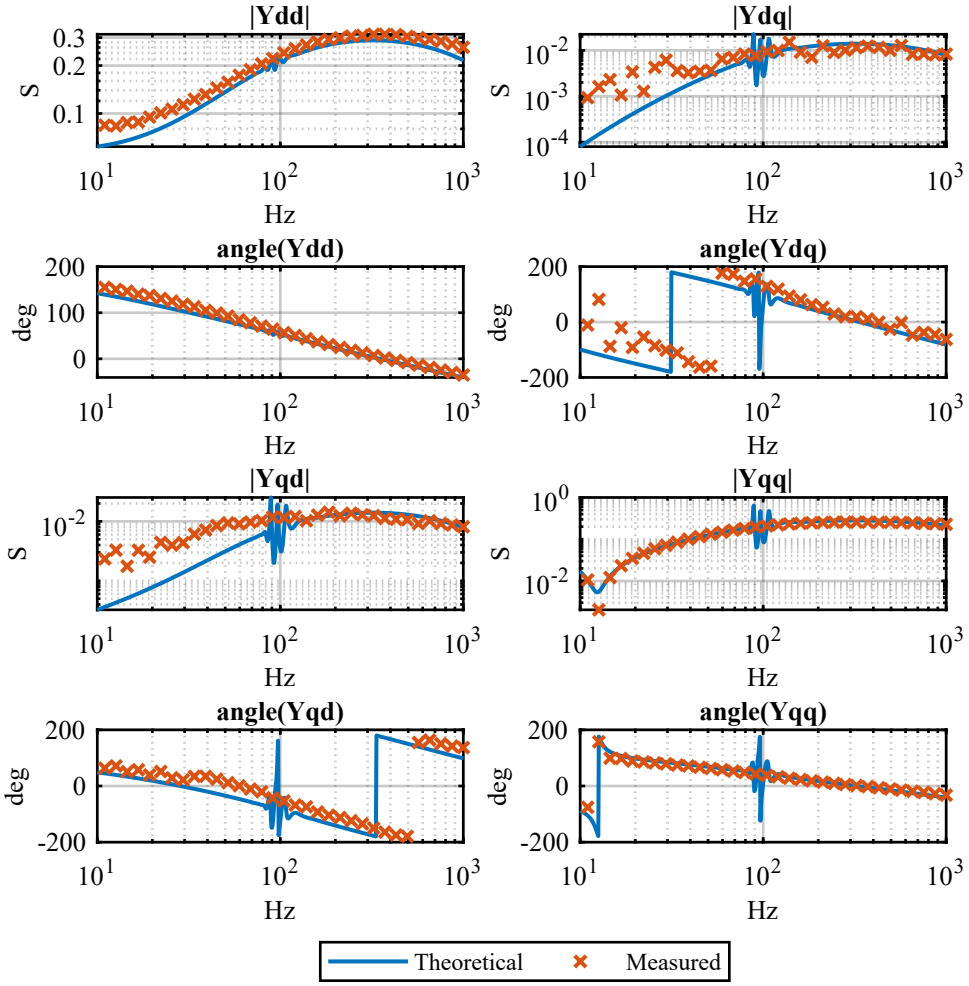

Figure 4.4: Comparison between the results on the experimental setup obtained by Small-Signal voltage injection and the theoretical results calculated for a converter with closed voltage-loop operating in Rectifier Mode.

As regards the analytical results obtained in chapters 2 and 3, the main aspect observed is that when the converter in analysis works by feeding energy into the grid the impedance Z_{qq} could destabilize the system due to its negative incremental resistance behaviour. It has also been seen how this penalizing behavior is influenced by the PLL: in fact, when its bandwidth increases, the spectrum of frequencies for which the phase of the impedance Z_{qq} is less than -90° increases, allowing an increasingly greater range of disturbances in the system to be affected

by this behavior.

The Small-Signal impedance model obtained in this thesis can therefore be used to evaluate the behavior of a converter based on its operating point, can validate estimation methods of the equivalent impedance of the converter, and therefore act as a benchmark. The final application is in grid stability analysis to evaluate the impact of the converter, during the operation, on the electrical grid.

Appendix A

Appendix

A.1 Code used for Impedance Model with Current-Loop only

```
clear
clc
% close all
% PARAMETERS FOR SIMULATION
Vg_rms = 120; %[V]
Vg_pk = 120*sqrt(2); %[V]
Vdc = 370; %[V]
Vd = Vg_pk; %[V]
Vq = 0; %[V]
fg = 50; %[Hz]
wg = 2*pi*fg; %[rad/s]
L = 0.000545; %[H]
R = 0.15; %[Ohm]
fsw = 10000; %[Hz]
Tdel = 1.5/fsw; %[s]
kp_i = 3.424/Vdc;
ki_i = 2151.57/Vdc;

Id = -10; %[A]
Iq = 0; %[A]

Dd = (Vd + R*Id - wg*L*Iq)/Vdc
Dq = (Vq + R*Iq + L*wg*Id)/Vdc

% Different PLL PI controllers
fbw_PLL1 = 10; %[Hz]
```

```
wbw_PLL1 = 2*pi*fbw_PLL1; %[rad/s]
wz_PLL1 = wbw_PLL1/10; %[rad/s]
kp_PLL1 = wbw_PLL1/Vg_pk
ki_PLL1 = (wbw_PLL1/Vg_pk)*wz_PLL1

fbw_PLL2 = 50; %[Hz]
wbw_PLL2 = 2*pi*fbw_PLL2; %[rad/s]
wz_PLL2 = wbw_PLL2/10; %[rad/s]
kp_PLL2 = wbw_PLL2/Vg_pk
ki_PLL2 = (wbw_PLL2/Vg_pk)*wz_PLL2

fbw_PLL3 = 100; %[Hz]
wbw_PLL3 = 2*pi*fbw_PLL3; %[rad/s]
wz_PLL3 = wbw_PLL3/10; %[rad/s]
kp_PLL3 = wbw_PLL3/Vg_pk
ki_PLL3 = (wbw_PLL3/Vg_pk)*wz_PLL3

% FUNCTIONS IN s DOMAIN CALCULATIONS
s = tf('s');
PI_i = kp_i + (ki_i)/s;

% First order Padè approximation
% delay = (1-0.5*Tdel*s)/(1+0.5*Tdel*s);
% Third order Padè approximation
delay = (120 +60*Tdel*s +12*Tdel^2*s^2 +Tdel^3*s^3)/(120 -60*Tdel*s +12*Tdel^2*s^2 -Tdel
    ^3*s^3);

PI_PLL1 = kp_PLL1 + (ki_PLL1/s);
PI_PLL2 = kp_PLL2 + (ki_PLL2/s);
PI_PLL3 = kp_PLL3 + (ki_PLL3/s);

T_PLL1 = PI_PLL1/(s + PI_PLL1*Vd);
T_PLL2 = PI_PLL2/(s + PI_PLL2*Vd);
T_PLL3 = PI_PLL3/(s + PI_PLL3*Vd);

% MATRIX CALCULATIONS

I = eye(2);
G_delay = [delay, 0; 0, delay];
G_PI_i = -[PI_i, 0; 0, PI_i];
Zrl = [s*L + R, -wg*L; wg*L, s*L + R];
Yrl = inv(Zrl);%Yrl = -inv_det_Zrl*[s*L + R, wg*L; -wg*L, s*L + R];

G_duty_PLL1 = [0, -Dq*T_PLL1; 0, Dd*T_PLL1];
G_i_PLL1 = [0, Iq*T_PLL1; 0, -Id*T_PLL1];

G_duty_PLL2 = [0, -Dq*T_PLL2; 0, Dd*T_PLL2];
G_i_PLL2 = [0, Iq*T_PLL2; 0, -Id*T_PLL2];
```

```
74
75 G_duty_PLL3 = [0, -Dq*T_PLL3; 0, Dd*T_PLL3];
76 G_i_PLL3 = [0, Iq*T_PLL3; 0, -Id*T_PLL3];
77
78 G_id = (-Vdc)*Yrl;
79 G_dec = [0, (wg*L)/Vdc; (-wg*L)/Vdc, 0];
80
81 % IMPEDANCES
82 Z_inverter_0 = Zrl;
83 Z_inverter = inv(Yrl + G_id*G_delay*G_duty_PLL1);
84
85 X = I - G_id*G_delay*(G_dec - G_PI_i);
86 Y1 = Yrl + G_id*G_delay*((G_dec - G_PI_i)*G_i_PLL1 + G_duty_PLL1);
87
88 Y2 = Yrl + G_id*G_delay*((G_dec - G_PI_i)*G_i_PLL2 + G_duty_PLL2);
89
90 Y3 = Yrl + G_id*G_delay*((G_dec - G_PI_i)*G_i_PLL3 + G_duty_PLL3);
91
92 Z_inverter_final1 = Y1\X;
93 Z_inverter_final2 = Y2\X;
94 Z_inverter_final3 = Y3\X;
```

A.2 Code used for Impedance Model with Voltage-Loop

```
1  clear
2  clc
3  close all
4  % PARAMETERS FOR SIMULATION
5  Vg_rms = 120; %[V]
6  Vg_pk = 120*sqrt(2); %[V]
7  Vdc = 370; %[V]
8  Vd = 120*sqrt(2); %[V]
9  Vq = 0; %[V]
10 Iload = -6.88;
11 fg = 50; %[Hz]
12 wg = 2*pi*fg; %[rad/s]
13 L = 545e-6; %[H]
14 R_L = 0.15; %[Ohm]
15 C = 0.0018; %[F]
16 R = abs(Vdc/Iload); %[Ohm]
17 fsw = 10000; %[Hz]
18 Tdel = 1.5/fsw;
19 kp_i = 3.424/Vdc;
20 ki_i = 2151.57/Vdc;
21
```

```
Id = -(2/3)*(Vdc/Vd)*Iload %[A]
Iq = 0 %[A]

Dd = (Vd - R_L*Id + wg*L*Iq)/Vdc   %0.3734;
Dq = (Vq - R_L*Iq -L*wg*Id)/Vdc   %0.0977;

% Different PLL PI controllers
fbw_PLL1 = 10; %[Hz]
wbw_PLL1 = 2*pi*fbw_PLL1; %[rad/s]
wz_PLL1 = wbw_PLL1/10; %[rad/s]
kp_PLL1 = wbw_PLL1/Vg_pk
ki_PLL1 = (wbw_PLL1/Vg_pk)*wz_PLL1

fbw_PLL2 = 50; %[Hz]
wbw_PLL2 = 2*pi*fbw_PLL2; %[rad/s]
wz_PLL2 = wbw_PLL2/10; %[rad/s]
kp_PLL2 = wbw_PLL2/Vg_pk
ki_PLL2 = (wbw_PLL2/Vg_pk)*wz_PLL2

fbw_PLL3 = 100; %[Hz]
wbw_PLL3 = 2*pi*fbw_PLL3; %[rad/s]
wz_PLL3 = wbw_PLL3/10; %[rad/s]
kp_PLL3 = wbw_PLL3/Vg_pk
ki_PLL3 = (wbw_PLL3/Vg_pk)*wz_PLL3

% FUNCTIONS IN s DOMAIN CALCULATIONS
s = tf('s');
PI_i = kp_i + (ki_i)/s;

PI_PLL1 = kp_PLL1 + (ki_PLL1/s);
PI_PLL2 = kp_PLL2 + (ki_PLL2/s);
PI_PLL3 = kp_PLL3 + (ki_PLL3/s);

% First order Padè approximation
% delay = (1-0.5*Tdel*s)/(1+0.5*Tdel*s);
% Third order Padè approximation
delay = (120 +60*Tdel*s +12*Tdel^2*s^2 +Tdel^3*s^3)/(120 -60*Tdel*s +12*Tdel^2*s^2 -Tdel
    ^3*s^3);

T_PLL1 = PI_PLL1/(s + PI_PLL1*Vd);
T_PLL2 = PI_PLL2/(s + PI_PLL2*Vd);
T_PLL3 = PI_PLL3/(s + PI_PLL3*Vd);

% inv_det_Zrl = 1/(((L*s + R_L)^2)+((wg*L)^2));
X_P = (R/(R*C*s + 1));
inv_det_Zrl = 1/((s*L + R_L + X_P*Dd^2)*(s*L + R_L + X_P*Dq^2) - ((X_P*Dd*Dq)^2 - (wg*L)
    ^2));
G_ve_1 = 1/((C*s + (1/R))*(((L*s + R_L)^2)+((wg*L)^2)) + ((Dd^2 + Dq^2)*(L*s + R_L)));
```

```
68 G_vd_1 = 1/((C*s + (1/R)) + (((L*s + R_L))*(Dd^2 + Dq^2))/(((L*s + R_L)^2)+((wg*L)^2)));
69
70 % MATRIX CALCULATIONS
71 I = eye(2);
72 G_delay = [delay, 0; 0, delay];
73 G_PI_i = -[PI_i, 0; 0, PI_i];
74 Zrl = [s*L + R_L + X_P*Dd^2, -wg*L + X_P*Dd*Dq; wg*L + X_P*Dq*Dd, s*L + R_L + X_P*Dq^2];
75 Yrl = inv_det_Zrl*[s*L + R_L + X_P*Dq^2, -(X_P*Dd*Dq - wg*L); -(X_P*Dd*Dq + wg*L), s*L +
       R_L + X_P*Dd^2];
76
77 Zrl_000 = [s*L + R_L, -wg*L; wg*L, s*L + R_L];
78 Yrl_000 = inv(Zrl_000);
79
80 G_duty_PLL1 = [0, -Dq*T_PLL1; 0, Dd*T_PLL1];
81 G_i_PLL1 = [0, Iq*T_PLL1; 0, -Id*T_PLL1];
82
83 G_duty_PLL2 = [0, -Dq*T_PLL2; 0, Dd*T_PLL2];
84 G_i_PLL2 = [0, Iq*T_PLL2; 0, -Id*T_PLL2];
85
86 G_duty_PLL3 = [0, -Dq*T_PLL3; 0, Dd*T_PLL3];
87 G_i_PLL3 = [0, Iq*T_PLL3; 0, -Id*T_PLL3];
88
89 G_id = -Yrl*[Vdc + X_P*Dd*Id, X_P*Dd*Iq; X_P*Dq*Id, Vdc + X_P*Dq*Iq];
90 G_dec = [0, (wg*L)/Vdc; (-wg*L)/Vdc, 0];
91
92 G_id_000 = (-Vdc)*Yrl_000;
93
94 GX = G_dec - G_PI_i;
95
96 % IMPEDANCES with CURRENT LOOP
97 Z_inverter_0 = Zrl;
98 Z_inverter_open_loop = inv(Yrl + G_id*G_delay*G_duty_PLL1);
99
100 X = I - G_id*G_delay*(GX);
101 Y1 = Yrl + G_id*G_delay*((GX)*G_i_PLL1 + G_duty_PLL1);
102 Y2 = Yrl + G_id*G_delay*((GX)*G_i_PLL2 + G_duty_PLL2);
103 Y3 = Yrl + G_id*G_delay*((GX)*G_i_PLL3 + G_duty_PLL3);
104
105 X_000 = I - G_id_000*G_delay*(G_dec - G_PI_i);
106 Y_000 = Yrl_000 + G_id_000*G_delay*((G_dec - G_PI_i)*G_i_PLL1 + G_duty_PLL1);
107
108 Z_inverter_final_000 = Y_000\X_000;
109
110 Z_inverter_closed_loop1 = Y1\X;
111 Y_inverter_closed_loop1 = X\Y1;
112
113 Z_inverter_closed_loop2 = Y2\X;
114 Y_inverter_closed_loop2 = X\Y2;
```

```
115
116 Z_inverter_closed_loop3 = Y3\X;
117 Y_inverter_closed_loop3 = X\Y3;
118
119 % VOLTAGE LOOP ADDED
120 kp_v = 0.3393;
121 ki_v = 6.3955;
122 PI_v = kp_v + (ki_v)/s;
123 G_PI_v = PI_v*[1, 0; 0, 0]; %((2*Vdc)/(3*Vd))
124 G_ve = G_ve_1*[Dd*(L*s + R_L) - (wg*L*Dq), Dq*(L*s + R_L) + (wg*L*Dd); 0, 0];
125 G_vd = G_vd_1*[Id - (Vdc/(((L*s + R_L)^2)+((wg*L)^2)))*(Dd*(L*s + R_L) - Dq*wg*L), Iq -
        (Vdc/(((L*s + R_L)^2)+((wg*L)^2)))*(Dd*wg*L + Dq*(L*s + R_L)); 0, 0];
126
127  G_dec = [0, (wg*L)/Vdc; (-wg*L)/Vdc, 0];
128  GX = G_dec - G_PI_i;
129
130 X_1 = I - G_id*(inv(I + G_delay*G_PI_i*G_PI_v*G_vd))*G_delay*(GX);
131 Y_1 = Yrl + G_id*(inv(I + G_delay*G_PI_i*G_PI_v*G_vd))*G_delay*((GX)*G_i_PLL1 - G_PI_i*
        G_PI_v*G_ve + G_duty_PLL1);
132 Y_2 = Yrl + G_id*(inv(I + G_delay*G_PI_i*G_PI_v*G_vd))*G_delay*((GX)*G_i_PLL2 - G_PI_i*
        G_PI_v*G_ve + G_duty_PLL2);
133 Y_3 = Yrl + G_id*(inv(I + G_delay*G_PI_i*G_PI_v*G_vd))*G_delay*((GX)*G_i_PLL3 - G_PI_i*
        G_PI_v*G_ve + G_duty_PLL3);
134
135 Y_inverter_final1 = X_1\Y_1;
136 Z_inverter_final1 = Y_1\X_1;
137
138 Y_inverter_final2 = X_1\Y_2;
139 Z_inverter_final2 = Y_2\X_1;
140
141 Y_inverter_final3 = X_1\Y_3;
142 Z_inverter_final3 = Y_3\X_1;
```

Bibliography

[1] Pooja Kholia, Mayank Chaturvedi, Pradeep K. Juneja, and Sheetal Kapoor. Effect of Padè First order Delay Approximation On Controller Capability designed for IPDT Process Model. In *2018 International Conference on Power Energy, Environment and Intelligent Control (PEEIC)*, pages 102–105, April 2018. ISSN: null.

[2] E. Mollerstedt and B. Bernhardsson. Out of control because of harmonics-an analysis of the harmonic response of an inverter locomotive. *IEEE Control Systems Magazine*, 20(4):70–81, August 2000.

[3] Xiongfei Wang, Lennart Harnefors, and Frede Blaabjerg. Unified Impedance Model of Grid-Connected Voltage-Source Converters. *IEEE Transactions on Power Electronics*, 33(2):1775–1787, February 2018.

[4] Bo Wen, Dushan Boroyevich, Rolando Burgos, Paolo Mattavelli, and Zhiyu Shen. Analysis of D-Q Small-Signal Impedance of Grid-Tied Inverters. *IEEE Transactions on Power Electronics*, 31(1):675–687, January 2016.

[5] Bo Wen, Dushan Boroyevich, Paolo Mattavelli, Zhiyu Shen, and Rolando Burgos. Influence of phase-locked loop on input admittance of three-phase voltage-source converters. In *2013 Twenty-Eighth Annual IEEE Applied Power Electronics Conference and Exposition (APEC)*, pages 897–904, March 2013. ISSN: 1048-2334.

[6] Luca Zeppegno. *Black-box Commissioning of Grid Converters*. Politecnico di Torino, March 2020.